# The function of Wnt/beta-catenin signaling in Ewing sarcoma and its contribution to pathogenesis

by

Elisabeth Anne Pedersen

A dissertation submitted in partial fulfillment
of the requirements for the degree of
Doctor of Philosophy
(Molecular and Cellular Pathology)
The University of Michigan
2016

Doctoral Committee:

Associate Professor Elizabeth R. Lawlor, Chair
Professor Kenneth Cadigan
Professor Colin Duckett
Professor Eric R. Fearon
Associate Professor Zaneta Nikolovska-Coleska
Professor Russell S. Taichman

*Dedicated to the patients for whom this work is intended,*
*and to my husband Chase, who spent many evenings in the lab too.*

## ACKNOWLEDGEMENTS

I would like to thank a the current members of the Lawlor lab for their scientific input technical assistance, and friendship, including Kelly Bailey, Ally Hawkins, Laurie Svoboda, Sudha Sud, Raelene Van Noord, and of course Beth Lawlor. Further thank you to former members Chris Scannell, Merlin Airik, Ashley Harris, Natashay Bailey, Katherine Ryland, Melanie Krook, and Jack Mosher. I am extremely grateful to temporary students Jay Read, Jenny Tran, Morgan Penny, and Jane Song, who all helped collect and interpret data in this dissertation. I would also like to acknowledge Raji Menon, Dafydd Thomas, Rashmi Chugh, Pingping Qu, Hongwei Wang, Antje Hoering, who all helped collect and interpret patient information and data for these studies.

Many additional thanks to the Medical Scientist Training Program members including Ron Koenig, Ellen Elkin, Laurie Koivupalo, and Hilkka Ketola, as well as Laura Labut and Zaneta Niklovska-Coleska, and Nick Lukacs from Molecular and Cellular Pathology. Thank you for helping me to get through the years smoothly. I am lucky to have been a part of such great programs.

An especially large thank you goes to my committee for always challenging me, providing me with guidance and scientific input. Thank you for meeting with me formally and individually – I have delighted in getting to know you all, and learn from you. Zaneta Nikolovska-Coleska has been especially supportive, and I would also like to thank her for being such a delightful and wonderful role model. A huge shout-out goes to Russ Taichman for his support and mentorship over the last ten (!) years. Thank you for inspiring me and teaching me more than I can express here.

A special note of thanks to my mentor Beth Lawlor – I will be eternally grateful for the opportunity to work in your lab and learn from you, and always will look fondly on these years. The immeasurable amount of scientific and career skills I have learned will

travel with me always, and I cannot thank you enough. On top of all of it all, it has really been so much fun. Thank you for everything!

I would also like to thank my parents Annemarie and Brian Pedersen, whose contribution to this process cannot be described, as well as my twin brother Nick and little sister Christina, who have been my best friends for life. Thank you to my parents-in-law, Chuck and Cindy Schuler, as well as Andrew and Claire Schuler, for not only their unending support but for always providing me with a beautiful place to rest. Thank you to my non-science friends Samantha Krench, Emily Baxter, and Anna James, who have been like family throughout these years.

Finally, a special thank you to my husband Chase Schuler. Thank you for listening, discussing, reading, and debating everything about this process through the years. Thank you for keeping me company in the lab during the odd hours. No, opening the freezer door for me will not get you authorship on my papers. Thank you for supporting me and loving me through everything.

## TABLE OF CONTENTS

Dedication ..... ii
Acknowledgements ..... iii
List of FIgures ..... viii
List of Tables ..... x
List of Abbreviations ..... xi
Abstract ..... xiii
Chapter 1: Introduction ..... 1
Rationale ..... 1
Ewing sarcoma overview ..... 2
Molecular genetics ..... 3
Developmental origins ..... 5
Mechanisms that promote aggressive disease ..... 6
Wnt/beta-catenin signaling ..... 7
Mechanism of signaling ..... 8
Regulation of Wnt/beta-catenin signaling ..... 9
Functions of Wnt/beta-catenin signaling in development and homeostasis ..... 10
Wnt/beta-catenin signaling in cancer ..... 12
Wnt signaling in sarcomas ..... 13
Wnt/beta-catenin signaling in Ewing sarcoma ..... 14
Non-canonical Wnt signaling in Ewing sarcoma ..... 17
Summary ..... 18
Chapter 2: Activation of Wnt/Beta-Catenin Signaling in Tumor Cell Subpopulations Promotes Ewing Sarcoma Progression by Antagonizing EWS/ETS Fusions ..... 19
Abstract ..... 19
Introduction ..... 21
Results ..... 23

The LGR-Wnt/beta-catenin signaling axis is heterogeneously active in Ewing sarcoma tumors in vivo ..... 23
The response of Ewing sarcoma cells to Wnt3a signaling in vitro is heterogeneous ..... 26
RNA profiling identifies novel targets of canonical Wnt-signaling in Ewing sarcoma cells ..... 33
Activation of Wnt/beta-catenin antagonizes EWS/ETS-dependent transcription ..... 37
Wnt/beta-catenin signaling promotes cytoskeleton changes and a migratory and metastatic phenotype ..... 44
Ewing sarcoma tumors with evidence of robust Wnt/beta-catenin activation are associated with a worse clinical outcome ..... 50
Discussion ..... 54
Experimental Procedures ..... 61
Chapter 3: Tenascin C is regulated by Wnt/beta-catenin signaling and promotes ewing sarcoma metastasis ..... 70
Abstract ..... 70
Introduction ..... 72
Results ..... 74
TNC is expressed by Ewing sarcoma cells ..... 74
TNC is regulated by Wnt/beta-catenin signaling in Ewing sarcoma ..... 75
TNC is variably regulated by Wnt/beta-catenin in stem cells and other tumors ..... 78
TNC promotes Ewing sarcoma cell migration and tumorigenicity in vivo ..... 81
TNC promotes in vivo metastasis of Ewing sarcoma cells ..... 83
Discussion ..... 87
Experimental Procedures ..... 91
Chapter 4: Prognostic and Therapeutic Significance of Wnt/beta-catenin signaling in the context of the ewing sarcoma microenvironment ..... 95
Abstract ..... 95
Introduction ..... 97
Results ..... 99
Beta-catenin/LEF1 expression results in poor clinical outcomes ..... 99
LEF1 expression is correlated with a stroma-enriched poor prognostic signature in Ewing sarcoma patients ..... 102
Activation of beta-catenin signaling induces cell spreading and an angiogenic phenotype in ovo ..... 109
Wnt/beta-catenin signaling induces expression of angiogenesis-related genes but does not induce secretion of pro-angiogenic factors ..... 111

Wnt/beta-catenin signaling induces TGF-beta genes ..... 115
Pharmacologic inhibition of RSPO2 does not affect tumor burden but inhibits the incidence of distant metastases ..... 116
Discussion ..... 122
Experimental Procedures ..... 126
Chapter 5: Discussion ..... 132
Introduction ..... 132
Implications for Wnt/beta-catenin biology ..... 135
Implications for Ewing sarcoma pathogenesis ..... 137
Considerations for therapy ..... 141
Concluding remarks ..... 142
References ..... 144

## LIST OF FIGURES

Figure 1.1. 1 Mechanism of Wnt/beta-catenin mediated transcriptional activation. ..... 9
Figure 2.1. Heterogeneous expression of LGR-Wnt-beta catenin ES cells *in vivo*. ..... 25
Figure 2.2. ES cells display heterogeneous response to Wnt stimulation *in vitro*. ..... 28
Figure 2.3. Characterization of Wnt3a timing, specificity, and heterogeneity of ES cells ..... 30
Figure 2.4 Wnt activity is reversible and subpopulations of Wnt-responsive cells are sustained. ..... 32
Figure 2.5 Context-specific targets of Wnt-beta catenin signaling are identified in ES. ..... 35
Figure 2.6 Transcriptional targets of canonical Wnt in ES are enriched for EWS/ETS targets and are inversely correlated. ..... 38
Figure 2.7. Wnt/beta-catenin activation antagonizes EWS/ETS-mediated transrcription of canonical EWS/ETS target genes as well genes involved in mitosis, microtubule cytoskeleton, and the actin cytoskeleton. ..... 40
Figure 2.8. Bi-directional transcriptional antagonism exists between EWS/FLI1 and Wnt-beta catenin signaling. ..... 43
Figure 2.9. Wnt signaling induces beta-catenin-mediated cytoskeleton changes and migration in ES cell lines. ..... 46
Figure 2.10. Activation of Wnt/beta-catenin signaling promotes lung metastasis. ..... 49
Figure 2.11. High *LEF1* expression is associated with poor outcomes in Ewing sarcoma and inversely correlates with EWS/ETS target genes. ..... 52
Figure 2.12. Schematic of heterogeneous RSPO/Wnt-mediated antagonism of EWS/ETS ..... 55
Figure 3.1. Tenascin C is variably expressed in Ewing sarcoma. ..... 75
Figure 3.2 TNC is regulated by Wnt/beta-catenin signaling in Ewing sarcoma ..... 77
Figure 3.3 TNC is expressed and variably induced by Wnt3a CM in stem cells and non-Ewing sarcoma tumors. ..... 80
Figure 3.4 Tenascin C promotes colony formation and migration *in vitro*. ..... 82
Figure 3.5 Tenascin C mediates Wnt-induced migration. ..... 83
Figure 3.6 Tenascin C promotes tumor engraftment and metastatic establishment *in* vivo. ..... 85
Figure 4.1. High LEF1 expression is associated with poor prognostic and stroma-associated genes. ..... 101
Figure 4.2. *LEF1* expression is associated with a poor prognostic signature and high stromal content. ..... 103

Figure 4.3. Beta-catenin activation promotes cell spreading and angiogenesis in the chick chorioallantoic membrane (CAM) assay ..... 110
Figure 4.4. Genes involved in angiogenesis are up-regulated by Wnt/beta-catenin signaling ..... 112
Figure 4.5. CM from Wnt-activated cells does not promote angiogenesis..... 114
Figure 4.6. TGFB2 and TGBR2 are induced by Wnt/beta-catenin signaling. ..... 116
Figure 4.7. The monoclonal antibody against RSPO2 MT130-230 blocks RSPO2-mediated potentiation of Wnt signaling but has no effect on subcutaneous tumor growth. ..... 118
Figure 4.8. Inhibition of RSPO2 does not affect tumor burden but inhibits the number of metastatic nodules in a sub-renal capsule model of metastasis..... 120
Figure 5.1. Model of the downstream effects of activated Wnt/beta-catenin signaling on Ewing sarcoma cells. ..... 135

## LIST OF TABLES

Table 2.1. List of most highly Wnt-responsive transcripts in Ewing sarcoma cells... ..... 36
Table 2.2 Primer sequences used for qRT-PCR ..... 64
Table 3.1. Primer sequences used for qRT-PCR ..... 92
Table 4.1. MSigDB gene signaure enrichment for patients with aggressive disease ..... 105
Table 4.2. MSigDB gene signature enrichment for genes upregulated in patients who experienced long-term survival. ..... 106
Table 4.3. MsigDB gene signature enrichment for genes significantly correlated with *LEF1.* ..... 108
Table 4.4. Primer sequences used for qRT-PCR. ..... 128

## LIST OF ABBREVIATIONS

**APC** adenomatous polyposis coli

**AQuA** Automated quantitative analysis

**CK1** casein kinase 1

**CNC** Cranial neural crest

**CRC** Colorectal carcinoma

**DKK** Dickkopf

**Dsh** Dishevelled

**EMT** Epithelial-to-mesenchymal transition

**EWS/ETS**

**Fz** Frizzled

**GSEA** Gene set enrichment analysis

**GSK3β** glycogen synthase kinase 3 beta

**HUVEC** Human umbilical vascular endothelial cells

**IGF-1** Insulin-like growth factor 1

**IGF-1R** Insulin-like growth factor 1 receptor

**ISH** *In situ* hybridization

**IP** Intraperitoneal

**JNK** Jun amino-terminal kinase

**LEF1** Lymphoid enhancer-binding factor 1

**LSD1** Lysine specific histone demethylase 1

**LGR5** Leucine-rich repeat-containing G-protein coupled receptor 5

**LRP5/6** low-density lipoprotein receptor

**MSC** Mesenchymal stem cell

**MSigDB** Molecular Signatures Database

**NCSC** Neural crest stem cell

**NuRD** Nucleosome remodeling deacetylase

**PcG** Polycomb group

**PCP** Planar cell polarity

**qRT-PCR** Quantitative real-time polymerase chain reaction

**ROR1** Receptor tyrosine kinase-like orphan receptor 1

**RSPO** R-spondin

**SQuISH** Semi-quantitative *in situ* hybridization

**TGF-beta** Transforming growth factor beta

**TGFBR2** Transforming growth factor beta receptor 2

**TNC** Tenascin C

**ZYX** Zyxin

## ABSTRACT

Ewing sarcoma is an aggressive bone and soft tissue tumor with a high propensity for metastasis; however, the mechanisms that contribute to this process are poorly understood. The Wnt/beta-catenin signaling pathway is critical for oncogenesis in numerous cancers, and although previous studies implicate a role for this pathway in Ewing sarcoma, its specific function and contribution is unknown. Previous work by our lab revealed that the Wnt-modulatory receptor LGR5 is highly expressed in patients with aggressive disease, and we hypothesized that LGR5 regulates activation of Wnt/beta-catenin signaling. Through investigation of primary tumors, we discovered that focal nuclear beta-catenin is detectable in a subset of Ewing sarcoma patients and strongly associated with LGR5 expression. Patients whose tumors have nuclear beta-catenin or high expression of the downstream Wnt/beta-catenin target LEF1, experienced worse clinical outcomes and overall survival.

We next used *in vitro* and *in vivo* models to determine the function of Wnt/beta-catenin signaling in Ewing sarcoma. Importantly, we found that LGR5 expression and Wnt activation were highly heterogeneous. We then investigated the downstream effects of Wnt/beta-catenin activation in the most highly Wnt-responsive cells. RNA-sequencing revealed that Wnt/beta-catenin paradoxically inhibits EWS-ETS transcriptional activity, resulting in a phenotypic change from a proliferative to a

migratory and metastatic state *in vitro* and *in vivo*. In addition, the metastasis-associated molecule Tenascin C was upregulated by Wnt/beta-catenin signaling, and was found to be a mediator of migration *in vitro* and metastasis *in vivo*. In the context of the tumor microenvironment, we further found that patient tumors with high Wnt/LEF1 expression had significant correlation with expression of stroma- and angiogenesis-related genes associated with a poor prognosis. Together, these data provide novel avenues of exploration for tumor-microenvironment interactions.

In conclusion these findings implicate a critical role for Wnt/beta-catenin-signaling in mediating migration and metastasis. This occurs in part through antagonism of EWS/ETS fusion protein activity and by up-regulation of the metastasis-associated gene Tenascin C. In addition, tumor-microenvironment interactions modulated by Wnt/beta-catenin further contribute to pathogenesis. Together these findings provide exciting new venues for therapeutic investigation.

# Chapter 1

# Introduction

## Rationale

Ewing sarcoma is an aggressive tumor that most commonly affects children and adolescents and young adults. It has an extremely high propensity to metastasize, and lower survival rates than other pediatric tumors [1]. In particular, patients with primary drug resistance or metastasis often have extremely poor outcomes, and novel therapeutic strategies are required. Ewing sarcoma is characterized by oncogenic EWS/ETS fusion proteins that result from chromosomal translocations, the most common of which is the t(11;22) translocation that encodes the fusion protein EWS/FLI-1 [1]. Although EWS/ETS fusions are the primary oncogenic insult in Ewing sarcoma, the mechanisms that confer particularly aggressive disease remain unclear. Recent evidence suggests that Ewing sarcoma tumors hijack stem cell pathways to promote oncogenesis [2]. Further, we have found that a molecule that regulates Wnt/beta-catenin signaling, namely the Wnt-modulatory stem cell marker LGR5, is highly upregulated in Ewing sarcoma patients with aggressive disease [3]. The Wnt/beta-catenin pathway is a highly conserved and promotes cellular proliferation and stem cell self-renewal during development and in adult stem cells [4]. Wnt signaling plays a major role in the development and progression of numerous tumors [4]; however, the specific

function of this pathway in Ewing sarcoma remains unclear. The aim of this dissertation is to determine the function of the Wnt/beta-catenin signaling pathway in Ewing sarcoma, and elucidate its contribution to tumor pathogenesis.

## Ewing sarcoma overview

Ewing sarcoma is an aggressive, undifferentiated tumor characterized by its small round blue-cell histology and pathognomonic chromosomal translocations that encode chimeric EWS/ETS fusion proteins [1]. The most common site of Ewing sarcoma development is the bone, with the highest prevalence of development in the pelvis (25%), femur (16.4%), and ribs (12%) [1]. Before current treatment regimens, survival for patients with Ewing sarcoma was fatal in 90% of patients. Today, the event free survival rate over 5 years is approximately 75% for patients with localized disease [5]. These advances are largely due to local control by surgery, radiation, and a chemotherapeutic regimen of alternating vincristine, doxorubicin, cyclophosphamide with ifosfamide and etoposide [6]. Despite these life-saving advances in local control, many pediatric patients suffer long-term side effects due to the highly toxic chemotherapy regimen [7]. Further, there has not been similar improvement for treatment of patients who experience metastasis and relapse. Patients who experience metastasis or relapse have an extremely poor prognosis, with only 20% of patients experiencing survival longer than five years [8]. When distant metastases develop, the most common locations are bone, bone marrow, and the lungs[1, 9].Histologically, Ewing sarcoma cells express CD99[10] and exhibit a primitive neuroectodermal phenotype[9], but the exact histogenesis of this tumor remains unknown.

### *Molecular genetics*

EWS-ETS chromosomal translocations are the defining genetic aberration in Ewing sarcoma. The most common translocation t(11;22) (q24,q12) encodes the EWS-FLI1 chimeric fusion protein, and occurs in approximately 85% of Ewing sarcoma tumors. The second most common translocation t(21;22)(q22,q12) encodes the EWS-ERG fusion and occurs in approximately 10-15% of tumors[11]. The remaining tumors express more rare fusions including EWS-ETV1, EWS-ETV4, and EWS-FEV [12]. EWS is a ubiquitously expressed RNA binding protein, and its function in normal homeostasis is not well understood but likely to be involved in RNA processing [13]. The ETS family encodes transcription factors that are involved in regulation of diverse cellular functions including differentiation, cell cycle regulation, and apoptosis, and are frequently involved in oncogenesis [13]. In EWS/ETS fusions, the transactivation domain of EWS is fused in frame to the DNA binding domain of the ETS family protein. This results in direct transcriptional activation which in part mediates its oncogenic effect [14]; however, the EWS/FLI-1 oncogene exerts widespread effects on the epigenome, mediating profound changes in promoters, enhancers, and super-enhancers [15, 16], resulting in extensive effects on gene expression. Important oncogenic genes that that contribute to pathogenesis and that are directly regulated by EWS-FLI-1 include *NKX2.2* [17, 18], *NR0B1*[19, 20], *VRK1 [15]* and *EZH2*[21]. EWS/FLI-1 also functions as a transcriptional repressor, and its function in this capacity is only beginning to become understood, but likely involves displacement of wild type ETS transcription factors from enhancers [15], as well as through direct interaction with LSD1 (lysine specific histone demethylase 1), a component of the nucleosome remodeling deacetylase (NuRD) complex [22, 23].

Important repressed targets of EWS-FLI1 are *TGFBR2* [24, 25], *LOX* [23, 26], and, which have evidence of tumor suppressive functions and repress growth in Ewing sarcoma cells.

` Recent whole-genome profiling studies have shown that few additional recurrent mutations are found in Ewing sarcoma apart from EWS/ETS rearrangements [27-29]. The most common recurrent secondary mutation is in the *STAG2* gene, which occurs in up to 21% of tumors, followed by *CDNK2A* (up to 14%), and *TP53* (7%) [27-29]. Although the majority of these tumors are genetically quiet at the time of diagnosis, with the median number of somatic mutations being 7 per tumor [29], the prevalence of mutations doubles on average after therapy [28]. Interestingly, some patients were found to harbor only the EWS/ETS fusion as a single mutation [28], indicating the EWS/ETS alone is sufficient to promote tumor formation. The paucity of somatic mutation suggests that EWS/ETS fusions are the predominant oncogenic driver of this tumor, and leaves little hope for adaption of personalized medicine where drug selection is guided based on the presence of targetable mutations. Despite this, targeting EWS/ETS fusions themselves is an active area of investigation. EWS/ETS targets are extremely desirable targets for therapy because Ewing sarcoma cells are dependent upon their expression for survival, and they are not expressed in normal tissue [30]. A number of compounds including cytarabine [31], trabectedin [32], and mithramycin [33, 34] have been shown to reverse the EWS/FLI-1 signature, but achieving therapeutic levels without toxicity has been challenging. Mithramycin analogs with improved targeted therapy are currently under investigation [34]. The design of small molecules targeting EWS/FLI-1 has also proven difficult, although the small molecule inhibitor YK-

4-279, which targets protein-protein interactions between EWS/FLI-1 and RNA helicase [35], may yield promising results [36].

### *Developmental origins*

Ewing sarcoma cells are characterized by a lack of obvious histological differentiation and arise in various tissues of the body. As a result, little is understood about the cell-of-origin of this tumor. There is no known precursor lesion, which further contributes to the difficulty in understanding its development. Although it most commonly arises in bone and soft tissues, thus warranting its classification as a sarcoma, Ewing sarcoma tumors have also been reported in epithelial tissues such as the kidney [37], intestine [38], and bladder [39], among other tissues types [40-44]. Further complicating its identity, it was originally classified by James Ewing as an endothelioma due to sheaths of intact blood cells found throughout the tumor [45], which may be caused by vascular mimicry by the tumor cells themselves [46]. Molecular characterization studies have found that Ewing sarcoma tumors express features of mesenchymal stem cells [47], neural crest stem cells [48], and endothelial cells[48]. Taken together, these findings result in the prevailing hypothesis that the cell-of-origin is likely a primitive stem cell with potential to differentiate along both neural and mesenchymal lineages [2]. In line with this observation, both mesenchymal stem cells [49] and neural crest stem cells[50] can tolerate expression of EWS/FLI-1 and undergo oncogenic transformation, despite the fact that EWS/FLI-1 is toxic to most cells [51, 52]. Although transformation can be achieved in stem cells *in vitro,* numerous investigators have unsuccessfully attempted to generate a transgenic mouse model of Ewing sarcoma. Given the highly variable clinical picture of this tumor, it is possible that the

cell-of-origin may vary among individual patients. Further, the EWS/ETS oncogenic mutation might occur at various times during development, in cells with varying degrees of neuro-mesenchymal differentiation. As it follows, the precise timing and specific cellular context that lead to Ewing sarcoma formation remain challenging and enigmatic.

### *Mechanisms that promote aggressive disease*

Advances in local tumor control have improved survival rates for Ewing sarcoma patients; however, for patients who experience upfront chemotherapy resistance, metastasis at diagnosis, or relapse, survival remains dismally low. In particular, the presence of overt metastases at diagnosis is the most significant factor that determines long-term prognosis for Ewing sarcoma patients [8]. Despite this, the mechanisms that mediate metastasis in this tumor remain surprisingly understudied. Because the genome of Ewing sarcoma tumors is largely devoid of mutations apart from EWS/ETS translocations, and EWS/ETS translocations are present in both primary and metastatic tumors, it is unlikely that genetic driver mutations of metastasis alone are account for the metastatic propensity of this tumor. Known mediators of metastatic disease include caveolin [53, 54], ZEB2 [55], CXCR4 [56, 57], and ERBB4 through activation of PI3-AKT-Rac1 [58]. These targets are promising and may likely have actionable therapeutic potential. In addition, emerging evidence suggests that modulation of EWS/FLI-1 activity changes the migratory and invasive potential of Ewing sarcoma cells. In addition to inhibition of proliferation, RNAi-mediated knockdown of EWS/ETS fusions promotes *in vitro* migration and invasion, as well as lung colonization by tumors cells *in vivo* [59, 60]. Up-regulation of critical cytoskeleton genes zyxin (*ZYX*) and alpha-5 integrin [59], which are normally repressed by EWS/FLI-1, in part mediates these effects. This paradoxically

suggests that low EWS/FLI-1 activity or expression levels may contribute to metastatic disease. Despite these findings, the mechanisms by which EWS/FLI1 levels or activity are altered, especially in patients, remain unknown.

## Wnt/beta-catenin signaling

The Wnt/beta-catenin pathway is a complex, evolutionary conserved signaling pathway that is critical for both development and adult tissue maintenance. Wnt ligands initiate a downstream signaling cascade which stabilizes the signaling molecule beta-catenin and results in activation of transcription in association with TCF/LEF transcription factors. Beta-catenin activation is the hallmark of the 'canonical' signaling cascade. There are 19 identified Wnt ligands in mammals, and the cellular response is highly dependent upon the Wnt ligand and context of the signal-receiving cell [61, 62]. Wnt/beta-catenin signaling is essential for normal embryogenesis and contributes to patterning and maintenance of a diverse set of tissues, including but not limited to the bones, intestinal system, skin, teeth, mammary gland, hematopoietic system, brain, and nervous systems. Depending on the cell type, Wnt/beta-catenin-dependent activation of target genes results in proliferation, patterning, migration, and/or self-renewal [63]. Wnt ligands can also activate beta-catenin-independent pathways, which are considered non-canonical Wnt signaling pathways. The best studied of these pathways include (1) Wnt/JNK (Jun amino-terminal kinase) pathway, also known as the planar cell polarity (PCP) pathway, (2) Wnt/Rho GTPase pathway, and (3) Wnt/Calcium pathway [64]. These pathways are important for cellular migration and separation of germ layers during development. Wnt signaling through both beta-catenin dependent and

independent mechanisms result in a large array of important mechanisms required for regulation of many critical cellular behaviors.

### *Mechanism of signaling*

Wnt/beta-catenin signaling is characterized by a signaling cascade that results in nuclear translocation of beta-catenin and transcriptional activation (Fig. 1.1). Briefly, in the absence of Wnt ligands, beta-catenin is sequestered in a destruction complex comprised of glycogen synthase kinase 3 (GSK3), and the scaffolding proteins Axin2 and adenomatous polyposis coli (APC) [4]. Together, these proteins serve to bind and phosphorylate beta-catenin, which targets it for degradation in the proteasome. Wnt signaling is activated when a Wnt ligand such as Wnt1 or Wnt3a engages with the transmembrane receptors frizzed and low-density lipoprotein receptor 5/6 (LRP5/6), which in turn causes the cytoplasmic protein Dishevelled (Dsh) to recruit the destruction complex to the cellular membrane [4]. GSK3-beta along with casein kinase 1 (CK1) then phosphorylate LRP5/6, causing inhibition the destruction complex and thereby resulting in stabilization of beta-catenin [4]. This allows beta-catenin to translocate into the nucleus, where it binds to members of the TCF/LEF family of transcription factors, alleviates transcriptional repression by Groucho/TCF, and results activation of Wnt target genes [4]. Depending on the cell and context, activation of these genes causes numerous responses including stem cell self-renewal, expansion, and lineage determination [63].

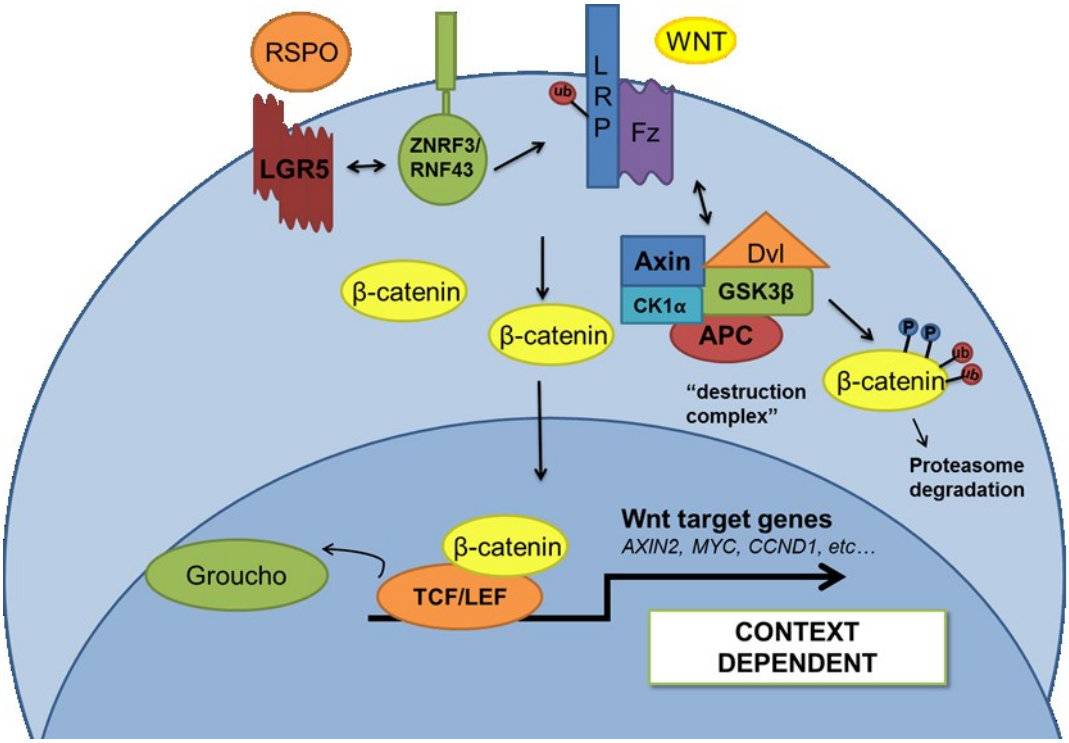


**Figure 1.1 Mechanism of Wnt/beta-catenin mediated transcriptional activation.**

In the absence of Wnt ligands, the destruction complex phosphorylates and ubiquitinates beta-catenin, resulting in proteasomal degradation. When a Wnt ligand associates with the frizzled (Fz)-LRP receptor complex, the destruction complex is recruited and beta-catenin is stabilized in the cytoplasm, resulting in nuclear translocation and association with TCF/LEF family transcription factors. The repressive Groucho/TCF complex is replaced and context-dependent transcription occurs. In the absence of RSPO ligands, transmembrane E3 ubiquitin ligase proteins ZNRF3 or RNF43 ubiquitinate Fz/LRP, which results in internalization and lysosomal degradation of the receptor complex. When RSPO is present and associates with LGRs, ZNRF/RNF and LGR proteins associate and are degraded, thus reducing Fz/LRP turnover, and allowing for potentiation of Wnt/β-catenin signaling.

### *Regulation of Wnt/beta-catenin signaling*

Wnt genes encode cysteine-rich glycoproteins that are secreted over relatively short distances. Wnt ligands require palmitoylation for secretion, and this is accomplished by an O-acyltransferase called Porcupine [65]. In addition to regulation of

secretion, the Wnt pathway can be modulated at the cell surface by a number of exogenous factors. The Dickkopf (DKK) family of proteins interact with the cell surface receptor Kremen, and promote internalization of LRP5/6, thereby inhibiting Wnt signal transduction [66]. The four members (DKK1-4) of this family of proteins are generally thought to be antagonistic of Wnt/beta-catenin signaling, with the exception of DKK2, which has been shown to be both antagonistic and agonistic [67, 68]. In addition, Wnt signaling can be modulated by proteins binding directly to Wnt ligands, such as secreted frizzled-related proteins (sFRPs). These proteins contain a domain that is homologous to the Wnt-binding domain of frizzleds [69]. Recently, it has been elucidated that Wnt signaling can be potentiated by the RSPO/LGR/RNF signaling complex, in which R-spondin (RSPO) ligands associate with the LGR family of membrane-bound receptors [70, 71]. This RSPO-LGR association recruits E3-ubiquitin ligase family members ZNRF3 and RNF43 away from the LRP5/6-frizzeld complex. This thereby stabilizes the membrane Wnt receptor complex, which results in increased and sustained Wnt signaling activity [72, 73] (Fig. 1.1).

### *Functions of Wnt/beta-catenin signaling in development and homeostasis*

During embryogenesis, Wnt/beta-catenin is essential for the development of numerous organ systems [63, 74]. In adult tissues, Wnt/beta-catenin is essential for regulation of intestinal homeostasis[4], and further contributes significantly to hematopoiesis [75] and regulation of hair follicle/ skin homeostasis[76]. The role of Wnt signaling in development homeostasis is broad, so the following introduction will focus on its role in normal cell types most likely to be relevant to Ewing sarcoma.

Wnt signaling plays a critical role in the development and function of the neural crest. The neural crest is a transient embryological structure found only in vertebrates which gives rise to peripheral nervous system structures such as sensory neurons, but also to non-neural cells such as melanocytes, bone, and cartilage. The neural crest arises from the ectoderm along the developing neuraxis at the border of neural and non-neural ectoderm [11]. At this stage, the ectoderm must be patterned, or “induced” into NCSCs. In experiments using model organisms, over-expression of canonical Wnts can induce neural crest formation [12, 13], and inhibition of the Wnt pathway can block induction [14]. After induction, NCSCs undergo an epithelial-to-mesenchymal transition (EMT) where they migrate as undifferentiated progenitors. The process of EMT in the neural crest requires the complex coordination of numerous signals, including Wnt/beta-catenin signaling. When the Wnt pathway is blocked during this process, NCSCs are unable to migrate; however, overexpression of beta-catenin allows cells to regain their ability to migrate [15]. Once NCSCs arrive at their destination, they must differentiate into their ultimate cellular fate. Like other stem cells, NSCS differentiation depends on an intricate milieu of signaling molecules to provide the correct balance of extracellular cues. Correct regulation of beta-catenin is necessary for proper lineage specification [18]. Together these studies indicate that a critical role exists for Wnt/beta-catenin signaling at multiple stages during the transient life of NCSCs.

The function of Wnt/beta-catenin signaling in mesenchymal stem cells (MSCs) and bone homeostasis is highly complex, but may also provide insight toward its role in Ewing sarcoma biology. In the bone, Wnts act as short-range signals, and are likely provided by osterix-positive bone progenitors cells [77]. MSCs reside in the bone marrow and have the capacity to differentiate into osteoblasts, chondrocytes,

myoblasts, and adipocytes. Wnt/beta-catenin signaling is important for allowing MSCs to remain in a self-renewing and proliferating, but undifferentiated state [19]. However, correct levels of endogenous Wnts are critically important for maintenance of this state, as high-doses of canonical Wnt signaling, as well as non-canonical signaling induced by Wnt5a, inhibit MSC proliferation [20, 21]. Wnt signaling further contributes to bone formation through MSC differentiation. Wnt/beta-catenin signaling has been shown to suppress osteogenesis [19], although this is likely dependent on the dose of Wnt3a, since overexpression of Wnt3a or beta-catenin can enhance osteogenesis and chondrogenesis [22, 23]. These studies have been elaborated upon further elsewhere (see [78]), and highlight the complexity of Wnt/beta-catenin regulation and function in bone and MSC homeostasis. Taken together, these studies demonstrate the vastly complex roles of Wnt/beta-catenin signaling in individual systems. The various developmental contexts in which the putative cells-of-origin of Ewing sarcoma may encounter Wnt signals are important, as they may provide insight and critical clues toward understanding the response of these tumor cells to Wnt ligands.

### *Wnt/beta-catenin signaling in cancer*

The best described role for Wnt/beta-catenin signaling in the pathogenesis of cancer is in epithelial cancers, with colorectal carcinoma (CRC) being particularly well-studied. Classically in CRC, a critical component of the beta-catenin destruction complex, often APC, is mutated, allowing constant stabilization of beta-catenin and thus constitutive activation of Wnt target genes. This drives proliferation of the intestinal stem cells, leading to the formation of thousands of adenomas along the intestinal tract, which inevitably transform into carcinomas [79]. CRC can similarly be driven by activating

mutations in beta-catenin [79], as well as newly discovered mutations encoding RSPO2 or RSPO3 fusions that occur in up to 10% of CRC and potentiate Wnt/beta-catenin signaling[80], underscoring the critical importance of this pathway in CRC pathogenesis. Activation of the Wnt signaling pathway has further been implicated in the progression of renal, bladder, prostate, breast, skin, and lung carcinomas [81-84]. In CRC and other epithelial cancers, a significant body of work has shown that activation of the Wnt/beta-catenin pathway leads to tumorigenesis through unchecked stimulation of proliferation [4, 79, 85]. This occurs through up-regulation of Wnt/beta-catenin target genes that mediate the cell cycle progression, such as cyclin D1 [86] and MYC [87]. As a result, significant effort is ongoing toward therapeutically inhibiting the proliferative effects induced by this pathway [88].

### *Wnt signaling in sarcomas*

The role of Wnt signaling in tumors arising in tissues of mesenchymal origin, known as sarcomas, is not straightforward, because Wnt/beta-catenin activation been reported to be both tumor suppressive and oncogenic in sarcomas [64, 89]. Increased Wnt activity is observed in a large proportion of human sarcomas including osteosarcoma, rhabdomyosarcoma, synovial sarcoma, and liposarcoma [89]. Similar to CRC, sarcomas exhibit activating mutations in Wnt/beta-catenin regulatory components, but Wnt/beta-catenin activation also occurs through autocrine stimulation via up-regulation of Wnt ligands [89]. In many types of sarcoma cells, up-regulation of CDC25A by Wnt/beta-catenin results in proliferative phenotypes, yet this is not true of all sarcomas [64]. Like its complex role in normal MSC homeostasis, the effects of beta-catenin in sarcomagenesis are strongly dictated by the degree and type of

mesenchymal lineage specification [64]. Thus, the effects of Wnt/beta-catenin in sarcomas cannot be generalized and should be considered in the context of each tumor type.

### *Wnt/beta-catenin signaling in Ewing sarcoma*

The first evidence for a role for Wnt/beta-catenin signaling in Ewing sarcoma was provided by Uren and colleagues [90], who characterized expression of multiple Wnt ligands and molecules involved in the signaling cascade in Ewing sarcoma cell lines, and showed that Wnt3a induces beta-catenin nuclear localization and a migratory phenotype, suggesting that Wnt3a may influence the metastatic potential of Ewing sarcoma [90]. Further, Wnt3a signaling results in the formation of long cytoplasmic extensions, which lead to investigation of mechanisms that regulate cytoplasmic extensions, or “neurites” that some Ewing sarcoma cells generate in response to Wnt3a [91, 92]. Critical components of both Wnt/beta-catenin and non-canonical Wnt/JNK signaling cascades are necessary for neurite formation [91], however, the functional significance of these structures remains unknown. Intriguingly, the Wnt inhibitor DKK1 also induces neurite formation [91, 93]. Taken together, these studies reveal that factors influencing both Wnt/beta-catenin and non-canonical Wnt signaling pathways may be responsible for neurite formation. Considering that canonical and non-canonical Wnt ligands can antagonize the functions of each other [94], it may be possible that the balance of exogenous Wnt modifying molecules may influence different behaviors in Ewing sarcoma cells. Despite this, the function relevance of these cytoplasmic extensions to Ewing sarcoma pathogenesis remains unknown.

Since these studies, a recently published model of EWS/FLI-1-induced transformation in murine osteochondrogenic progenitors highlighted the Wnt/beta-catenin axis as a key regulator of tumorigenesis [95]. In this study, expression of EWS/FLI-1 in primary murine osteochondrogenic precursor cells resulted in formation of Ewing sarcoma-like tumors. Gene set enrichment analysis (GSEA) and qRT-PCR revealed significant up-regulation of Wnt pathway genes in early tumor formation. Further, these tumors had immunohistochemical evidence of nuclear beta-catenin, and inhibition of tumor formation was achieved through shRNA-mediated silencing of beta-catenin as well as by the beta-catenin inhibitor iCRT14 [95]. Taken together, these data provide the first evidence that Wnt/beta-catenin signaling is essential for *in vivo* oncogenic transformation by EWS/FLI-1.

DKKs have also been implicated in the progression of Ewing sarcoma. Ewing sarcoma cells express low levels of DKK1 [96], but overexpress DKK2 [97, 98]. Ectopic DKK1 but not DKK2 expression inhibits the growth of Ewing sarcoma cells [97]. Recently, Hauer and colleagues confirmed that DKK2 was overexpressed in Ewing sarcoma, and discovered that DKK2 regulates invasion and metastasis through up-regulation of numerous genes including the matrix metalloproteinase MMP1 [98]. The authors suggest that this may be due to activation of Wnt/beta-catenin signaling, although scant evidence was provided [98]. The role of DKK2 and its involvement in Wnt/beta-catenin activation in Ewing sarcoma is in need of further clarification, but initial studies provide intriguing evidence toward a significant role in pathogenesis.

The EWS/FLI-1 fusion protein has been implicated in modulating Wnt activity, however, the data regarding its specific role is not clear. When EWS/FLI-1 was ectopically expressed in heterologous cell types, a strong up-regulation of neural crest-

related genes was observed in addition to a Ewing sarcoma-like phenotype. Of these genes, a large proportion of them are associated with previously described Wnt/beta-catenin as well as non-canonical Wnt target genes [99]. Despite this induction of downstream Wnt genes, no nuclear beta-catenin was observed in these cells. Thus, a subset of the target genes of EWS/FLI-1 may serve to hijack the Wnt signaling genes that drive proliferation during development and contribute to tumorigenesis. In direct contrast to this study, Navarro and colleagues shows that EWS/FLI-1 directly inhibits transcription of Wnt target genes [96]. The proposed mechanism by which this occurs is through EWS/FLI-1 binding to the TCF family transcription factor LEF1. Thus, EWS/FLI-1 may inhibit beta-catenin mediated transcription by interfering with transcriptional co-activators, but may itself directly influence Wnt transcription through its own aberrant transcription factor activity. Further EWS/FLI-1 binds to the DKK1 promoter and inhibits its expression[96], consistent with earlier observations that DKK1 is found at very low levels in Ewing sarcoma and suppress proliferation [97]. Evidence for regulation of DKK2 by EWS/FLI-1 is conflicting, as DKK2 is shown to be regulated both directly [97] and independently [98] of EWS/FLI-1. Together, it is likely that EWS/FLI-1 and Wnt/beta-catenin cross-talk occurs, and EWS/FLI-1 may both activate and repress Wnt-associated genes.

Work by our lab has shown that the stem cell marker LGR5 is heterogeneously expressed by Ewing sarcoma cells, and associated with aggressive disease[3]. Importantly, we showed that RSPO potentiates Wnt/beta-catenin activation through LGR5, and that shRNA-mediated silencing of LGR5 abrogates this effect. Unlike carcinomas, this robust and potentiated Wnt/beta-catenin signaling has no effect on

tumor proliferation[3]. Apart from *AXIN2*, the downstream target genes and phenotypic effects of Wnt/beta-catenin remained unknown.

### *Non-canonical Wnt signaling in Ewing sarcoma*

When Uren and colleagues first characterized expression of Wnt signaling mediators in Ewing sarcoma, it was noted that the prototypical 'non-canonical' Wnt ligands Wnt5a and Wnt11 are expressed by Ewing sarcoma cell lines [90]. Further studies have confirmed Wnt5a and Wnt11 expression in ES [100, 101]. Recently, it was shown that Wnt5a results in up-regulation of CXCR4 through JNK pathway activation, resulting in increased chemotaxis to CXCL12 [101]. Further, ROR1 (Receptor tyrosine kinase-like orphan receptor 1)/Wnt5a signaling has recently been implicated in Ewing sarcoma migration. ROR1 is a member of the ROR family of receptors known to function as Wnt5a receptors and induce PCP signaling [102]. In Ewing sarcoma, ROR1 silencing blocks migration, and may function as a receptor of Wnt5a [103], suggesting another mechanism of Wnt5a-mediated migration. As aforementioned, non-canonical Wnt/JNK signaling has also been implied in neurite extension [91], but relevance of this phenomenon is unclear. Thus, the implications non-canonical Wnt signaling in Ewing sarcoma is only beginning to be explored, and is in need of further characterization.

## Summary

Ewing sarcoma is a highly aggressive disease and novel therapeutic strategies to prevent and treat metastasis are severely needed. The Wnt/beta-catenin signaling pathway is a key regulator of normal development and homeostasis that is frequently deregulated in cancers. Although studies have alluded to a role for Wnt/beta-catenin signaling in Ewing sarcoma pathobiology, few comprehensive studies have been performed, and little clinical evidence has yet been reported to implicate its relevance in disease. The studies that follow in this dissertation set out to establish whether or not there is a role for Wnt/beta-catenin signaling in Ewing sarcoma pathogenesis, and to determine the specific functions and downstream target genes regulated by this pathway. Together, these studies have elucidated a previously unknown role of the Wnt/beta-catenin signaling pathway in Ewing sarcoma biology.

## Chapter 2

## Activation of Wnt/Beta-Catenin Signaling in Tumor Cell Subpopulations Promotes Ewing Sarcoma Progression by Antagonizing EWS/ETS Fusions


### Abstract

Mutations that deregulate Wnt/beta-catenin signaling underlie the pathogenesis of several human cancers, but the role of Wnt/beta-catenin in sarcomas in general, and Ewing sarcoma specifically, is not well understood. We evaluated beta-catenin levels and localization in primary Ewing sarcomas and found evidence of marked intra- and inter-tumor heterogeneity. Further, RNA sequencing studies showed that Wnt/beta-catenin activation is associated with a distinct gene expression signature. Specifically, activation of Wnt/beta-catenin signaling in Ewing sarcoma cells was found to antagonize the transcriptional activity of EWS/ETS fusion oncoproteins. Moreover, activation of Wnt-beta-catenin signaling induced changes in Ewing sarcoma cells that phenocopy effects of EWS/ETS loss-of-function, including actin cytoskeleton changes and transition to a migratory cell state. Further, activation of Wnt/beta-catenin signaling promoted metastatic lung engraftment *in vivo.* The findings suggested that Wnt/beta-catenin activation results in the acquisition of a more aggressive cellular phenotype. These cell-based findings were validated in a cohort of clinically annotated Ewing sarcoma tumors, where high expression of *LEF1* was associated with poor outcome. Moreover, *LEF1* levels in primary patient tumors were significantly correlated with a poor prognosis gene

signature and inversely related to expression of EWS/ETS target genes. Our results reveal a critical role for Wnt/beta-catenin signaling as a key mediator of tumor heterogeneity and disease progression in Ewing sarcoma patients.

## Introduction

Despite in-depth investigations of the role of Wnt signaling pathway alterations in other cancer types, a key functional contribution for Wnt signaling in Ewing sarcoma pathogenesis has yet to be elucidated. Prior *in vitro* studies have shown that Wnt signaling induces morphological changes rather than changes in cell proliferation and/or survival in Ewing sarcoma cells [90]. Consistent with these findings, work by our own group has shown that exposure of Ewing sarcoma cells to canonical Wnt ligands leads to stabilization and nuclear localization of beta-catenin but does not promote cell proliferation [3]. Recent evidence suggests that Wnt activation via DKK2 may contribute to Ewing sarcoma metastasis *in vivo* [98]. In addition, a recently published model of EWS/FLI-1-induced transformation in murine osteochondrogenic progenitors highlighted the Wnt/beta-catenin axis as a key regulator of tumorigenesis [95]. Thus, while the current body of data suggests canonical Wnt/beta-catenin signaling may contribute to human Ewing sarcoma pathogenesis, the specific functions of and downstream target genes regulated by Wnt pathway activation in the context of Ewing sarcoma remain unknown.

In the current work, we investigated whether activation of Wnt/beta-catenin signaling is evident in primary Ewing sarcoma tumors. We defined the transcriptional targets of Wnt/beta-catenin signaling in Ewing sarcoma cells and used *in vitro* models and patient tumors to investigate the biologic and clinical significance of Wnt/beta-catenin activation. Our data show that very significant intra- and inter-tumor heterogeneity exists in Ewing sarcoma with respect to Wnt/beta-catenin activation and that transcriptional and functional antagonism between EWS/ETS fusion proteins and

Wnt/beta-catenin signaling contributes to Ewing sarcoma cell plasticity and tumor progression.

## Results

### *The LGR-Wnt/beta-catenin signaling axis is heterogeneously active in Ewing sarcoma tumors in vivo*

Previous work by our group showed that the R-spondin receptor *LGR5*, which acts to enhance Wnt signaling, is expressed by Ewing sarcoma tumors, and that high levels of *LGR5* are associated with aggressive disease [3]. *LGR5* is a Wnt pathway-regulated marker of intestinal stem cells in the intestine and is often elevated in colorectal cancers [104-106]. Having established that *LGR5* is highly variably expressed between Ewing sarcoma tumors and cell lines [3], we next sought to determine if *LGR5* expression varies at the level of individual Ewing sarcoma cells. We performed *in situ* hybridization (ISH) assays on both Ewing sarcoma cell lines (Fig. 2.1A) as well as tumor biopsies (Fig. 2.1B). Among the cell lines, there was clear evidence of heterogeneity with respect to the total levels of *LGR5* expression, as well as variable numbers of positive and negative cells apparent in the cell lines studied. Likewise, in primary tumors, *LGR5*-positive cells could be detected adjacent to *LGR5*-negative cells (arrows, Fig. 2.1B). In keeping with our prior qRT-PCR-based studies [3], expression of *LGR5* was generally very low in primary tumors, with few to no *LGR5*-positive cells detected. To better quantify *LGR5* expression in primary tumor biopsies we performed fluorescence-based, semi-quantitative ISH (SQUISH) on a tumor tissue microarray (TMA) that contained 58 Ewing sarcoma tumor cores. These studies showed that most of the CD99-positive Ewing sarcoma cells expressed very little to no detectable *LGR5* (Fig. 2.1C). In contrast, a small proportion of tumors were found to contain a large number of *LGR5*-positive cells (Fig. 2.1C). Next, we performed beta-catenin immunofluorescence staining of an adjacent section of the same TMA to

determine if tumors with high expression of *LGR5* also showed evidence of active Wnt/beta-catenin signaling. Using CD99 as a marker of Ewing sarcoma cells and DAPI as a nuclear stain, we observed that a subset of tumors showed strong nuclear beta-catenin nuclear and cytoplasmic staining (Fig. 2.1D). These findings were quantified using AQuA technology (see Methods), which confirmed that only a minority of cases displayed evidence of beta-catenin activation (Fig. 2.1E). Significantly, in the tumor cells, there was a positive correlation between *LGR5* expression and nuclear beta-catenin staining (Fig. 2.1F).

Together these studies confirm that Ewing sarcoma cells express LGR5 and nuclear beta-catenin, providing evidence for activation of the LGR-Wnt/beta-catenin signaling axis. In addition, there is a high degree of tumor cell heterogeneity with respect to both *LGR5* expression and beta-catenin activation, both among tumors and within individual tumor specimens. Further, these studies reveal that tumors with high expression of *LGR5* have increased evidence of beta-catenin activation *in vivo*.

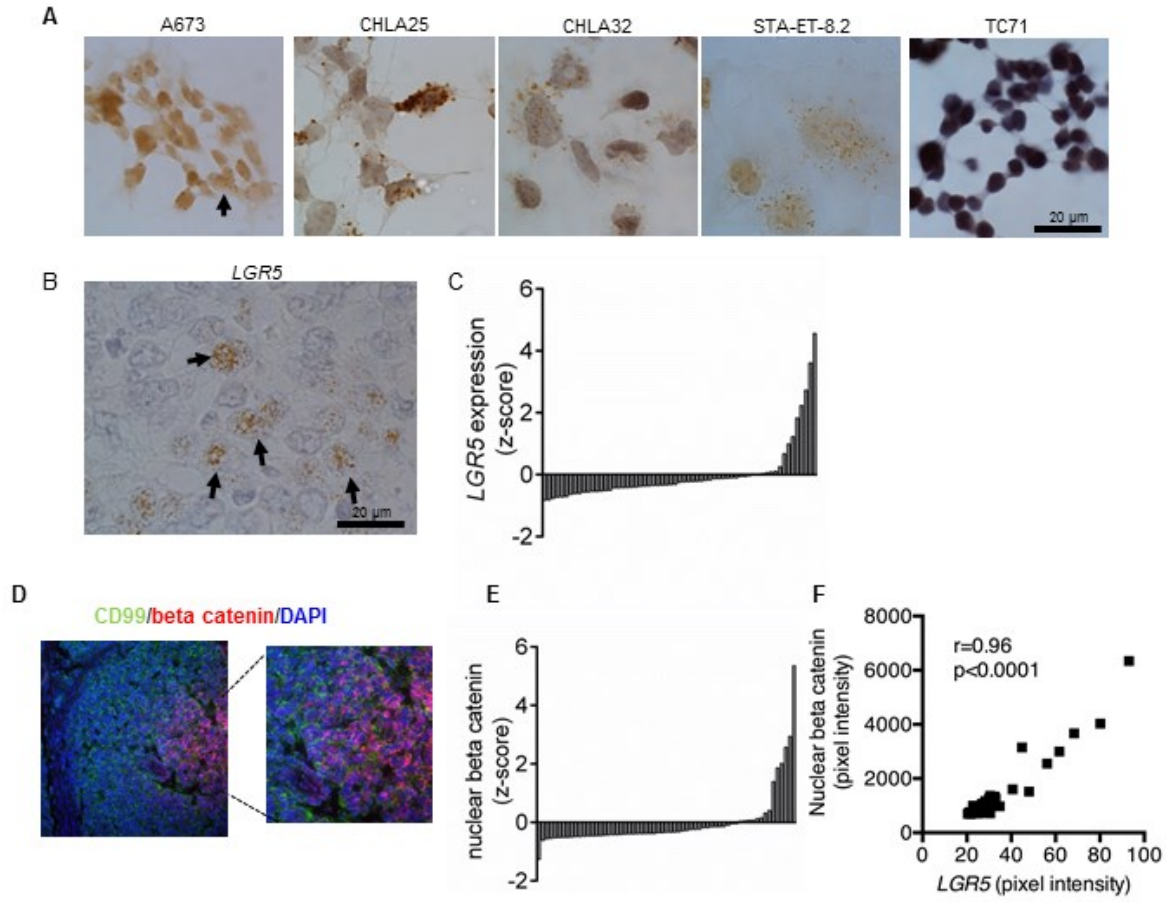


**Figure 2.1. Heterogeneous expression of LGR-Wnt-beta catenin ES cells *in vivo*.**

(A) *In situ* hybridization for *LGR5* was performed on primary ES tumors. A representative *LGR5*-positive tumor is shown. Note marked heterogeneity among individual tumor cells (arrows). Scale bar = 20 μm. (C) Quantification of *LGR5* expression in 52 ES tumors by SQUISH of tumor TMA as described in methods. Data is shown as z-score (z= (sample-mean)/standard deviation). A small number of tumors expressed high levels of *LGR5.* (D) Beta catenin (red) staining of CD99-postive ES cells (green). Note marked heterogeneity of staining within the biopsy (left panel). Beta catenin staining is detected in a subset of nuclei in this representative image of a positive tumor (inset, right). (E) Quantification of nuclear beta-catenin in ES tumors (TMA as in D), as determined by AQUA (see methods). (F) *LGR5* correlates with nuclear beta-catenin *in vivo. r*=Pearson's correlation between *LGR5* (C) and nuclear beta catenin (E) expression in ES tumor biopsies.

### *The response of Ewing sarcoma cells to Wnt3a signaling in vitro is heterogeneous*

To further study the potential significance of the apparently marked intra-tumoral heterogeneity of Wnt/beta-catenin signaling in Ewing sarcoma, we evaluated the response of individual Ewing sarcoma cells to the canonical Wnt ligand, Wnt3a. Sub-confluent cultures of Ewing sarcoma cells were exposed to control L-cell conditioned media (CM) or Wnt3a CM for 48 hr and beta-catenin expression and localization were studied in individual cells by immunocytochemistry. Under control conditions, cytoplasmic and/or nuclear staining for beta-catenin was lacking, and beta-catenin staining was predominately located at the cytoplasmic membrane (Fig. 2.2A). As expected, stimulation with Wnt3a CM led to increased beta-catenin staining in the cytoplasm and the nucleus (Fig. 2.2B). Importantly, however, the response among the cells studied was not uniform. While robust nuclear beta-catenin staining was evident in some cells, little to no increase in beta-catenin staining was observed in other cells (Fig. 2.2B). To determine if this heterogeneous response in beta-catenin stabilization and nuclear localization resulted in heterogeneous activation of Wnt/beta-catenin-dependent transcription, we evaluated Wnt activation in Ewing sarcoma cells that had been modified to express a 7x TCF-promoter/GFP reporter (7TGP) construct. The 7TGP-transduced Ewing sarcoma cells were exposed to L-cell or Wnt3a CM and then flow cytometry was used to measure activation of GFP as readout of Wnt/beta-catenin transcriptional signaling at the level of individual cells. Although all cell lines showed an increase in GFP-positive cells following Wnt3a stimulation (Fig. 2.2C), the responses were highly variable, ranging from <20% of GFP-positive cells in the case of the CHLA32 cell line to nearly 80% GFP-positive cells for TC71 cells (Fig. 2. 2D). Notably,

in all cell lines studied, many cells did not activate the GFP reporter, as evidenced by a failure to induce GFP. In addition, consistent with the variability in LGR5 expression, both within and between cell lines, the LGR5 ligand RSPO2 was able to potentiate the Wnt response in only a subset of cells and was most effective in CHLA25 cells, the cell line with the highest basal expression of *LGR5* [3] (Fig. 2.2D). RSPO2 is highly expressed in both developing [107] and adult [108] bones, and likely to be a key mediator in the Ewing sarcoma microenvironment. Taken together, these data show that individual Ewing sarcoma cells do not respond equivalently to exogenous Wnt ligand and that the heterogeneity of the cellular response is variable in the context of primary tumors *in vivo* as well as cell lines *in vitro*.

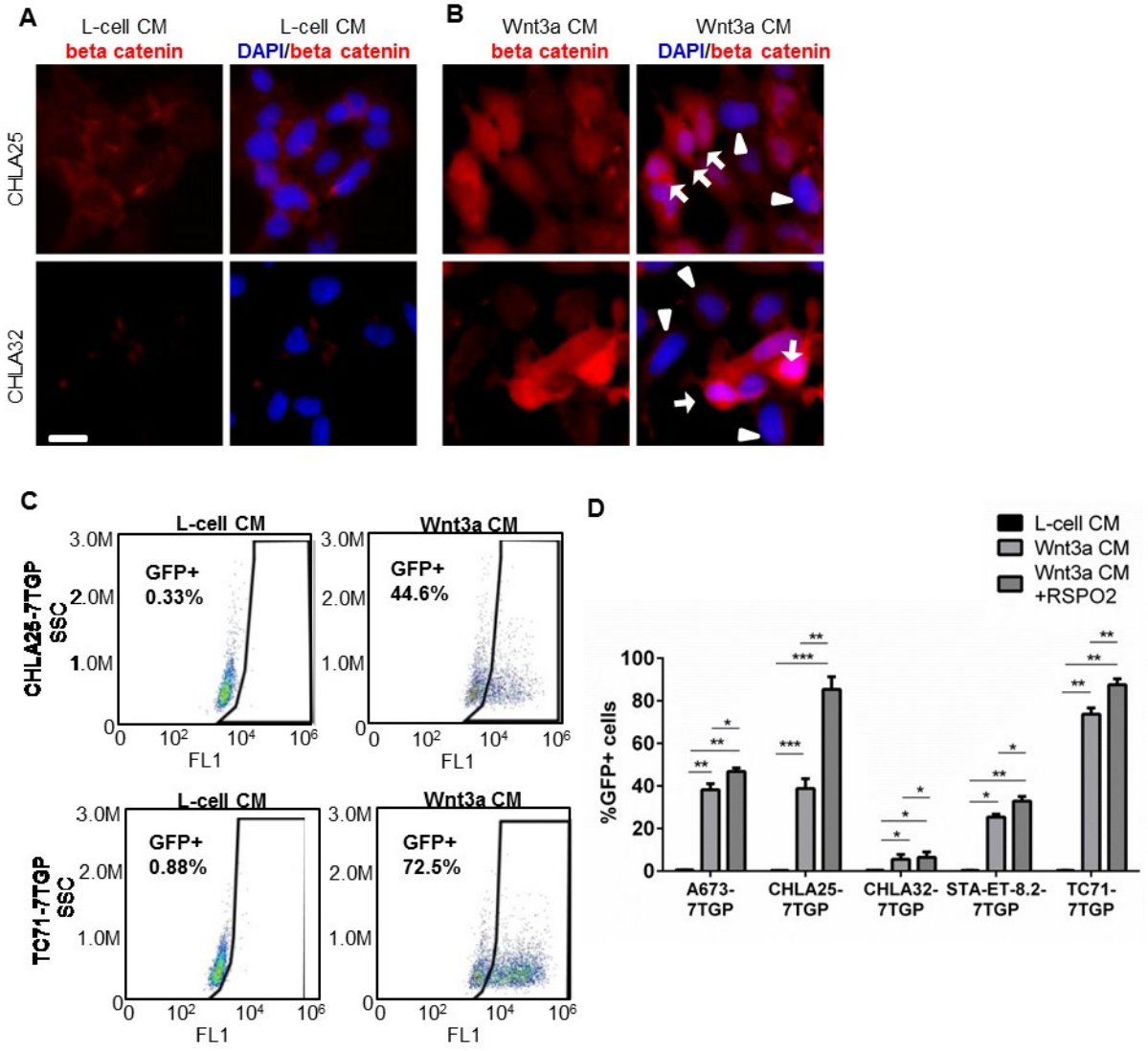


**Figure 2.2. Ewing sarcoma cells display heterogeneous response to Wnt stimulation *in vitro.***

(A) Cultured Ewing sarcoma cells were stained with anti-beta catenin antibody (red) and counterstained with DAPI (blue) 48 hr after exposure to control (L-cell) or (B) Wnt3a conditioned media (CM). Cells were visualized by immunofluorescence microscopy and representative high-power images are shown. Note highly heterogeneous response of cells to Wnt3a stimulation, both between and within cell lines. In particular in (B), cells with strong nuclear localization of beta catenin (arrows) are observed alongside cells with weak nuclear localization (arrowheads). Representative of *n*=3 independent experiments. Scale bars = 20 μm. (C) Ewing sarcoma cell lines were stably transduced with a TCF reporter construct (7xTCF-GFP (7TGP)) and then stimulated with either L-cell, Wnt3a CM, or Wnt3a CM for 48 hr prior to analysis of GFP by flow cytometry. Representative dot plots showing GFP activation are shown. (D) 7TGP-transducedcells as in (C) were exposed to Wnt3a CM, alone or in combination with RSPO2. Flow

cytometry for GFP shows tumor cell heterogeneity with respect to response to both Wnt3a and RSPO2. Quantification of $n$=3 independent experiments (mean ± SEM). Significance was determined using a paired Student's t-test. *$p$<0.05, **$p$<0.01 ***$p$<0.001, ****$p$<0.0001.

To further characterize the response of Ewing sarcoma cells to Wnt ligands, we performed a time course assay using 7TGP reporter cells. Cells were stimulated with CM for 8, 24, and 48 hr, and the percentage of GFP positive cells at each time point was assessed by flow cytometry. As shown in Fig. 2.3A, little GFP positivity was observed after 8 hr, and peak induction of GFP positivity was noted at 48 hr in all cell lines. We next sought to determine the extent to which other ligands induce TCF activity. We observed no induction of reporter activity with RSPO2 alone, Wnt5a CM alone, or with Wnt 5a CM +RSPO2, but robust induction of reporter activity with Wnt3a CM +/- RSPO2 (Fig 2.3B). These results are largely concordant with published literature, as RSPOs do not activate Wnt/beta-catenin activity in the absence of Wnt signals [71], and Wnt5a is a prototypical 'non-canonical' ligand that does not induce Wnt/beta-catenin/TCF signaling in other cell types. Next, we stimulated reporter cells with recombinant Wnt3a and observed a weak, dose dependent induction of 7TGP reporter activity (Fig. 2.3C), verifying that 7TGP reporter activity is specific to Wnt3a. We next tested to see if pharmacological activation of Wnt/beta-catenin signaling induced reporter activity. Using the GSK3-beta inhibitor SB-216763, we observed induction of nearly 100% of cells in both A673 and CHLA25 (Fig. 2.3D). This suggests that Ewing sarcoma cell all have the intracellular beta-catenin signaling machinery required to activate TCF-dependent transcription, and that heterogeneity of Wnt responsiveness likely occurs at the level of Wnt receptors.

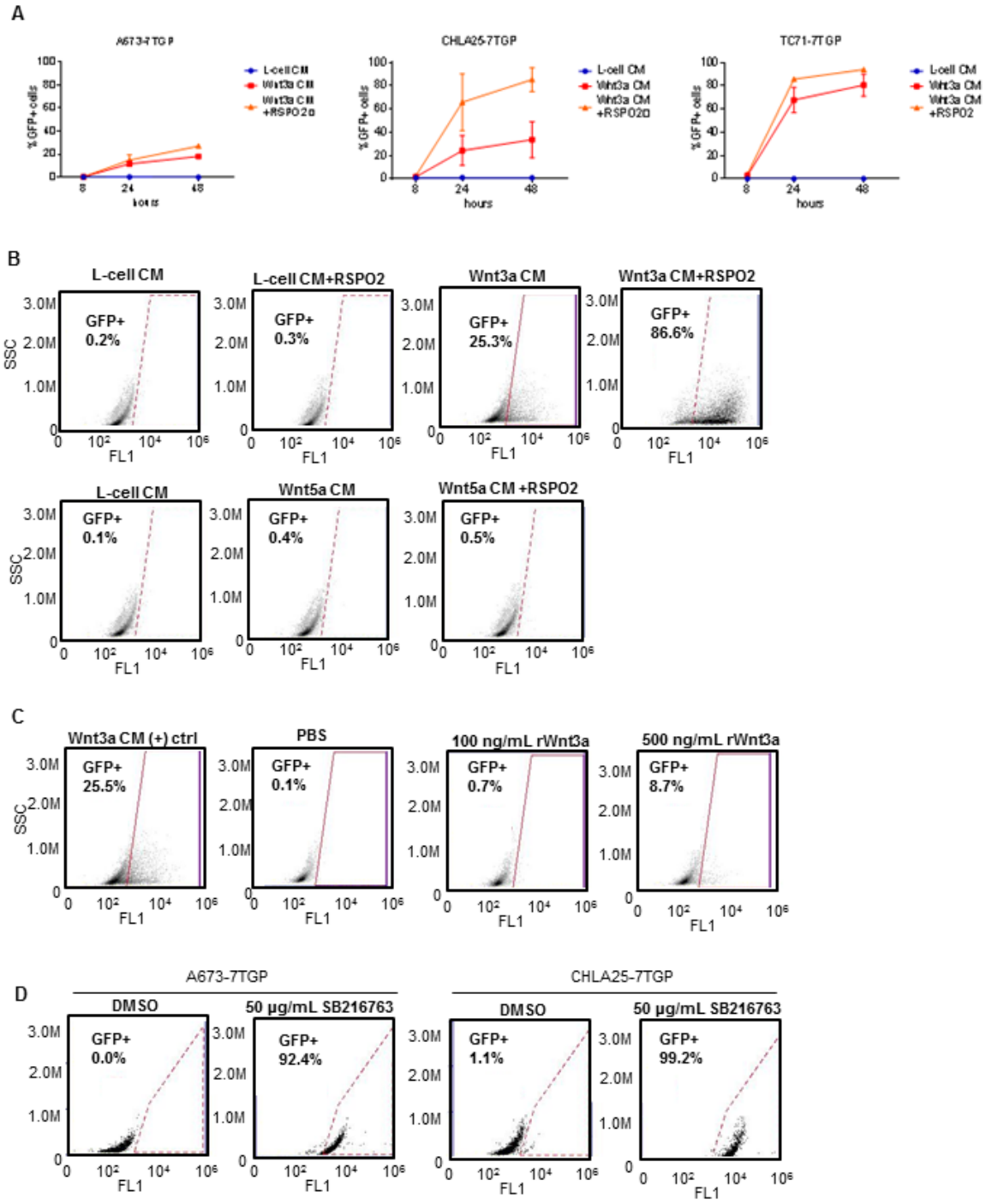


**Figure 2.3. Characterization of Wnt3a timing, specificity, and heterogeneity of ES cells.**

(A) 7TGP cell lines were stimulated with L-cell, Wnt3a CM, or Wnt3a CM for 8, 24, or 48 hr prior to analysis of GFP by flow cytometry. The average percent of GFP-positive cells at each time point is shown. In all three cell lines tested, peak %GFP+ induction was achieved at 48 hr. (B) CHLA25-7TGP cells were exposed to Wnt3a CM, Wnt5a CM, and/or RSPO2 for 48 hr. RSPO2 alone and Wnt5a do not induce 7TGP reporter activity.

(C) A673-7TGP cells were exposed to Wnt3a CM as a positive control, and conditions of either PBS, 100 ng/mL, or 500 ng/mL recombinant Wnt3a (rWnt3a). Stimulation with rWnt3a induces 7TGP reporter activity, although to a lesser extent that Wnt3a CM. (D) A673-7TGP (left two panels) and CHLA25-7TGP were stimulated for 24 hr with 0.1%DMSO as vehicle control or 50 μg/ml SB216763, a GSK3-beta inhibitor and activator of Wnt/beta-catenin activity. Over 90% of cells activated the reporter in both cell lines, indicating that the response to this chemical is not heterogeneous.

Having established that Wnt3a CM heterogeneously activates TCF-dependent transcription, we next sought to determine the extent to which subpopulations are sustained. First, A673-7TGP cells were stimulated with CM as previously described, and sorted on the basis of reporter activity. Specifically, the top 10% of GFP-positive cells and the bottom 10% of GFP-negative cells were isolated using fluorescence activated cell sorting (FACS). Cells stimulated with L-cell CM were run through the flow cytometer as a control, but were not sorted. Cells were then re-plated and maintained in culture. After one week, each isolate of cells was re-stimulated with CM and reporter activity was determined by flow cytometry. Cells originally stimulated with L-cell CM had few GFP+ cells upon re-stimulation with L-cell CM, and 16.4% and 32.7% GFP-positive cells following exposure to Wnt3a CM and Wnt3a CM+RSPO2, respectively (Fig. 2.4A). These percentages were consistent with percentages observed at the time of initial stimulation (data not shown). Interestingly, in cells initially stimulated with Wnt3a CM (Fig. 2.4B) or Wnt3a CM +RSPO2 (Fig. 2.4C), the originally non-responsive cells (lowest 10% GFP+) were responsive to Wnt ligands after one week, albeit weaker than unsorted. Cells that were originally Wnt responsive (highest 10% GFP+) reverted back to negligible Wnt activity after one week as seen by little reporter activity in L-cell CM re-stimulation conditions. These cells, however, were more Wnt responsive than unsorted cells, and this effect was even more dramatic in cells that were exposed to RSPO2 (Fig. 2.4C). Taken together, these data suggest that subpopulations of highly Wnt-responsive

and weakly Wnt-responsive cells exist in standard tissue culture conditions, and that these subpopulations remain respectively enriched in culture for at least one week.

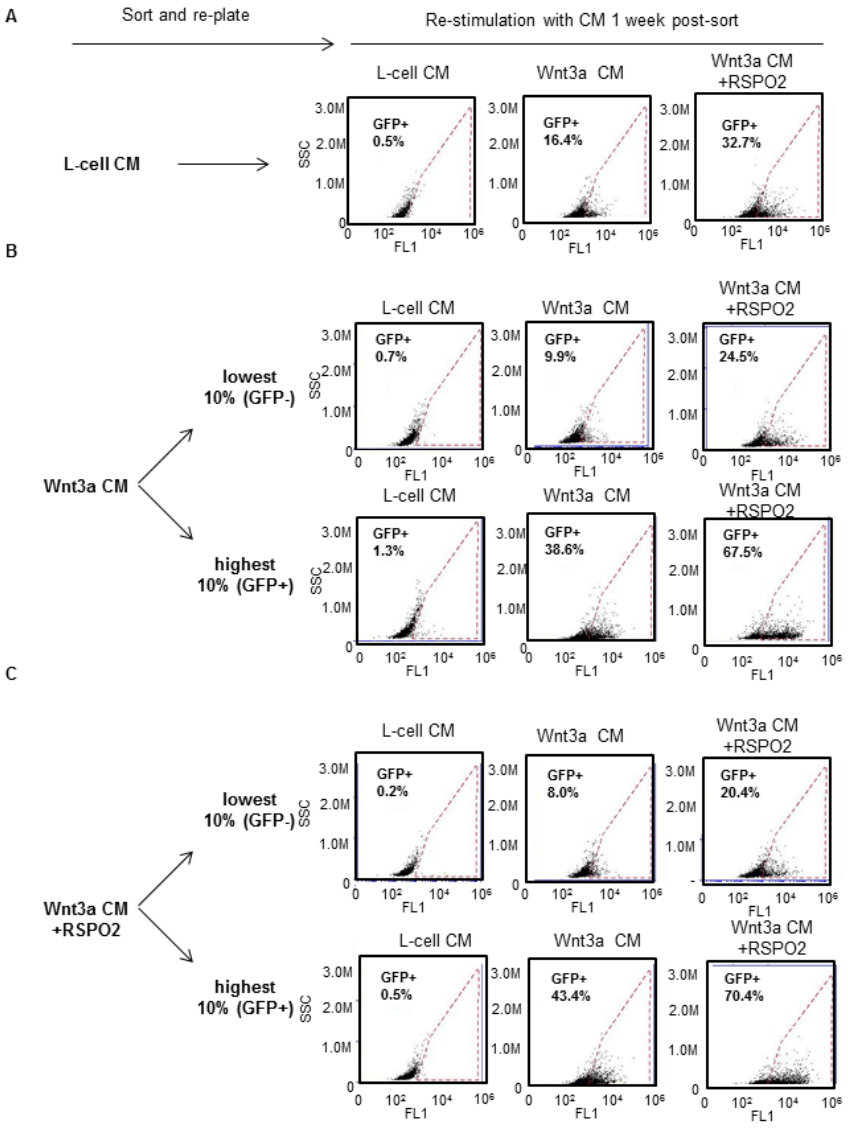


**Figure 2.4 Wnt activity is reversible and subpopulations of Wnt-responsive cells are sustained.**
(A)A673-7TGP cells were stimulated for 24 hr with L-cell CM, Wnt3a CM, or Wnt3a CM+RSPO2. Cells were sorted into the top 10% of most Wnt-responsive, GFP-positive cells (10% GFP+) and bottom 10% of least Wnt-responsive, GFP-negative cells (10% GFP-) and re-plated, and allowed to grow in standard tissue culture conditions for one week. After one week, cells were re-stimulated for 24 hr with either L-cell CM, Wnt3a CM, or Wnt3a CM+RSPO2, and flow cytometry analysis was performed. (A) As

expected, cells that were initially stimulated with L-cell CM and re-plated heterogeneously induce GFP expression in response to Wnt3a CM, and this is potentiated upon addition of RSPO2. (B) Cells that were initially stimulated with Wnt3a CM and sorted responded differentially to re-stimulation. Non-responsive (bottom 10% GFP-) cells were less responsive than unsorted cells (A) or their top 10% GFP- counterparts. Highly Wnt-responsive cells (top 10% GFP+) were more responsive to Wnt ligands than unsorted cells in panel A. (C) Cells that were initially stimulated with Wnt3a CM +RSPO2 reveal a similar but even more dramatic pattern of responsiveness compared to cell in (B). Notably, under all sorted conditions, little to no Wnt activity was maintained after 1 week in standard culture conditions, indicating that cells revert back to a Wnt-OFF state in the absence of ligands.

### *RNA profiling identifies novel targets of canonical Wnt-signaling in Ewing sarcoma cells*

The function of Wnt signaling in development and disease is highly context-dependent. To study further the role of canonical Wnt signaling in Ewing sarcoma, we performed experiments to define downstream transcriptional targets of Wnt/beta-catenin signaling in Ewing sarcoma cells. First, we used qRT-PCR to determine if Wnt3a, alone or in combination with RSPO2, modulates the expression of genes that were previously established to be canonical Wnt targets in other cell types. Interestingly, although the well-known Wnt/beta-catenin target gene *AXIN2* was reproducibly induced in all Ewing sarcoma cell lines by Wnt3a and Wnt3a plus RSPO2 treatment, other reported target genes showed no change in expression, including *C-MYC*, *CDC25A*, and *CCND1* (Fig. 2.5A). We next used RNA-sequencing to define, in an unbiased manner, downstream transcriptional targets. We used CHLA25 cells stably transduced with the 7TGP reporter gene and FACS of GFP-expressing cells to isolate the most highly-Wnt responsive cells. We compared gene expression between high GFP-expressing cells and unstimulated control cells (Fig. 2.5B). Expression of over 1,000 transcripts was altered by Wnt3a alone or by Wnt3a plus RSPO2, with slightly more genes being up-regulated

than down-regulated by either treatment (Fig. 2.5C). Analysis of the RNA-seq data indicated that numerous previously described Wnt/beta-catenin target genes were not induced by Wnt3a or Wnt3a plus RSPO2 treatment even in robustly Wnt-responsive cells (Fig. 2.5D). Besides *AXIN2*, we did find that two established Wnt target genes, *LEF1* and *NKD1,* were among genes most responsive to Wnt3a or Wnt3a plus RSPO2 (Fig. 2.5D and E). Genes for which expression was up-regulated more than two-fold by Wnt3a alone and more than ten-fold by Wnt3a plus RSPO2 are listed in Table 2.1. The RNA profiling studies of Wnt and Wnt plus R-spondin activated genes in Ewing sarcoma identified only a few known and many novel, transcriptional targets of the Wnt/beta-catenin signaling axis.

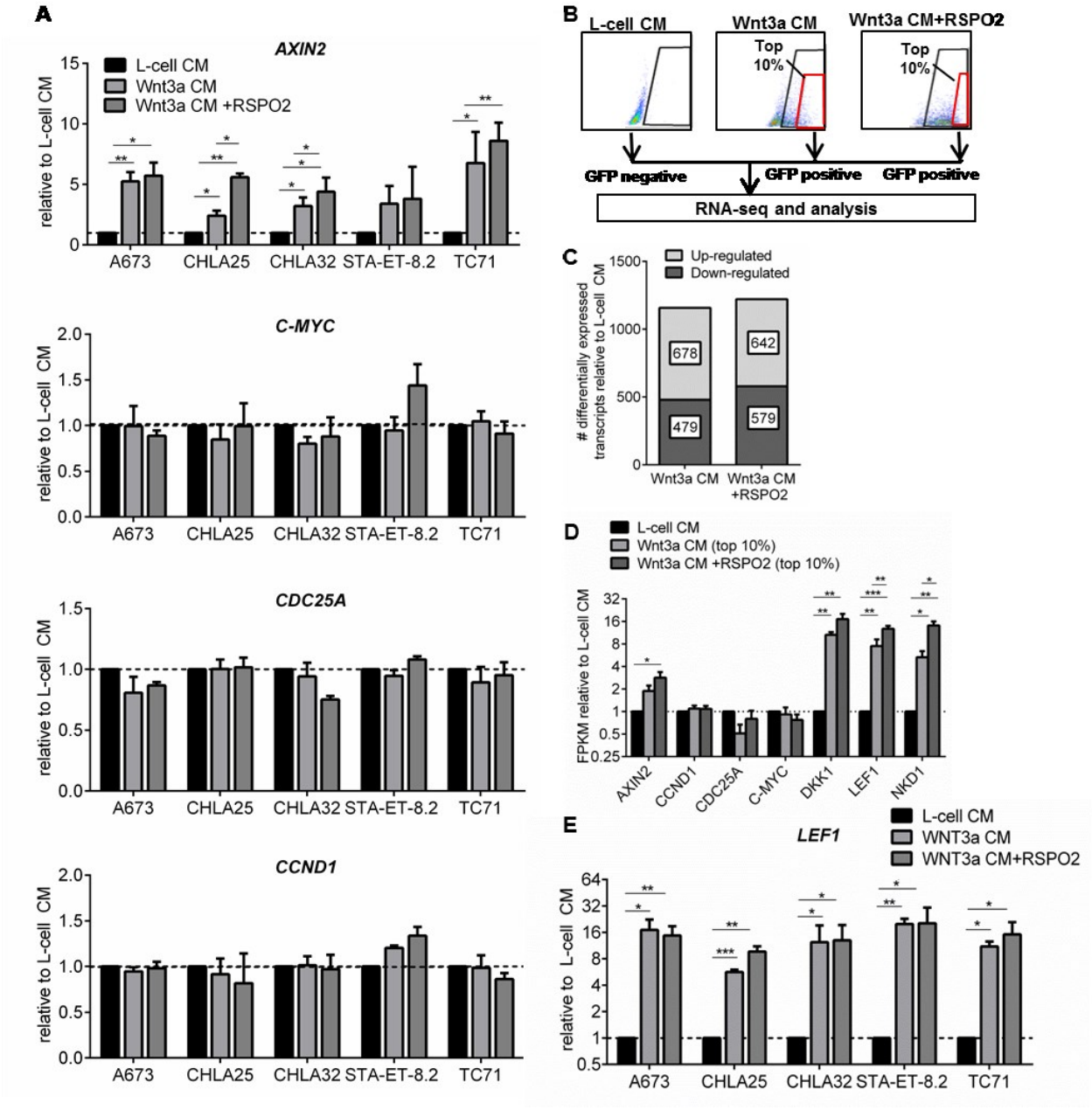


**Figure 2.5 Context-specific targets of Wnt-beta catenin signaling are identified in Ewing sarcoma.**

(A) qRT-PCR was performed on cells exposed to L-cell CM, Wnt3a CM, or Wnt3a CM+RSPO2 for 24 hr to assess induction of canonical Wnt target genes *AXIN2, CMYC, CDC25A,* and *CCND1*. Mean ± SEM relative to L-cell CM expression in *n=3* independent experiments. (B) CHLA25-7TGP cells were exposed to conditions as in (A) and FACS-sorted on the basis of GFP. (C) Over 1000 genes were significantly regulated *(p*<0.05) compared to L-cell controls for Wnt3a and Wnt3a+RSPO2 conditions. (D) RNA-seq data validates induction of *AXIN2, DKK1, LEF1* and *NKD1* but

an absence of induction of other known canonical target genes identified in other cell types. (E) qRT-PCR validation of *LEF1* induction in multiple Ewing sarcoma cell lines.

| Transcript ID | Gene symbol | Fold change Wnt3a | Fold change Wnt3a+RSPO2 |
|---|---|---|---|
| **ENST00000440284** | ACSM3 | 12.6 | 40.5 |
| **ENST00000397137** | BLCAP | 12.7 | 21.4 |
| **ENST00000378615** | C11orf49 | 9.3 | 15.4 |
| **ENST00000592872** | C19orf25 | 9.8 | 13.0 |
| **ENST00000274368** | CRHBP | 14.2 | 20.0 |
| **ENST00000510508** | DIO3 | 32.2 | 67.9 |
| **ENST00000373970** | DKK1 | 7.7 | 13.6 |
| **ENST00000344257** | GAD1 | 6.7 | 13.7 |
| **ENST00000429473** | GNGT1 | 13.3 | 20.6 |
| **ENST00000391588** | KRTAP3-1 | 13.0 | 19.8 |
| **ENST00000379951** | LEF1 | 6.5 | 11.6 |
| **ENST00000438313** | LEF1 | 9.1 | 11.9 |
| **ENST00000323851** | NDRG1 | 8.6 | 11.1 |
| **ENST00000397853** | NDRG2 | 8.9 | 11.9 |
| **ENST00000268459** | NKD1 | 4.6 | 12.9 |
| **ENST00000361478** | PJA1 | 37.3 | 44.3 |
| **ENST00000436066** | PLEKHF1 | 14.3 | 21.3 |
| **ENST00000338415** | QPCT | 5.6 | 10.0 |
| **ENST00000399409** | RABGGTA | 12.8 | 15.5 |
| **ENST00000586686** | RPS15 | 10.1 | 11.9 |
| **ENST00000373068** | SLC25A25 | 11.9 | 17.9 |
| **ENST00000397517** | STK24 | 13.7 | 20.7 |
| **ENST00000222543** | TFPI2 | 8.1 | 16.1 |
| **ENST00000350763** | TNC | 4.1 | 10.5 |
| **ENST00000367315** | TNNT2 | 13.0 | 16.0 |
| **ENST00000376368** | WDR45 | 8.8 | 10.3 |

**Table 2.1. List of most highly Wnt-responsive transcripts in Ewing sarcoma cells.**

List of 26 transcripts (encoding 25 unique genes) that were significantly induced at least 2-fold following Wnt3a and more than 10-fold following exposure to both Wnt3a and RSPO2.

### *Activation of Wnt/beta-catenin antagonizes EWS/ETS-dependent transcription*

To gain further insight into the Ewing sarcoma-specific Wnt/beta-catenin transcriptional profile, we determined the extent of overlap between the identified target genes and previously published gene datasets in the Molecular Signatures Database (MSigDB) [109]. Strikingly, genes that were induced two-fold by Wnt3a plus RSPO2 in Ewing sarcoma overlapped most significantly with genes that are repressed by EWS/FLI-1 in Ewing sarcoma cells [20] (Fig. 2.6A). Conversely, genes that were repressed 2-fold by Wnt3a plus RSPO2 overlapped most significantly with genes that are up-regulated by EWS/FLI-1 (Fig. 2.6B). To further understand this potential inverse relationship between Wnt/beta-catenin and EWS/FLI-1, we next evaluated the entire list of genes regulated by Wnt3a plus RSPO2, ranked by log-fold change in gene expression, using gene set enrichment analysis (GSEA). GSEA confirmed that published EWS/ETS-induced and EWS/ETS-repressed targets were among the most the significantly correlated gene sets. Specifically, expression of genes that were altered by Wnt3a plus RSPO2 significantly and directly correlated with genes that are down regulated by EWS/FLI-1 (Fig. 2.6C top), and inversely correlated with genes that are up regulated by EWS/FLI-1 (Fig. 2.6C, bottom). These same genes were similarly correlated with EWS/ERG-regulated genes (Fig. 2.6D), indicating this antagonistic relationship extends beyond EWS/FLI-1 to include other EWS/ETS fusions. Thus, genes that are regulated by canonical Wnt signaling in Ewing sarcoma are enriched and inversely correlated with genes that are regulated by EWS/ETS fusions.

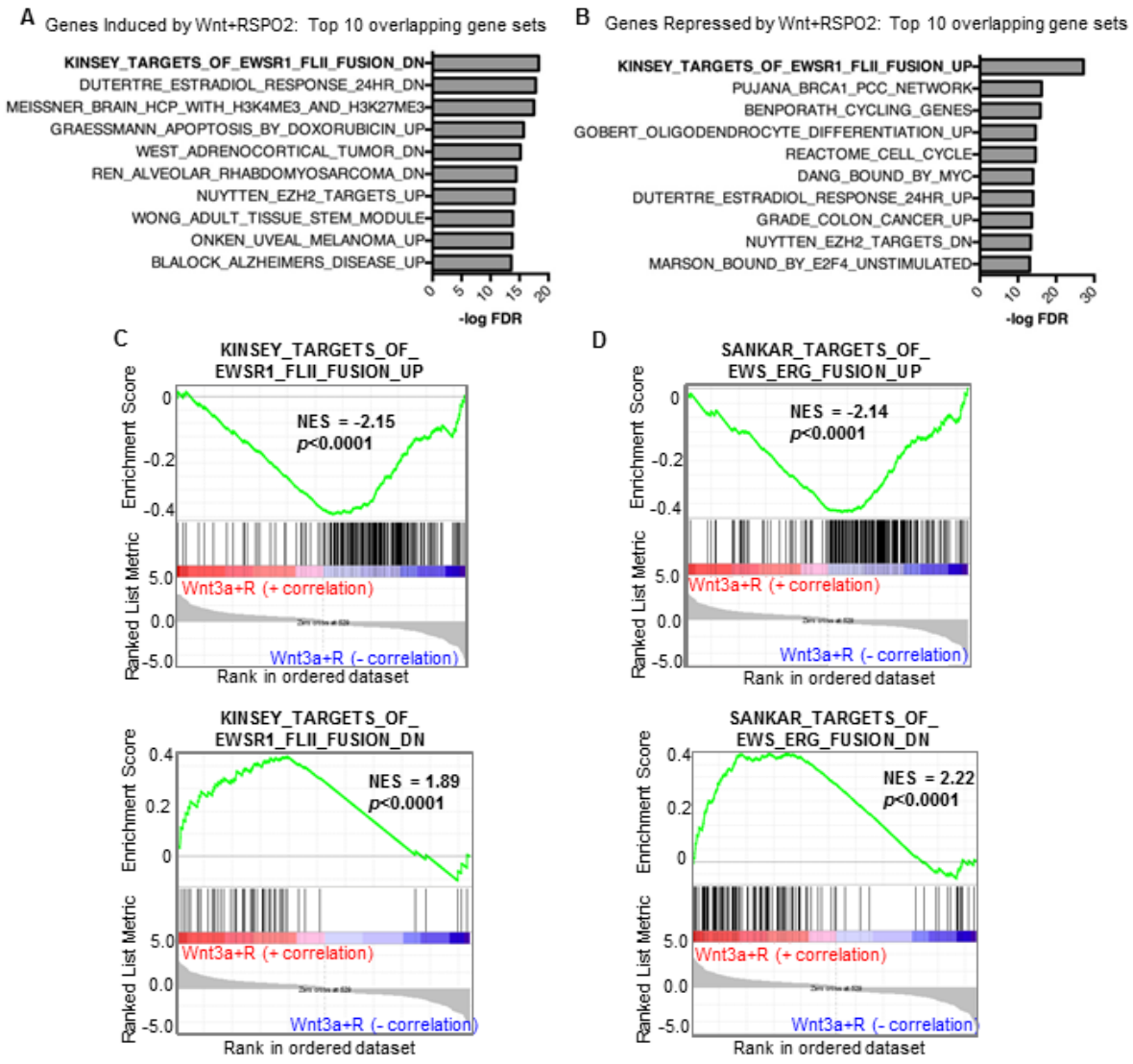


**Figure 2.6 Transcriptional targets of canonical Wnt in ES are enriched for EWS/ETS targets and are inversely correlated.**

Molecular signatures database analysis of genes that were significantly induced (A) or repressed (B) at least 2-fold following stimulation with Wnt3a + RSPO2. Top 10 most significantly overlapping gene sets are shown ranked by –log FDR. Rank-ordered gene set enrichment analysis (GSEA) of 1146 genes identified to be significantly modulated in CHLA25 cells by Wnt3a CM+RSPO2 showed a significant inverse relationship between Wnt target genes and EWS-ETS target genes. (C) Comparison of Wnt targets to EWS/FLI1 target genes. (D) Comparison of Wnt targets to EWS/ERG target genes. Wnt target genes in each case were rank-ordered on the basis of fold change and compared to published datasets. NES indicates the normalized enrichment score.

Upon more in-depth analysis of the observed antagonism of the EWS/ETS signature, we noted that there was incomplete overlap between the gene sets (Fig. 2.7A) and that the extent of Wnt/beta-catenin-dependent modulation of individual EWS/ETS target genes was highly variable (Fig. 2.7B). To understand the nature of the Wnt/beta-catenin response we focused our functional analyses on the identified set of 236 co-regulated genes. Hierarchical clustering of these genes showed a clear segregation between Wnt/beta-catenin-induced and –repressed genes and confirmed both the opposing pattern of regulation by EWS/FLI1 and the potentiating effect of RSPO2 on gene modulation (Fig. 2.7C). Gene ontology analysis of the overlapping genes revealed that cell cycle and mitosis genes were most prominent among EWS/FLI1- induced genes that were repressed by Wnt/beta-catenin while actin cytoskeleton and adhesion genes that are normally repressed by EWS/FLI1 were induced in Wnt/beta-catenin activated cells (Fig. 2.7C). In addition, although cell cycle genes were classified to be the most highly enriched category among Wnt/beta-catenin-repressed EWS/FLI1 targets, it is noteworthy that many of these genes encode for proteins that regulate the biomechanics of mitotic cell division including sister chromatid segregation (e.g. aurora kinases) and microtubule cytoskeleton structure and function (e.g. kinesins) (Fig. 2.7D). Thus, activation of beta-catenin in Ewing sarcoma cells partially antagonizes EWS/ETS transcriptional activity and results in altered expression of key regulators of actin and microtubule cytoskeleton structure and function.

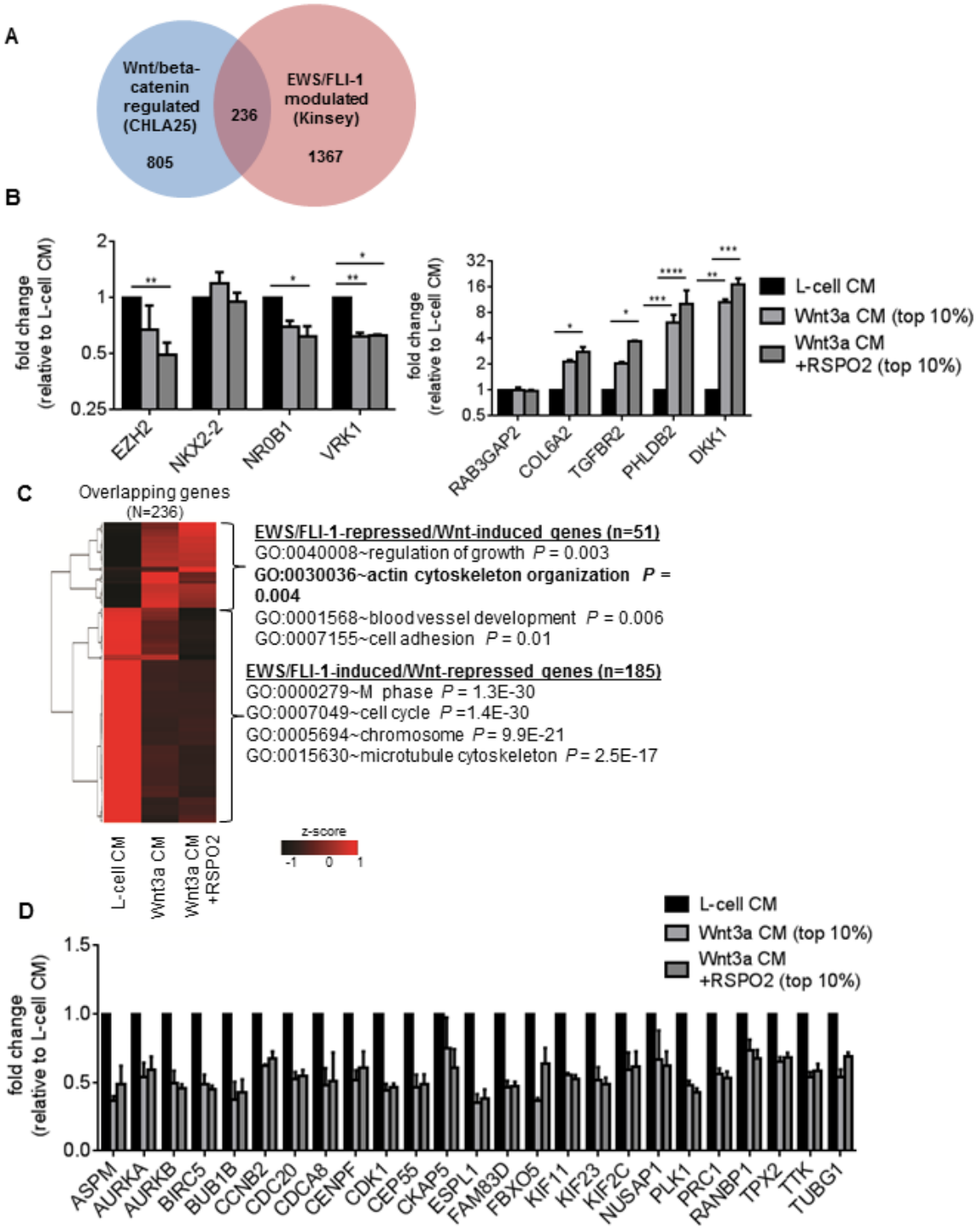


**Figure 2.7. Wnt/beta-catenin activation antagonizes EWS/ETS-mediated transcription of canonical EWS/ETS target genes as well genes involved in mitosis, microtubule cytoskeleton, and the actin cytoskeleton.**

(A) Overlap between published EWS/FLI-1 target genes and Wnt/beta-catenin regulated genes in Ewing sarcoma. (B) Expression of EWS/ETS-induced (left panel) and

EWS/ETS-repressed (right panel) genes is oppositely regulated by Wnt/beta-catenin activation but not all EWS/ETS genes are equally impacted. FPKM data shown as fold change. *$p$<0.05, **$p$<0.01, ***$p$<0.001, ****$p$<0.0001.(C) Hierarchical clustering of gene expression of 236 overlapping genes from (A). Gene ontology analysis shows that genes involved in cytoskeleton organization and adhesion are significantly enriched among Wnt/beta-catenin induced genes. Conversely, genes involved in proliferation and mitosis are among Wnt/beta-catenin repressed genes. (D) EWS/ETS-induced cytoskeleton and microtubule genes are repressed by Wnt/beta-catenin activation. FPKM data shown as fold change relative to L-cell CM control.

Given the striking inverse correlation between expression of Wnt/beta-catenin and EWS/ETS transcriptional targets, we investigated whether activation of the Wnt/beta-catenin axis resulted in transcriptional repression of EWS/ETS fusions themselves. Although EWS/ETS transcript levels were largely unchanged by Wnt/beta-catenin activation, levels of expression did decrease in a dose-dependent manner in the most highly Wnt-responsive cells, TC71 (Fig. 2.8A). This raised the possibility that highly Wnt-responsive cells may down-regulate EWS-ETS fusions in response to Wnt/beta-catenin activation. To test this hypothesis, we measured expression of EWS/ETS transcripts in 7TGP-transduced reporter cells that had been sorted to isolate the most highly GFP-positive cells. Interestingly, this analysis showed reduced expression of the fusion transcript in the most responsive cells in all three EWS/FLI-1 expressing cell lines, albeit to varying degrees (Fig. 2.8B). In contrast, levels of EWS/ERG transcript were unchanged in CHLA25 cells (Fig. 2.8B). Thus, the dramatic changes in EWS/ETS target gene expression that occur downstream of Wnt in Ewing sarcoma cells are unlikely to be mediated by down-regulation of EWS/ETS fusions themselves.

Having shown that activation of Wnt/beta-catenin inhibits the transcriptional activity of EWS/ETS fusions, we next tested whether the inverse is also true – i.e. do

EWS/ETS fusions inhibit Wnt/beta-catenin? To test this we used A673 cells that stably express an inducible EWS/FLI-1 knockdown shRNA (shA673-1C) [47]. Exposure of these cells to doxycycline led to both reduced *EWS/FLI-1* transcript expression as well as reduced expression of the canonical EWS/FLI-1 target gene, *NR0B1* (Fig. 2.8C). To determine if loss of EWS/FLI-1 impacted Wnt responsiveness, we transduced shA673-1C cells with a 7xTCF-luciferase (7TFP) reporter of Wnt activity [110], and then stimulated cells with Wnt3a in the presence or absence of doxycycline. Cells with reduced expression of EWS/FLI-1 demonstrated a more than two-fold increase in TCF reporter activity in response to Wnt3a compared to control cells (Fig. 2.8D). Likewise, induction of Wnt target genes, *AXIN2, LEF1,* and *NKD1* was significantly enhanced following EWS/FLI-1 knockdown (Fig. 2.8D). Thus, these data indicate that transcriptional antagonism between Wnt/beta-catenin and EWS/ETS signaling is bi-directional.

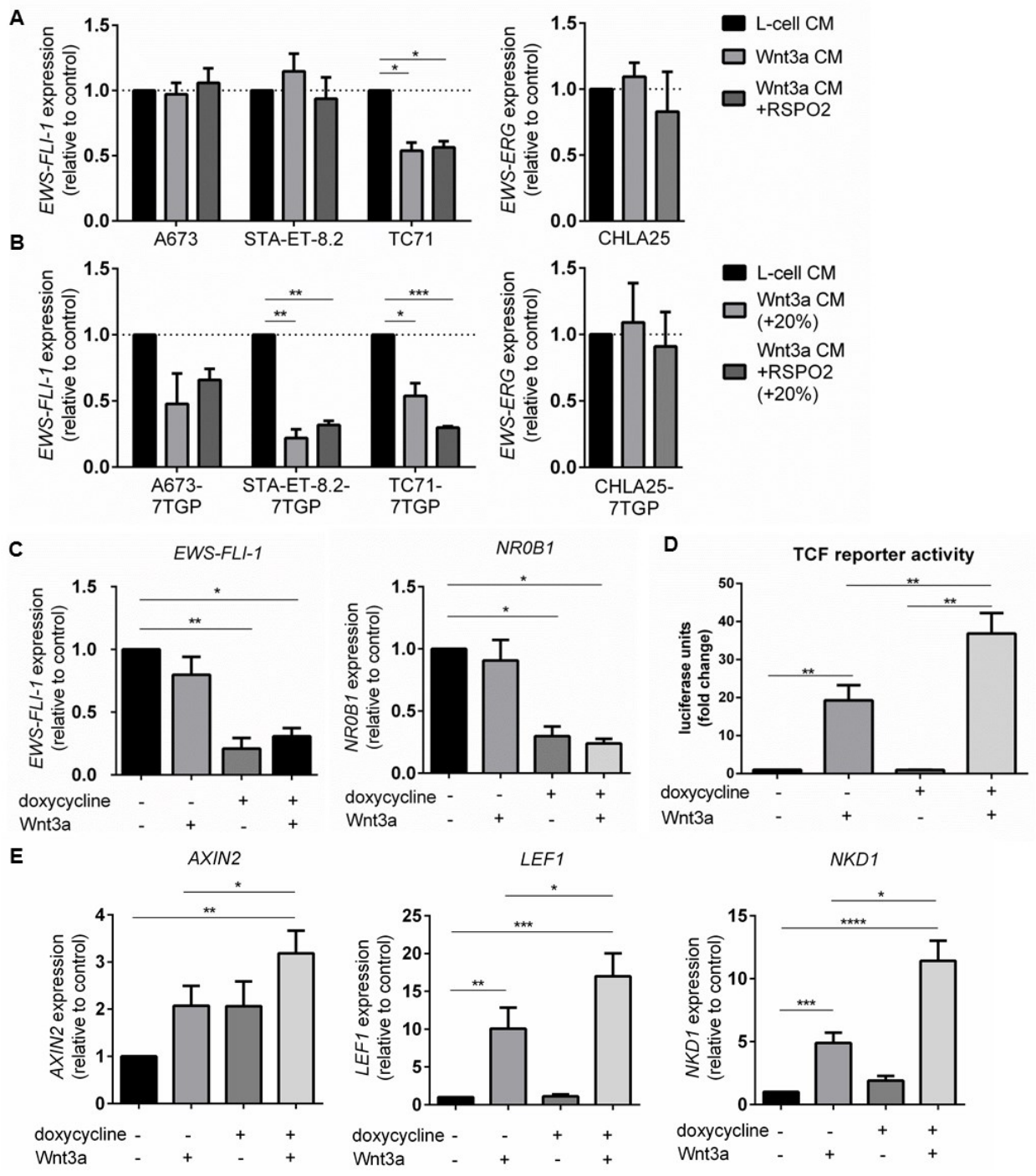


**Figure 2.8. Bi-directional transcriptional antagonism exists between EWS/FLI1 and Wnt-beta catenin signaling.**

(A) Expression of EWS/FLI1 (A673, STA-ET-8.2, and TC71) or EWS/ERG (CHLA25) was assessed by qRT-PCR in cells stimulated with Wnt3a or Wnt3a + RSPO2. In the highly Wnt-responsive cell line TC71, EWS/FLI1 levels are reduced twofold upon stimulation of Wnt signaling. (B) The top 20% of Wnt responsive 7TGP reporter cells

were sorted and EWS/ETS expression was assessed as in (A). In all cell lines except CHLA25, EWS/ETS levels are decreased approximately twofold or more. (C) A673 cells containing a doxycycline-inducible EWS/FLI1 construct (shA673-1C) were stimulated with doxycycline and/or recombinant Wnt3a. In cells treated with doxycycline, expression of *EWS/FLI1* and the EWS/FLI1 target gene *NR0B1* transcripts are reduced. (D) shA673-1C cells were transduced with a 7xTCF-luciferase (7TFP) reporter of Wnt activity and stimulated with doxycycline and/or Wnt3a. Induction of reporter activity is observed upon addition of Wnt3a, but not after knockdown of EWS/FLI1 alone. Induction of reporter activity is significantly increased upon both stimulation with Wnt3a and knockdown of EWS/FLI1. (E) Endogenous gene expression was assessed by qRT-PCR of Wnt target genes *AXIN2, LEF1, and NKD1.* Addition of Wnt3a induced expression of all genes, and knockdown of EWS/FLI1 induced further expression.

### *Wnt/beta-catenin signaling promotes cytoskeleton changes and a migratory and metastatic phenotype*

*In vitro* EWS/ETS inhibition results in a decrease in Ewing sarcoma cell proliferation, but recent evidence showed that EWS/ETS inhibition also results in induction of actin stress fibers, and acquisition of a more migratory cell phenotype, enhanced tumor cell adhesion in the lung [59, 60]. These changes are mediated in part by de-repression of the actin-associated gene zyxin (ZYX). Our observation that activation of Wnt/beta-catenin leads to de-repression of numerous cytoskeleton genes, including ZYX (Fig. 2.9A), led us to test whether activation of Wnt/beta-catenin signaling in Ewing sarcoma cells would phenocopy EWS/ETS inhibition. Therefore, we investigated the impact of Wnt/beta-catenin signaling on the actin cytoskeleton and on cell migration. We used phalloidin staining to visualize the actin cytoskeleton in 7TGP-transduced Wnt reporter cells and found that, compared to controls, Wnt3a treatment resulted in an increase in cell size and actin stress fibers that was further enhanced by the addition of RSPO2 (Fig. 2.9B). Notably, the differences in the actin cytoskeleton were most pronounced in the GFP-positive populations, demonstrating the direct relationship between morphologic, cytoskeletal changes and Wnt activation (Fig. 2.9B).

We next sought to determine if Wnt-dependent changes in the cytoskeleton had functional effects on cell migration. As shown, cells stimulated with Wnt3a +/-RSPO2 were more migratory than control cells in a transwell migration assay, and migration was further enhanced by the presence of RSPO2 (Fig. 2.9C). To determine if changes in the cytoskeleton were mediated by beta-catenin, we transduced cells with a constitutively active beta-catenin construct (EβP)[110] or empty vector control (empty). Ectopic expression of activated beta-catenin induced cytoskeleton changes (Fig. 2.9D) and a migratory phenotype (Fig. 2.9E) that reproduced those seen in highly Wnt-responsive cells, confirming that the effects of Wnt activation on the Ewing sarcoma cytoskeleton are mediated, at least in part, by beta-catenin. Finally, we evaluated the formation of podosomes in Wnt-stimulated Ewing sarcoma cells. Podosomes are actin-rich cytoskeletal structures that are essential for cell migration and can be visualized by their distinct morphology and cortactin immunocytochemical staining [111, 112]. Consistent with induction of migratory cytoskeleton architecture, podosomes were increased in Ewing sarcoma cells following exposure to Wnt3a (Fig. 2.9F). Thus, Wnt/beta-catenin signaling in Ewing sarcoma promotes cytoskeleton changes and a migratory phenotype that are strongly reminiscent of the EWS/FLI-1 knockdown phenotype.

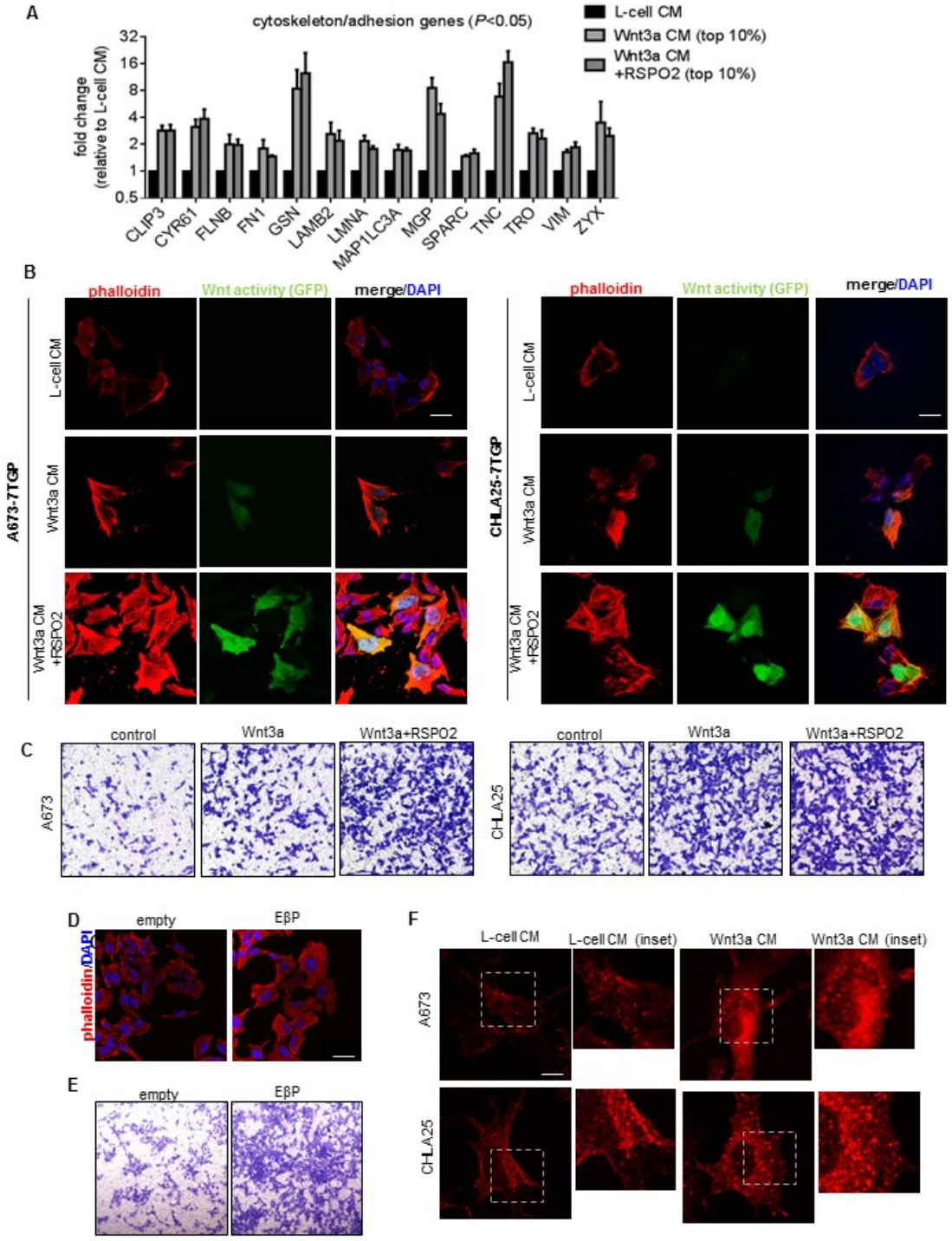


**Figure 2.9. Wnt signaling induces beta-catenin-mediated cytoskeleton changes and migration in ES cell lines.**

(A) EWS/ETS-repressed cytoskeleton and migration genes are induced by Wnt/beta-catenin activation. FPKM data shown as fold change relative to L-cell CM control.

(B) A673 and CHLA25 7TGP-reporter cells were stimulated with Wnt3a CM or Wnt3a CM + RSPO2 and F-actin filaments evaluated by phalloidin staining (red). Highly Wnt-responsive cells are GFP-positive (green). Nuclei are stained with DAPI (blue). Stress fibers are most abundant in GFP-positive cells. Scale bar = 20 μM. (C) Migration of A673 and CHLA25 was assessed using transwell assays containing Wnt3a with our without RSPO2 and stained with crystal violet. Wnt3a and Wnt3a +RSPO2 induced more migration compared to control. (D) A673 cells were transduced with either an empty vector or a vector containing a constitutively active beta-catenin (EβP) and stained with phalloidin. EβP cells are larger and exhibit more stress fibers than those containing an empty vector. Scale bar = 20 μM. (E) Migration was assessed using transwell assays and stained with crystal violet. Cells containing the EβP vector were more migratory than those containing an empty vector. (F) A673 and CHLA25 were stimulated with L-cell CM or Wnt3a CM and podosomes were evaluated by cortactin staining (red). Insets show higher magnification of area demarcated by dotted lines of punctate staining indicating podosomes. Podosomes were increased in cells stimulated with Wnt3a compared to control. Scale bar = 5 μM.

In order to determine if an increased migratory phenotype results in increased metastasis *in vivo*¸ luciferase-tagged A673 and TC32 cells were stimulated *in vitro* with either L-cell CM or Wnt3a CM +RSPO2 and injected via tail vein into NOD-SCID mice. Tumor establishment and growth was monitored by bioluminescence imaging over the course of six weeks (Fig. 2.10A). In A673 cells, Wnt3a CM +RSPO2 tumors initially grew faster than L-cell CM stimulated tumors (Fig. 2.10B). By six weeks, mice receiving Wnt3a CM +RSPO2-treated cells had an increased incidence of tumor formation (Fig. 2.10C), as 9/10 mice formed tumors, compared to only 5/10 for L-cell CM recipient mice. However, among mice in which tumors were present there was no significant difference in overall tumor burden (data not shown), indicating that there was little difference in tumor growth once tumors were established. Although no differences were observed in the size of tumors, the tissue tropism was markedly different between the two groups. Of the five tumors that formed in the L-cell group, three tumors were in the subcutaneous space, one tumor was in the mandible, and one tumor was on the exterior chest wall. No lung nodules were detectable by bioluminescence or inspection

upon dissection (Fig. 2.10A, D). In striking contrast, 7/10 mice in the Wnt3a CM+RSPO2 group had tumor formation in the lungs, in addition to tumors in the subcutaneous space, ovary, and limbs (Fig. 2.10A, D). In mice receiving TC32 cells, Wnt3a CM+RSPO2 treated cells had a similar but modest trend toward earlier onset (Fig. 2.10E), and little difference between groups in regards to overall tumor incidence (Fig. 2.10F) and metastasis location (Fig. 2.10G). In both groups, TC32 cells formed multiple metastases per mouse, with an equally strong prevalence of lung tumors, suggesting that Wnt activation does not further increase the tumorigenicity of cells that are already highly aggressive.

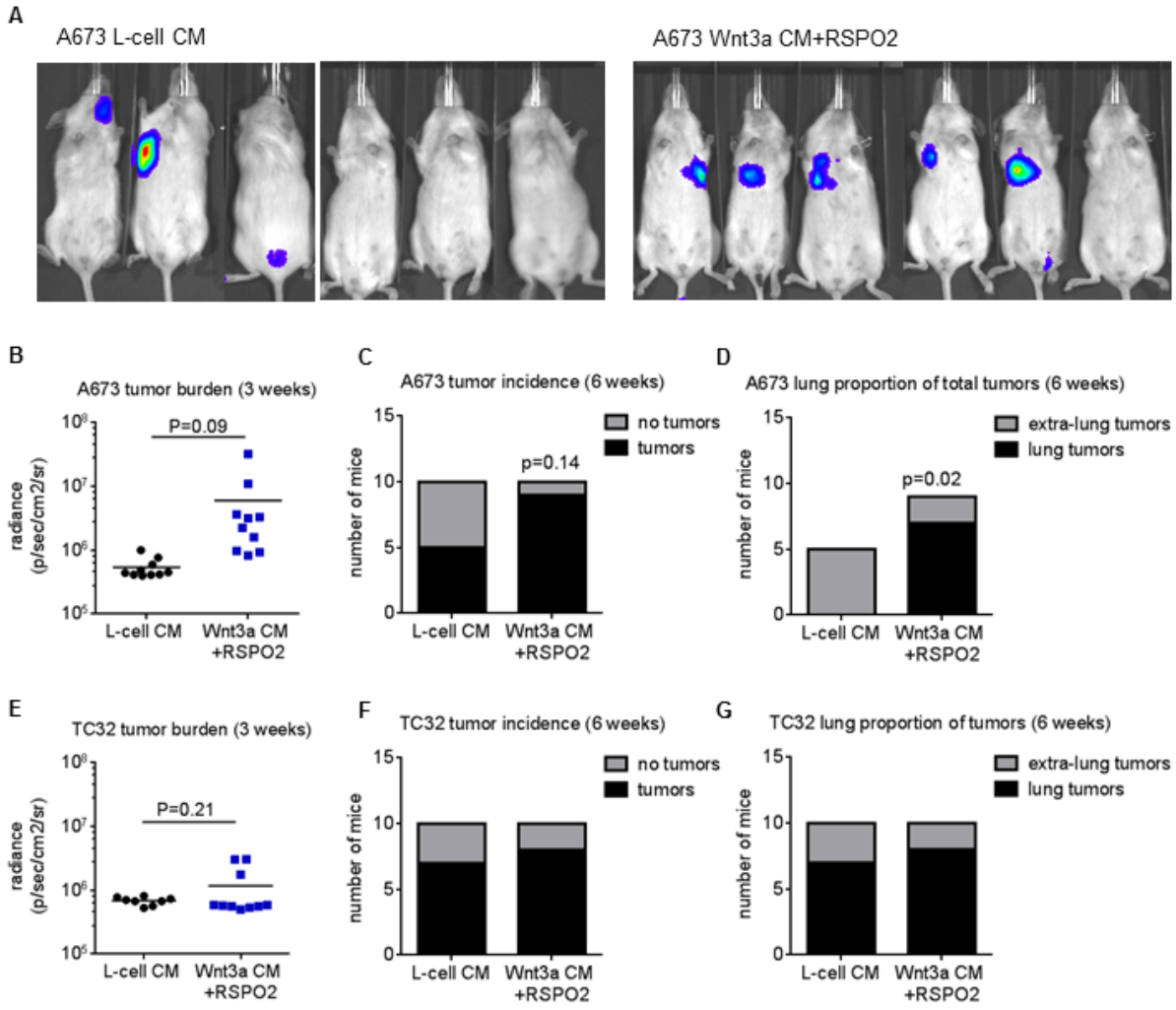


**Figure 2.10. Activation of Wnt/beta-catenin signaling promotes lung metastasis.**

(A) Representative bioluminescent images of mice injected with L-cell CM stimulated A673 cells (left panels) or Wnt3a CM +RSPO2 treated cells. Upon dissection, tumors were located in in the mandible, exterior chest wall, and subcutaneous spaces in mice with L-cell CM treated cells. In mice receiving cells stimulated with Wnt3a CM + RSPO2, tumors were located in the lungs, subcutaneous space, ovary, and limbs. (B) The onset of tumor formation was assessed by bioluminescence imaging at 3 weeks, and revealed that mice receiving A673 cells stimulated with Wnt3a CM+RSPO2 had higher tumor burden at 3 weeks compared to mice receiving L-cell CM stimulated cells. Data is expressed as radiance. P-values were determined using Student's t-test. (C) After 6 weeks, tumor incidence was determined by the presence or absence of bioluminescent signal in each mouse. More tumors formed from cells with Wnt stimulation compared to controls. P-values were determined using Fisher's exact test. (D) The location of each tumor was assessed by bioluminescent imaging and confirmed by dissection. Significantly more lung tumors were observed as a result of Wnt stimulation P-values were determined using Fisher's exact test. Tumor burden at 3 weeks (E), incidence (F),

and tumor location (G) for TC32 cells was similarly determined as in (B), (C), and (D), respectively. No significant differences exist between TC32 cells stimulated with Wnt3a CM+RSPO2 compared to controls.

### *Ewing sarcoma tumors with evidence of robust Wnt/beta-catenin activation are associated with a worse clinical outcome*

Our *in vitro* and *in vivo* studies demonstrate that activation of Wnt/beta-catenin in Ewing sarcoma leads to phenotypic changes that are associated with more aggressive disease. To assess if these observations are relevant in the clinical setting, we analyzed patient tumors for evidence of canonical Wnt/beta-catenin activation and determined if activity associated with tumor relapse and/or patient survival. First, we assessed nuclear beta catenin staining in clinically annotated tumor specimens from 37 patients at the University of Michigan. These cases were included in the aforementioned TMA (Fig. 2.1D). Six tumors robustly expressed nuclear beta-catenin and all six of these patients relapsed. Nuclear beta-catenin was low or undetectable in 31 patients, and 18 (58%) relapsed. Given the heterogeneity of this patient cohort, with respect to clinical presentation and treatment regimens, conclusions cannot be drawn, although a trend toward worse outcome was observed in patients whose tumors showed evidence of robust Wnt/beta-catenin activation. To assess Wnt/beta-catenin activation in a more homogeneous cohort of equivalently treated patients, we turned to gene expression microarray data that was obtained from 46 Ewing sarcoma patients who were treated according to the most recent Children's Oncology Group (COG) protocols [113]. In the absence of nuclear beta-catenin data for these cases, we used expression of *LEF1* as a biomarker of Wnt/beta-catenin activation. *LEF1* was chosen given that it is not highly expressed by Ewing sarcoma cells in the absence of Wnt ligand, but is robustly and

reproducibly transcriptionally induced by treatment with Wnt3a or Wnt3a plus RSPO2 (Fig. 2.5D,E), and by expression of constitutively active beta-catenin (Fig. 2.11A). Notably, this induction is not associated with an increase in proliferation (Fig. 2.11B and [3]). In keeping with the potential of Wnt/beta-catenin as a mediator of aggressive disease, increased expression of *LEF1* was associated with worse event free and overall survival rates in this patient cohort (Fig. 2.11C). Finally, given our observation that Wnt/beta-catenin and EWS-ETS display transcriptional antagonism *in vitro*, we hypothesized that tumors that display evidence of activated beta catenin *in vivo* would show reduced levels of EWS-ETS transcriptional activity. To address this, we ranked genes by correlation with *LEF1* expression in primary tumors and performed GSEA. Comparison of the Wnt-activated gene set to EWS-ETS target gene signatures revealed a striking and reproducible inverse correlation that was entirely consistent with our *in vitro* studies (Fig. 2.11D). Together, these patient tumor-derived data further demonstrate that activation of Wnt/beta-catenin signaling in Ewing sarcoma antagonizes EWS-ETS-dependent transcription.

Together these findings reveal that beta-catenin activation in Ewing sarcoma leads to activation of a gene expression program that promotes adoption of a more clinically aggressive phenotype and results in worse clinical outcomes. Furthermore, this is mediated, at least in part, by Wnt/beta-catenin-dependent antagonism of EWS-ETS transcriptional activity.

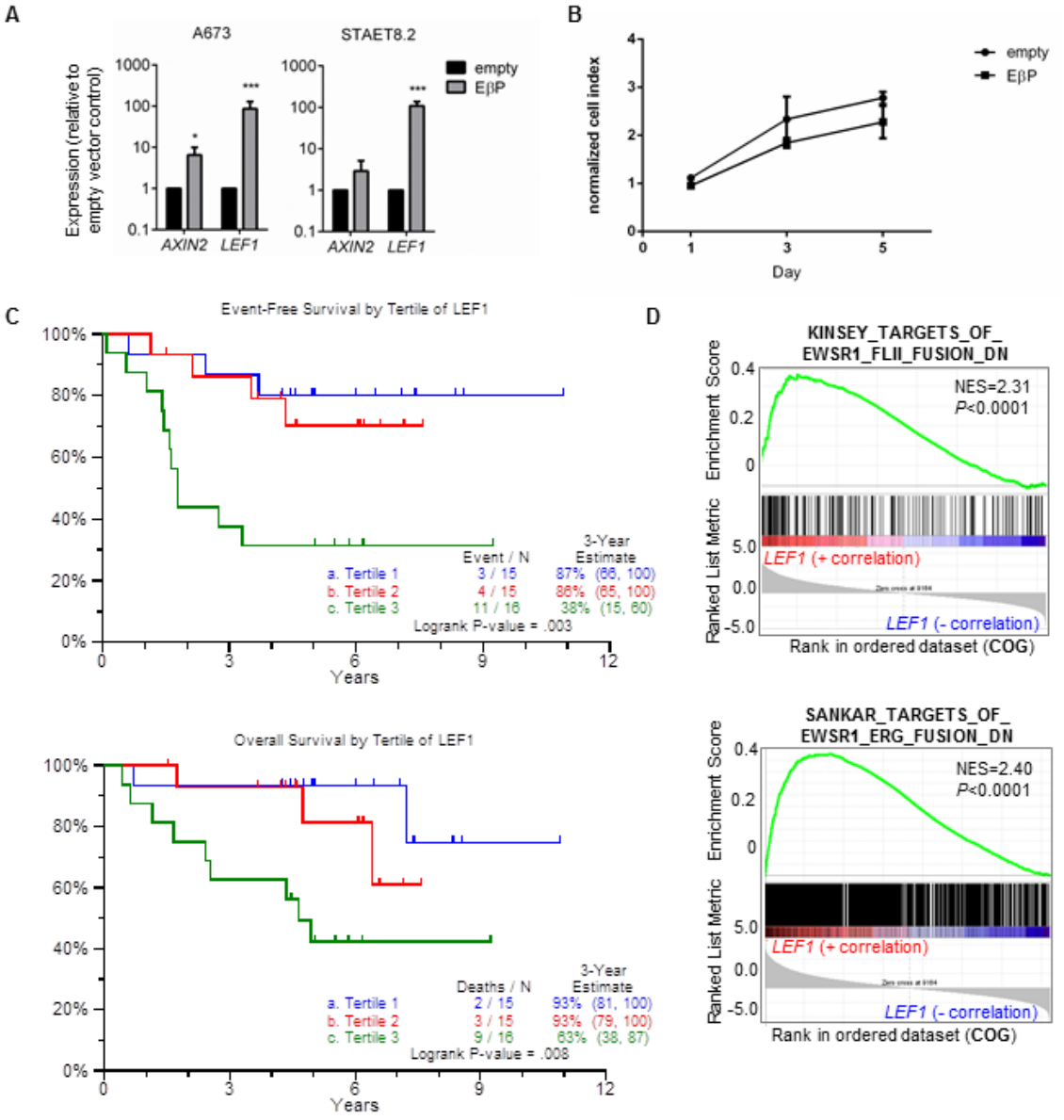


**Figure 2.11. High *LEF1* expression is associated with poor outcomes in Ewing sarcoma and inversely correlates with EWS/ETS target genes.**

(A) A673 and STA-ET-8.2 were transduced with a constitutively active beta catenin construct (EβP), and expression of *LEF1* was assessed by qRT-PCR. *LEF1* was found to be a highly sensitive readout of Wnt signaling. (B) Constitutively active beta-catenin and LEF-1 induction do not result in significant changes in proliferation. (C) Event free survival and (C) overall survival based on LEF1 expression was assessed in the COG patients. (D) An in vivo signature of Wnt/beta-catenin activation was generated from 46

primary tumors by ranking genes based on their correlation with LEF1 expression. Genes that are highly correlated with LEF1 expression in primary tumors are enriched for genes that are repressed by EWS/FLI-1 (top panel) and EWS/ERG (bottom panel).

## Discussion

A seminal role for Wnt/beta-catenin exists in colorectal carcinoma, where germ line and somatic genetic mutations contribute to constitutive pathway activation, resulting in tumor initiation and progression [63]. Involvement of canonical Wnt signaling in other cancer types has also been described [82, 114, 115] including in the sarcomas, although genetic mutations in the pathway are less frequent than in colorectal tumors and other carcinomas [89]. Prior studies of established Ewing sarcoma cell lines [3, 90, 96, 99] as well as a new murine model of EWS/ETS-induced malignant transformation [95] suggest that the Wnt/beta-catenin axis contributes to the pathogenesis of Ewing sarcoma. Nevertheless, the potential oncogenic role of Wnt signaling in Ewing sarcoma tumors *in vivo,* and the nature of Wnt/beta-catenin transcriptional targets in these tumors, had yet to be fully elucidated. In the current study we combined cell line models, patient tumors, gene expression and functional studies to investigate the impact of Wnt/beta-catenin signaling on Ewing sarcoma transcriptional profiles, biology and clinical behavior. The combined results of these studies converge on a model in which activation of canonical Wnt/beta-catenin signaling, by ligands in the tumor microenvironment, induces Ewing sarcoma cells to transition from relatively non-motile to more migratory and metastatic states. Paradoxically, this phenotypic transition is associated with functional inhibition of EWS/ETS-dependent transcription, thus revealing a highly complex and context-specific interplay between the tumor microenvironment, tumor cell autonomous Wnt/beta-catenin signaling molecules, and EWS/ETS fusion proteins (Fig. 2.12).

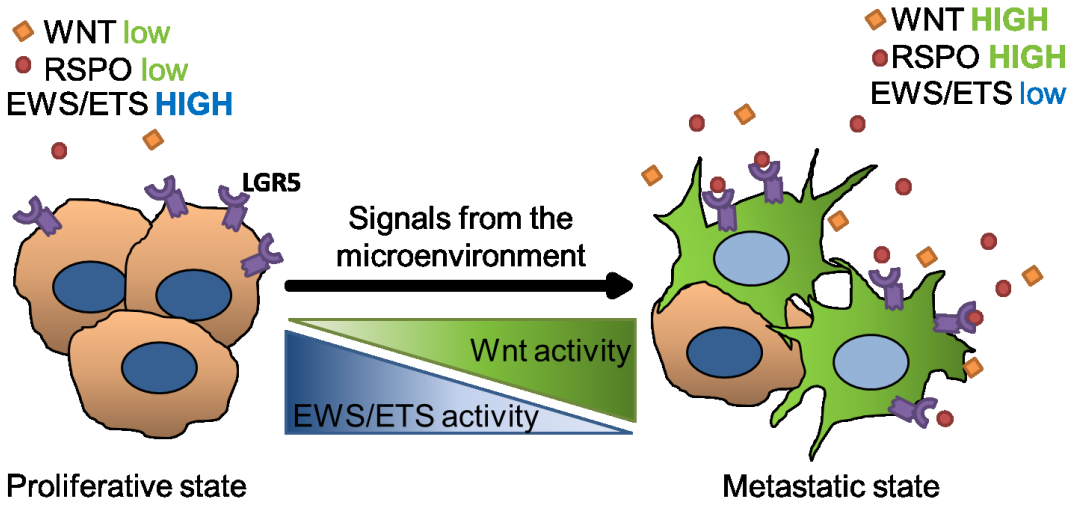


**Figure 2.12. Schematic of heterogeneous RSPO/Wnt-mediated antagonism of EWS/ETS antagonism**

Wnt responsive LGR5-positive cells respond to RSPO2 and Wnt ligands in the microenvironment, and undergo phenotypic changes to switch from a proliferative to a migratory and metastatic phenotype through inhibition of EWS/ETS fusion activity.

The transcriptional targets of Wnt/beta-catenin, both in normal development and in cancer, are highly context dependent and, as such, the functional impact of pathway activation varies between tissues and tumors of different ontogenies [68, 114]. Given the critical role that canonical Wnt signaling plays in modulating mesenchymal cell migration and morphogenesis during embryonic development [115], it is highly consistent that we have found that the axis plays a similar role in Ewing sarcoma. Prior studies showed that Wnt3a promotes Ewing sarcoma cell migration *in vitro* [90] and our current findings demonstrate that this is mediated by beta-catenin-dependent changes in the actin cytoskeleton. In particular, nuclear localization of beta-catenin in Ewing sarcoma cells results in cell spreading, an increase in actin stress fibers and the creation of podosomes, actin-rich cytoskeletal structures that are dynamically induced on the leading front of migratory and invasive cancer cells [112]. Significantly, the

observed changes in cell shape, stress fiber formation, and lung engraftment that we observed in Wnt-activated cells were highly reminiscent of a phenotype that was recently described in the context of RNAi-mediated EWS/ETS knockdown [59, 60]. In these studies, EWS/ETS knockdown cells were also shown to be more migratory and to harbor enhanced capacity for lung engraftment, observations that lead to the intriguing, and somewhat counterintuitive hypothesis, that a relative loss of EWS/ETS function could promote Ewing sarcoma metastasis [59]. Remarkably, our unbiased RNA profiling studies of Wnt-stimulated Ewing sarcoma cells identified a striking, and highly statistically significant, inverse relationship between Wnt/beta-catenin-dependent and EWS/ETS-dependent transcriptional targets. In addition, two genes that have been convincingly shown to be mediators of tumor metastasis in other tumor types, *LEF1* [116] and *TNC* [117], were both robustly induced by activated beta-catenin in Ewing sarcoma cells. Thus, canonical Wnt signaling in Ewing sarcoma antagonizes EWS/ETS transcriptional activity, promotes acquisition of a migratory phenotype, and induces expression of metastasis-associated genes.

The precise molecular mechanisms underlying transcriptional antagonism between EWS/ETS and beta-catenin remain to be elucidated, although several potential possibilities now demand further study. First, prior work using A673 Ewing sarcoma cells and EWS/FLI-1-transduced heterologous cell types showed that EWS/FLI-1 can physically associate with LEF1, leading to reduced interactions between LEF1 and beta-catenin and subsequent inhibition of TCF/LEF target gene activation [96]. We have discovered that *LEF1* is strongly induced upon Wnt stimulation and that Wnt/beta-catenin antagonizes the EWS/ETS transcriptional signature. Therefore, we speculate that high levels of LEF1 in Wnt-stimulated Ewing sarcoma cells may result in increased

LEF1-EWS/ETS protein-protein interactions, which could negatively impact on EWS/ETS transcriptional activity by blocking localization of the fusion to its DNA targets. Alternatively, activated Wnt signaling might directly repress expression of the fusions themselves. In support of this, we observed down regulation of *EWS/FLI-1* transcript expression in the most robustly Wnt-responsive cells. Conversely, despite intense beta-catenin activation, EWS/ERG levels were unaffected by Wnt3a or Wnt3a plus RSPO2 in CHLA25 cells. Moreover, expression of many established EWS/ETS target genes, including *NR0B1* [19, 20] and *NKX2.2* [17, 18] was unaffected by Wnt/beta-catenin activation, demonstrating that transcriptional antagonism between Wnt/beta-catenin and EWS/ETS does not extend to all targets of EWS/ETS fusions. Further investigations are required to elucidate the molecular mechanisms that account for these differential responses to Wnt/beta-catenin signaling among different EWS/ETS target genes, although it is likely that the different interactions of fusions with different transcriptional and chromatin regulatory complexes at target gene promoters and enhancers is likely to be key [15, 16].

Another potential explanation for the relative reduction in *EWS/FLI-1* levels in the most Wnt-responsive cells is that heterogeneity exists among Ewing sarcoma cells with respect to fusion gene expression levels. In this scenario, cells with the lowest levels of EWS/FLI-1 expression would be most responsive to Wnt stimulation, resulting in detection of relatively fewer fusion transcripts in the most beta-catenin-active cell population. Our finding, also previously observed by Navarro *et al.* [96], that experimental down regulation of EWS/FLI-1 results in enhanced Wnt-responsiveness supports this possibility. The concept of non-mutational tumor cell heterogeneity is not new but it has recently emerged as a key player in the context of emergent drug

resistance and tumor progression [118-120]. In particular, plasticity of tumor cells that permits cell state transitions between proliferative and migratory states, such as epithelial to mesenchymal transitions in carcinoma, has been linked to metastasis [121, 122]. The current studies identify a novel mechanism of phenotypic plasticity in Ewing sarcoma cells that is responsive to provision of an exogenous Wnt signal from the microenvironment. Significantly, however, our studies showed that not all cells respond to Wnt stimulation, and that the relative responsiveness varies both within and between cell lines and between neighboring cells in tumors *in vivo*. Numerous factors could contribute to this heterogeneity of response. We have discovered that expression of the Wnt-potentiating ligand, *LGR5,* is heterogeneous on a cell-to-cell basis and our previous studies showed that LGR5 modulates Wnt signaling in the absence of exogenous R-spondins [3]. Thus, variability in the availability of endogenous or exogenous R-spondins and Wnt ligands, as well as heterogeneous expression of LGR5*,* frizzleds, LRPs, and other Wnt-modulating receptors, would all impact on an individual cell's ability to activate beta-catenin. Other cell-intrinsic factors, such as cell cycle state, may also have an effect. For instance, G2/M-phase is most permissive for Wnt signaling [123], so differences in cell cycle state might also contribute to differences in response among neighboring cells. The finding that heterogeneous Wnt signaling occurs in Ewing sarcoma is supported by data from other tumor systems. In colorectal cancer, nuclear beta-catenin is heterogeneous among tumor cells, despite the universal presence of activating mutations [124]. In lung adenocarcinoma, cells isolated from metastatic lesions were more Wnt responsive than their corresponding primary tumors, and aggressive phenotypes were enhanced *in vitro* in the presence of conditioned media from metastatic sites [116]. This further supports the idea that differences in Wnt

responsiveness among tumor cells can be dictated by the signaling microenvironment. Thus, these studies, together with our own findings, reinforce the conclusion that cellular heterogeneity in Wnt signaling is determined by both cell intrinsic and cell extrinsic factors.

Finally, our studies of patient tumors support the conclusions from our experimental systems that activation of Wnt/beta-catenin in Ewing sarcoma cells promotes tumor metastasis and progression. In a small cohort of adult patient tumors, we were able to identify six patients with evidence of high nuclear beta-catenin staining and all of them relapsed. In an independent cohort of equivalently treated pediatric Ewing sarcoma patients we discovered that high expression of *LEF1,* a sensitive biomarker of Wnt/beta-catenin activation in Ewing sarcoma cells, was associated with relapse and worse survival. In summary, through extensive molecular, cellular and tumor studies we have identified a Wnt/beta-catenin-dependent response in Ewing sarcoma that promotes transition of cells from less motile to highly migratory and metastatic states. This cell plasticity is heterogeneous and dependent on both cell intrinsic and extrinsic factors. The phenotypic transition of Ewing cells to a more migratory state is mediated by beta-catenin-dependent changes in the actin cytoskeleton and by transcriptional antagonism with EWS/ETS proteins. Activation of Wnt/beta-catenin in tumors *in vivo* is associated with worse clinical outcomes, including increased rates of relapse and diminished rates of survival. Together these data support further investigation of Wnt pathway-targeted agents as adjuvant therapy for Ewing sarcoma patients. In particular, given that activation of Wnt/beta-catenin in Ewing sarcoma is likely to be mediated, in the vast majority of cases, by the microenvironment rather than through activating mutations, agents that inhibit the extracellular ligand-receptor interaction, as well as those that

target intracellular downstream signaling components, are strong candidates for testing in Ewing sarcoma.

## Experimental Procedures

*Cell culture and lentiviral transductions*

Ewing sarcoma cell lines A673, CHLA25, CHLA32, STA-ET-8.2, TC71, and TC32 were kindly provided by Dr. Timothy Triche (CHLA, Los Angeles, CA, USA), Dr. Heinrich Kovar (CCRI, St. Anna Kinderkrebsforschung, Vienna, Austria), and the COG cell bank (cogcell.org). Identities of the cells were verified by short tandem repeat (STR) profiling. Cells were routinely tested for mycoplasma contamination, and were verified to be negative for all studies. Cells were cultured in RPMI 1640 media (Gibco) supplemented with 10% fetal bovine serum (FBS)(Atlas Biologicals) and 2mM L-glutamine (Life Technologies). CHLA25, CHLA32, and STA-ET-8.2 were grown on plates coated with 0.2% gelatin. L-cells (ATCC CRL-2648) and Wnt3a L-cells (ATCC CRL-2647) were cultured in DMEM (Gibco) supplemented with 10% FBS. The identity of the cells was confirmed by short tandem repeat (STR) profiling. Lentiviral production and transduction was performed as previously described [3]. For generation of 7TGP and 7TFP reporter cells, plasmids #24305 and #24308 (Addgene) were used, respectively [110]. For generation of EβP cells, plasmid #24313 (Addgene) was used. The constitutively active beta-catenin element was removed using BamHI to generate EβP-empty vector. Luciferase-tagged cells were generated with a pLentilox-luciferase/GFP vector provided by the University of Michigan Vector Core.

*Reporter assays and cell sorting*

For luciferase assays, $5x10^3$ stably transduced 7TFP cells were plated in triplicate on 96-well plates in RPMI1640 containing 10% tetracycline-free FBS and 1% L-glutamine. The next day, the media was changed to contain either stimulated with 1:1 RPMI1640

supplemented with 5% FBS and 1% L-glutamine and CM +/- RSPO2 for 48 hr, or PBS or 1ug/mL of doxycycline, and/or 500 ng/mL recombinant Wnt3a (R&D Systems) for shA673-1C cells. After 48 hr, luciferase activity was measured using the Steady-Glo Luciferase Assay System (Promega) according to manufacturer's protocol and measured on white opaque plates on a Synergy H1 Multi-mode plate reader (BioTek Instruments). Data is expressed as relative luciferase units (RLU), which is the mean value of luciferase activity normalized to the mean of the background signal in media-only wells.

To visualize and sort Wnt/beta-catenin active cells, stably transduced 7TGP cells were stimulated with 1:1 RPMI1640 supplemented with 5% FBS and 1% L-glutamine and CM +/- RSPO2 for 48 hr. Cells were dissociated using Accutase (Millipore) and fluorescence was measured and cells counted using an Accuri C6 cytometer. For fluorescence-activated cell sorting (FACS), cells were similarly stimulated and dissociated, and sorted on the basis of GFP expression using the MoFlo Astrios instrument at the University of Michigan Flow Cytometry Core.

*Immunofluorescence microscopy*

Cells were plated on gelatin-coated coverslips. The next day, the media was changed to RPMI 1640 containing 5% FBS and 1% L-glutamine and an equal volume (1:1) of L-cell conditioned media (CM) or L-cell Wnt3a CM either with or without 20ng/mL recombinant R-spondin 2 (RSPO2) (R&D Systems). Cells were fixed in 4% PFA for 15 min at room temperature (RT), then permeabilized in PBS containing 0.5% Triton-X for 5 min. Cells were blocked in 5% donkey serum for 1 hr, then incubated with anti-beta-catenin (BD Transduction Laboratories, 1:300) for 1 hr at RT followed by 1 hr secondary antibody

(Alexafluor 594, 1:500) at RT. Cortactin was detected using a directly conjugated Alexa 555 anti-cortactin antibody, clone 4F11 (EMD Millipore. 1:1000). For phalloidin staining, cells were fixed and permeabilized, and then incubated with 100 nM Acti-stain 555 phalloidin (Cytoskeleton, Inc.) for 30 minutes in in the dark at RT. GFP expression was directly visualized by fluorescent microscopy in 7TGP reporter cells. Slides were counterstained using DAPI (1:10,000) (Invitrogen) for 10 minutes in the dark at RT, were mounted using Prolong Gold (Molecular Probes, Life Technologies) and imaged using an Olympus CKX41 or Nikon A1 spectral confocal microscope at 40X with Nikon Elements software version 3.

*Migration Assays*

Cells were dissociated with Accutase (Millipore), washed twice with PBS, and re-suspended in serum-free RPMI1640. 2x10^5 cells were plated on a transwell coated with 0.2% gelatin, and media containing 10% FBS was used in the bottom chamber. 500 ng/mL of Wnt3a with or without 20 ng/mL RSPO2 was added to the bottom chamber as indicated. Cells were allowed to migrate through the transwell for 24 hr, and then fixed using a solution of 25% crystal violet and 25% methanol.

*Proliferation assay*

$5x10^3$ cells were plated in triplicate on 96 well plates, and cells were allowed to proliferate for five days. Cell proliferation was monitored at days 0, 1, 3, and 5 using the CellTiter 96 AQueous One Solution Cell Proliferation Assay (Promega, Madison, WI) according to the manufacturer's instructions. Colorimetric absorbance (490 nm) was quantified on a BioTek plate reader. Background readings for each day were subtracted

from blank wells. Data is expressed as the normalized cell index, which is the background-corrected absorbance normalized to the day 0 reading.

*Analysis of Wnt pathway gene expression*

Expression of Wnt pathway genes in primary Ewing sarcoma and colorectal carcinoma tumors was determined using publicly available data (GSE 34630 [125], and GSE 4554 [126]. Graphical representation of the data was achieved using the R2: Genomics Analysis and Visualization Platform (http://r2.amc.nl). Expression of Wnt pathway genes cell lines was determined by RNA–sequencing (see below) and by quantitative RT-PCR, using standard methods as previously described [3] . Primers are listed in Table 2.2.

| Gene | Forward primer sequence | Reverse primer sequence |
|---|---|---|
| *AXIN2* | AAGTGCAAACTTTCGCCAAC | ACAGGATCGCTCCTCTTGAA |
| *CCND1* | CCGTCCATGCGGAAGATC | ATGGCCAGCGGGAAGAC |
| *CDC25A* | CCAGCCCCAAAGAGTCAAC | AAGGTCCCTTGGGTCATTGT |
| *CMYC* | CGTAGTTGTGCTGATGTGTGG | CTCGGATTCTCTGCTCTCCTC |
| *EWS/ERG* | GTCAACCTCAATCTAGCACAGGG | CTGTCCGACAGGAGCTCCAG |
| *EWS/FLI1* | CGACTAGTTATGATCAGAGCAGT | CCGTTGCTCTGTATTCTTACTGA |
| *HPRT1* | TGACACTGGCAAAACAATGCA | GGTCCTTTTCACCAGCAAGCT |
| *LEF1* | TGGATCTCTTTCTCCACCCA | CACTGTAAGTGATGAGGGGG |
| *NKD1* | TCGCCGGGATAGAAAACTACA | CAGTTCTGACTTCTGGGCCAC |
| *NR0B1* | AGCACAAATCAAGCGCAGG | GAAGCGCAGCGTCTTCAAC |

**Table 2.2 Primer sequences used for qRT-PCR**

In vivo *metastasis assay*

To assess metastatic capacity, luciferase-labeled A673 or TC32 were stimulated with L-cell CM or Wnt3a CM +RSPO2 for 48 hr, dissociated with Accutase, and then injected via tail vein into 10-12 week-old NOD SCID mice. Each mouse received $1x10^6$ cells in 100 µl PBS. Satisfactory injection of viable cells was confirmed by detection of light

emission in the lungs of recipient mice 30 minutes after cell injection on a Xenogen IVIS bioluminescence system (Perkin Elmer, Waltham, MA). Imaging was repeated weekly and tumor burden quantified using Living Image software (Perkin Elmer, Waltham, MA). Mice were monitored for 6 weeks, at which point mice were euthanized and examined for metastases. The location and amount of macroscopic tumors that correlated with bioluminescent signal was assessed with the assistance of the Unit for Laboratory Animal Medicine (ULAM) Pathology Core for Animal Research (PCAR).

*TMA Construction*

Formalin-fixed, paraffin-embedded tissue blocks (FFPE) of 65 cases of Ewing sarcoma tumors were obtained from the files of the Department of Pathology, University of Michigan Medical Center, Ann Arbor, MI. The University of Michigan Institutional Review Board provided a waiver of informed consent to obtain these samples. After pathological review, a tissue microarray was constructed from the most representative area using the methodology of Nocito *et al.* [127]. Each case was represented by one 1 mm diameter core obtained from the most representative, non-necrotic area of the tumor.

*Immunohistochemistry and Automated Quantitative Assay (AQUA)*

After deparaffinization and rehydration, sequential TMA sections were subjected to microwave epitope retrieval in 10 mM sodium citrate buffer, pH 6.0. After rinsing several times in 10 mM Tris/HCl buffer, pH 8 containing 0.154 M NaCl and 0.05% (v/v) Tween-20 (TBST), endogenous peroxidase activity was blocked with Peroxidazed (BioCare Medical) for 15 min. Non-specific binding of the antibodies was extinguished by 30 min incubation with Background Sniper (BioCare Medical). The TMA slide was then

incubated with the tumor-specific antibody, CD99 (clone EPR309Y, 1:200, BioCare Medical) overnight at 4°C. The slides were then washed with TBST and subsequently incubated with an antibody to beta-catenin (BD Biosciences, Clone #14, 610153, 1:7000) for 60 min at RT. Slides were then washed as described above and incubated with Alexafluor 555 (AF555) (Molecular probes, A21422, 1:200) secondary antibody in Envision+ (DAKO, K4003) or goat anti-rabbit IgG conjugated to AF555 (Molecular probes, A21429, 1:200) in goat anti mouse Envision+ (DAKO, K4001) for 60 min at RT in the dark. The slides were then washed and the target image was developed by a CSA reaction of Cy5 labeled tyramide (PerkinElmer, 1:50). The slides were washed with water, stained with DAPI, and mounted with in a ProLong Gold.

AQUA was performed as previously described [128]. Briefly, images of each stained TMA core were captured with an Olympus BX51 microscope at 3 different extinction/emission wavelengths. Within each TMA spot, the area of tumor was distinguished from stromal and necrotic areas by creating a tumor specific mask from the anti-CD99 protein, which was visualized from AF555 signal. The DAPI image was then used to differentiate between the cytoplasmic and nuclear staining within the tumor mask. The pixel intensity of the protein/antibody complex was determined from the Cy5 signal and reported as pixel intensity. The beta-catenin signal was further differentiated into the nuclear-associated pixel intensity and the non-nuclear-associated (membrane and cytoplasm) fraction.

*RNA In-situ Hybridization*

RNA in-situ hybridization (ISH) was performed using a commercially available kit and probes according to the manufacturer's instructions (Advanced Cell Diagnostics Inc., Haywood, Ca) and detailed in ([129]). Briefly, 4-µm thick sections of the EFT TMA were pretreated with 1 mM EDTA pH9 microwave epitope retrieval and protease digestion before digestion. Three sequential TMA sections were hybridized with *UBC* (positive control, catalog #310041), *LGR5* (catalog #311021) and *DAPB* (negative control, catalog #310043). The preamplifier, amplifier and horseradish peroxidase-labeled probes were then sequentially applied to the sections with appropriate washing steps between each application. Hybridizations and all incubations were carried out at 42C in a humidified environment. This was followed by color development with diaminobenzadine and light counterstaining with hematoxylin. Specific staining signals were identified as brown well-defined dots present in the cytoplasm of the cell. For *in vitro* analysis of cell lines, cells were cultured on glass chamber slides coated with 0.2% gelatin, fixed in 4% paraformaldehyde, and ISH was similarly performed according to the manufacturer's instructions using probes against *PPIB* (positive control, catalog # 313901), *LGR5*, and *DAPB*.

*Semi-Quantitative In-Situ Hybridization (SQUISH).*

SQUISH was performed using the protocol described above for ISH with the exception that a CSA reaction of Cy5 labeled tyramide was used instead of DAB. Prior to the addition of the Cy5 tyramide, the slides were sequentially incubated with antibody to CD99 (1:200) for 1 hr at RT, followed by Alexafluor 555 (1:200) for 1 hr at RT, and

Background Sniper. The slides were washed water and stained with DAPI in ProLong Gold. Analysis was performed as described for AQUA.

*RNA profiling and identification of Wnt target genes*

CHLA25-7TGP cells were stimulated with CM and FACS sorted on the basis of GFP expression. RNA was extracted for RNA sequencing (RNA-seq) and analysis. Total RNA was isolated from 3 sample sets: L-cell CM, Wnt3a CM, and the Wnt3a CM +RSPO2. RNA-seq libraries were prepared according to Illumina TruSeq standard procedures. Three biological replicates per sample were used and further three technical replicates for each of the biological sample were sequenced on the Illumina HiSeq 2000 instrument (50 cycle single read). Fastq generation was performed using Illumina's CASAVA-1.8.2 software. Quality control (QC) analyses were done on the fastq files using FASTQC. The fastq sequences that passed the QC were then aligned to Human genome (Ensembl GRCh37) using Tophat (v.2.0.5) embedded with Bowtie (v.2.2.0) with a maximum number of 2 mismatches. The RNA-seq data was aligned using Sailfish, a rapid alignment-free isoform quantification software[130]. The transcript coverage is accurately estimated using counts of k-mers occurring in reads instead of alignments of reads[130]. The criterion for considering a transcript as expressed was that more than one replicate from at least one sample group have RPKM (reads per kilobase per million mapped reads) greater than 1. For differential expression analysis, RPKM calculated using Sailfish methodology was used to estimate the expression levels of the transcripts, as it is based on the abundance of the unique read sequences of the transcripts. We used the statistical R package, edgeR[131] to determine differential transcript expression. This package uses an over-dispersed Poisson model

to account for both biological and technical variability. We performed two comparisons for the differential expression analyses: L-cell CM versus Wnt3a CM and L-cell CM versus Wnt3a CM +RSPO2. A $p$ value < 0.05 was considered as significant. Heat map analysis was generated using the heatmap.2 function in the gplots R package.

*Gene set enrichment analysis (GSEA)*

Generation of a list of significantly overlapping datasets was computed using the Molecular Signatures Database v4.05 (MSigDB)[109]. Gene set enrichment analysis (GSEA) was performed by using the GseaPreranked function of GSEA v2.1.0 software (Broad Institute). For *in vitro* targets of Wnt/beta-catenin signaling, rank-ordered GSEA was performed by generating a rank-ordered list based on fold-change gene expression for either Wnt3a CM or Wnt3a CM+RSPO2 conditions relative to L-cell CM. EWS/ETS antagonism was determined in patient data by ranking genes based on correlation with *LEF1* expression in the clinically annotated dataset from the Children's Oncology Group (COG) (GSE 63157 [113], and gene set enrichment analysis (GSEA) was similarly performed.

*Statistics*

Unless otherwise indicated, data are expressed as mean ± standard error of the mean (SEM) from a minimum of three independent experiments. The data were analyzed using GraphPad Prism software by a Student's *t*-test and a *p*-value of 0.05 or less was considered significant.

## Chapter 3

## Tenascin C is regulated by Wnt/beta-catenin signaling and promotes ewing sarcoma metastasis


### Abstract

Metastasis is a major cause of mortality for patients with Ewing sarcoma. We have recently shown that Wnt/beta-catenin signaling can be strongly induced in Ewing sarcoma cells, that it promotes metastatic phenotypes, and that signaling is potentiated by the LGR5 ligand, R-spondin 2 (RSPO2). Interrogation of RNA-sequencing data identified the metastasis-associated extracellular matrix glycoprotein tenascin C as a putative downstream mediator of this metastatic phenotype. Quantitative real-time PCR and immunocytochemistry studies of multiple Ewing sarcoma cell lines validated that tenascin C is regulated by Wnt/beta catenin signaling. Given the context-dependent nature of downstream gene regulation by Wnt/beta-catenin ligands, we further investigated putative cells-of-origin, as well as other cancer cell lines to determine if regulation of *TNC* by Wnt/beta-catenin was unique to Ewing sarcoma cell lines. Through these studies, we found that regulation of *TNC* by Wnt3a/RSPO2 is variable among adult and pediatric cancers, while *TNC* is reproducibly induced by Wnt/beta-catenin in stem cells and variably potentiated by RSPO2. Functionally, we found that knockdown of TNC inhibits Wnt-induced as well as Wnt-independent Ewing sarcoma cell migration and metastasis both *in* vitro and *in vivo.* Thus, we have shown that Wnt/beta-catenin

signaling induces metastasis-associated genes, including *TNC,* in Ewing sarcoma. Furthermore, we have identified that autocrine production of tenascin C promotes Ewing sarcoma cellular migration and metastasis, thus implicating the RSPO2-Wnt-TNC axis as a candidate effector of tumor metastasis.

## Introduction

Ewing sarcoma is an aggressive bone and soft tissue that has a high propensity for metastasis. The mechanisms that mediate migration, invasion and metastasis in this tumor remain poorly understood. For epithelial tumors, a predominant hypothesis is that extracellular signals, often from the microenvironment, promote transcriptional programs that upregulate proteins that are critical for metastasis. Most notably, cells undergo a program that induces an epithelial to mesenchymal transition (EMT) and become highly invasive [122]. By nature, Ewing sarcoma already exhibits a mesenchymal phenotype, yet not all Ewing sarcoma tumor or cells have the ability to invade or metastasize. It is becoming increasingly recognized that expression of mesenchymal factors alone are not sufficient to promote metastatic and invasive states, but rather that cells must undergo functional cell state transitions.

In the previous chapter, we provided evidence that Wnt/beta-catenin signaling upregulates pro-metastatic adhesion and migration genes, and this results in cytoskeleton changes and induction of a migratory phenotype. It remains unclear which genes specifically mediate phenotypic changes. One of the genes most highly upregulated by Wnt3a CM and RSPO2 is tenascin C (TNC). TNC is strongly associated with metastasis and poor outcomes in numerous tumors [132, 133]. Thus, we hypothesized that tenascin C mediates aggressive phenotypes in Ewing sarcoma. TNC, encoded by the gene *TNC,* is a matricellular glycoprotein that functions as a modulator of interactions between the cell and the extracellular matrix [134]. It is minimally expressed in normal adult tissues, but up-regulated in numerous and diverse solid tumors including carcinomas [117, 132, 133, 135], melanoma [136], glioblastoma [135], and sarcomas [137]. TNC is a large multimeric protein composed of six similar subunits.

The *TNC* gene encodes a large region subject to alternative splicing, which generates 190-300 kDa variants that ultimately associate to form the larger oligomeric complex. During embryogenesis, tenascin C is broadly expressed and promotes a wide range of cellular functions including proliferation, migration, adhesion, immune modulation, and regulation of angiogenesis [134]. Notably, during the physiological EMT that neural crest cells undergo during normal development, TNC is strongly upregulated, and expression is essential for proper neural crest migration [138-140]. In tumors, TNC is frequently expressed by the stroma of a tumor, but in some contexts is also expressed by the tumor cells themselves [134, 141]. In some cancer cells, TNC promotes proliferation and migration [132-134]. Further, TNC is required for metastatic survival of breast cancer cells, as shown in a xenograft model of metastasis, where breast cancer cells that disseminated from a primary tumor were shown to upregulate and maintain expression of TNC in as in micro-metastatic foci [117]. Once tumors progressed from micro-metastases to macro-metastases, a marked increase in stromal expression of TNC was observed, thus suggesting that TNC acts as a niche component necessary for metastatic survival and outgrowth [117]. In this chapter, we sought to further investigate the regulation of tenascin C by Wnt/beta-catenin signaling, and to determine the function of this protein in Ewing sarcoma.

## Results

### *TNC is expressed by Ewing sarcoma cells*

Although TNC is highly expressed by many tissues during development, in adults its expression is limited with the exception of during wound healing. In contrast to normal tissue, adult and pediatric cancers frequently express TNC, but the expression patterns of TNC in Ewing sarcoma tumors and cell lines are only beginning to become understood [142]. To better understand TNC expression, we first interrogated publicly available microarray expression data for *TNC* in 117 Ewing sarcoma primary tumors relative to expression in 24 normal tissues (Fig. 3.1A). Here, we observed that *TNC* expression is on average higher in tumor samples than in normal tissue. In addition, a wide range of expression among patient samples is observed, indicating heterogeneity of expression among patients. We next used qRT-PCR to determine expression in a panel of Ewing sarcoma cells lines (Fig. 3.1B), and similarly observed heterogeneity of expression among cell lines. Immunocytochemistry studies were next performed in order to determine protein expression in the panel of cell lines (Fig. 3.1C). Here, we saw that TNC was detectable, albeit to varying degrees, in all cell lines, and was heterogeneous not only between cell lines, but also highly heterogeneous among individual cells. Taken together, these studies reveal that TNC is expressed by Ewing sarcoma tumor cells and this expression is heterogeneous among tumors, as well as variably expressed by individual cells.

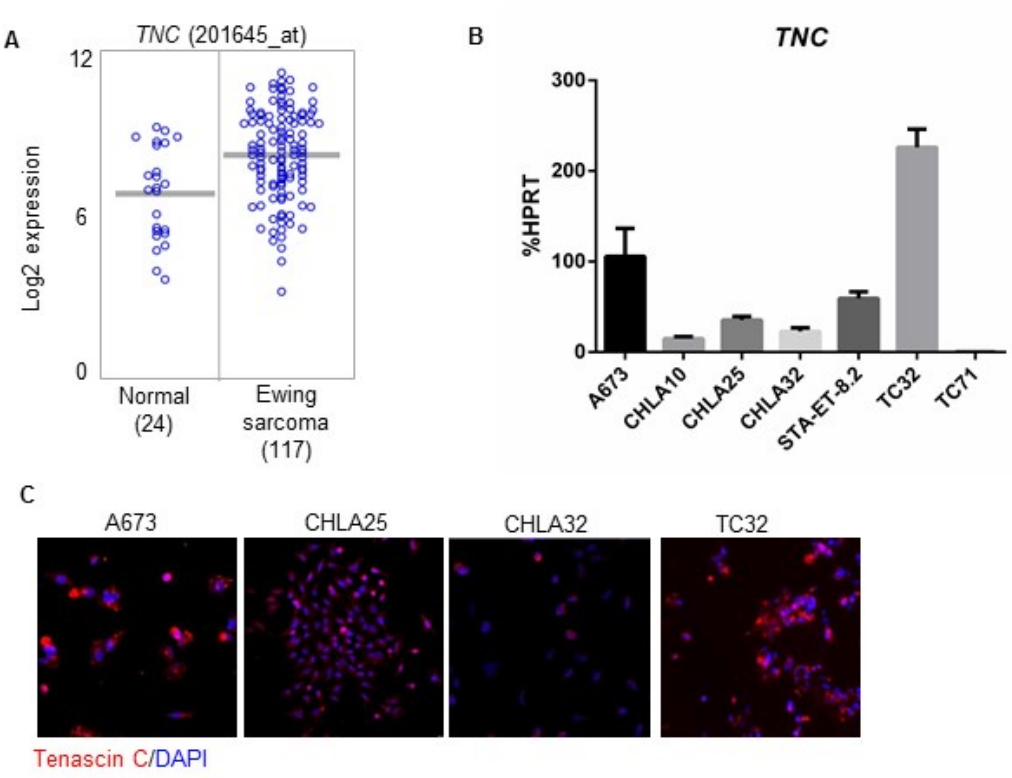


**Figure 3.1. Tenascin C is variably expressed in Ewing sarcoma.**

(A) Published microarray gene expression profiling data from 117 primary Ewing sarcoma samples (GEO accession # GSE34620) reveals that on average, *TNC* expression is higher in primary Ewing sarcoma tumors than in normal tissue. (B) qRT-PCR of seven Ewing sarcoma cell lines reveals highly variable *TNC* transcript expression among cell lines with very high expression in TC32 cells and nearly undetectable levels in TC71. (C) Immunocytochemistry for tenascin C reveals both inter- and intra-cell line heterogeneity of tenascin C expression in Ewing sarcoma cell lines.

### *TNC is regulated by Wnt/beta-catenin signaling in Ewing sarcoma*

The mechanisms that regulate TNC expression in Ewing sarcoma are largely unknown. Interrogation of the list of Wnt/beta-catenin and EWS/ETS co-regulated genes identified *TNC* as one of the most highly up-regulated genes by Wnt3a/RSPO2 in CHLA25 cells (see Table 2.1, Fig 2.9A ). We next sought to determine if regulation of *TNC* by Wnt3a is reproducible in other Ewing sarcoma cell lines. qRT-PCR (Fig. 3.2A)

and immunocytochemistry (Fig. 3.2B) confirmed that *TNC* is induced two-fold or more in Ewing sarcoma cells in response to exogenous Wnt ligands in all cell lines tested, although potentiation with RSPO2 was variable. In most cell lines, TNC induction was unaffected by RSPO2. As expected, the two cell lines that express high levels of *LGR5,* CHLA25 and CHLA32, had the most robust potentiation of *TNC* in response to RSPO2. Next, we investigated if Wnt activation was associated with *TNC* expression in primary tumors. Using *LEF1* as readout of Wnt/beta-catenin activation, we found a positive and significant correlation between *LEF1* and *TNC* expression (Fig. 3.2C), suggesting that high Wnt activity contributes to *TNC* expression *in vivo.* To establish that *TNC* is directly regulated by beta-catenin signaling, A673 cells were transduced with a constitutively active beta-catenin (EβP) construct. In EβP cells, and *TNC* expression was upregulated in the absence of exogenous ligands, confirming that Wnt-dependent regulation is, at least in part, mediated by beta-catenin (Fig. 3.2D). Evidence that EWS/FLI-1 regulates *TNC* is conflicting. In one report, *TNC* was induced upon introduction of EWS/FLI-1 into heterologous cells [142], while two other studies demonstrated *TNC* induction following EWS/FLI1 knockdown in Ewing sarcoma cells [19, 22]. We measured *TNC* expression with and without doxycycline-mediated silencing of EWS/FLI-1 in shA673-1C cells and observed a robust induction of *TNC* in cells with reduced EWS/FLI-1 (Fig. 3.2E). This induction was slightly enhanced upon addition of Wnt3a. These data indicate that *TNC* is indeed an EWS/ETS-repressed gene, and this repression is antagonized by Wnt/beta-catenin signaling.

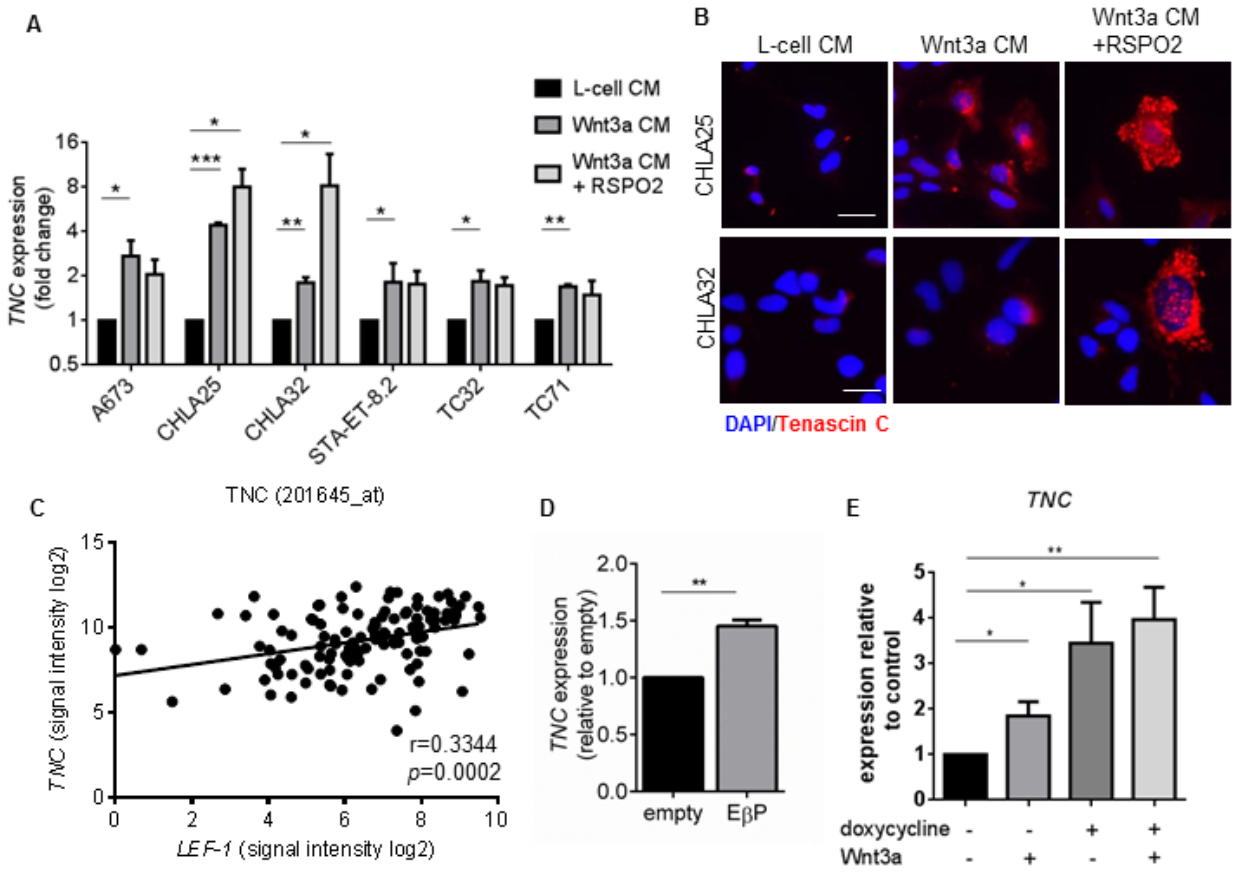


**Figure 3.2 TNC is regulated by Wnt/beta-catenin signaling in Ewing sarcoma**

(A) Ewing sarcoma cells were stimulated with Wnt3a CM +/- RSPO2 for 24 hr and *TNC* expression was measured by qRT-PCR. *TNC* was significantly induced by Wnt3a CM in all cell lines tested, but variably potentiated by RSPO2. *P*-values were determined using the Student's t-test. **p*<0.05, ***p*<0.01, ****p*<0.001. (B) Tenascin C expression, assessed by immunocytochemistry, is induced by Wnt3a CM and potentiated by RSPO2 in LGR5-high expressing cell lines CHLA25 and CHLA32. Scale bar = 20 μm. (C) High *LEF1* expression in primary Ewing sarcoma tumors is positively correlated with *TNC* expression. *r*=Pearson's correlation between *TNC* and *LEF1.* (D) A673 cells transduced with a constitutively active beta-catenin construct (EβP) express significantly higher *TNC* compared to empty vector control cells. *P*-values was determined using the Student's t-test. ***p*<0.01 (E) A673 cells transduced with a doxycycline-inducible shRNA against EWS-FLI1 (shA673-1C) reveal an induction of *TNC* both with addition of recombinant Wnt3a and doxycycline, indicating that *TNC* is repressed by EWS-FLI1. *P*-values were determined using the Student's t-test. **p*<0.05, ***p*<0.01.

### *TNC is variably regulated by Wnt/beta-catenin in stem cells and other tumors*

Regulation of *TNC* by Wnt/beta-catenin is evident in Ewing sarcoma, but it is unknown if expression of *TNC* in other tissues is governed by Wnt/beta-catenin signaling, including during normal development. In order to better understand the context in which *TNC* is a transcriptional target of Wnt/beta-catenin, we specifically focused on stem cells representing putative cells-of-origin. The stem cells assessed were of varying neural crest and mesenchymal potential, and included human embryonic stem cell-derived neural crest stem cells (hNCSC), human patient-derived mesenchymal stem cells (hMSC), and mouse cranial neural crest cells (mCNCs), which are considered to be of neuro-mesenchymal lineage. We interrogated basal *TNC* expression and found that hMSCs expressed over ten-fold as much *TNC* as hNCSCs, while mCNC cells had intermediate expression (Fig. 3.3A). To determine if expression was regulated by Wnt3a +/- RSPO2, we stimulated cells as aforementioned and found that hNCSC robustly induced *TNC* in response to Wnt3a, and this was further potentiated by RSPO2 (Fig. 3.3B). Regulation of *TNC* was only induced by Wnt3a CM in hMSCs but not Wnt3a +RSPO2, and not significantly induced in mCNC (Fig. 3.3B).

In colorectal carcinoma, TNC is expressed at the invasive borders of tumors with nuclear beta-catenin [143] but regulation of *TNC* by Wnt/beta-catenin in other cancer cells has not been reported. To better understand the context in which *TNC* is regulated, we stimulated other non-Ewing sarcoma cell lines of differing lineages, and included both pediatric (Fig. 3.3C,D) and adult (Fig. 3.3E) cancers. Upon stimulation with Wnt3a CM +/- RSPO2, neuroblastoma cells SH-SH-5Y (5Y), SHEP, and IMR32 variably regulated *TNC.* The highly aggressive cell line IMR-32 showed a pattern of regulation most similar to hNCSCs and Ewing sarcoma cell lines, whereas the less

aggressive cell line SHEP down-regulated *TNC* (Fig. 3.3C). Osteosarcoma cell lines SaOS2 and U2OS similarly showed variable regulation, although the pattern of regulation in SaOS2 was highly reminiscent of the pattern observed with hMSCs (Fig. 3.3D), likely reflecting its mesenchymal origin. The adult epithelial cancers A549 (lung adenocarcinoma), HeLa (cervical cancer), and MDA-MB-231 (breast cancer) showed inconsistent induction of *TNC* (Fig. 3.3E). Of all cell types tested, hNCSCs had a pattern of *TNC* regulation most similar to that seen in Ewing sarcoma. Other pediatric cancer and epithelial cancers exhibited divergent regulation of *TNC*, underscoring the context-specificity of downstream Wnt/beta-catenin target genes.

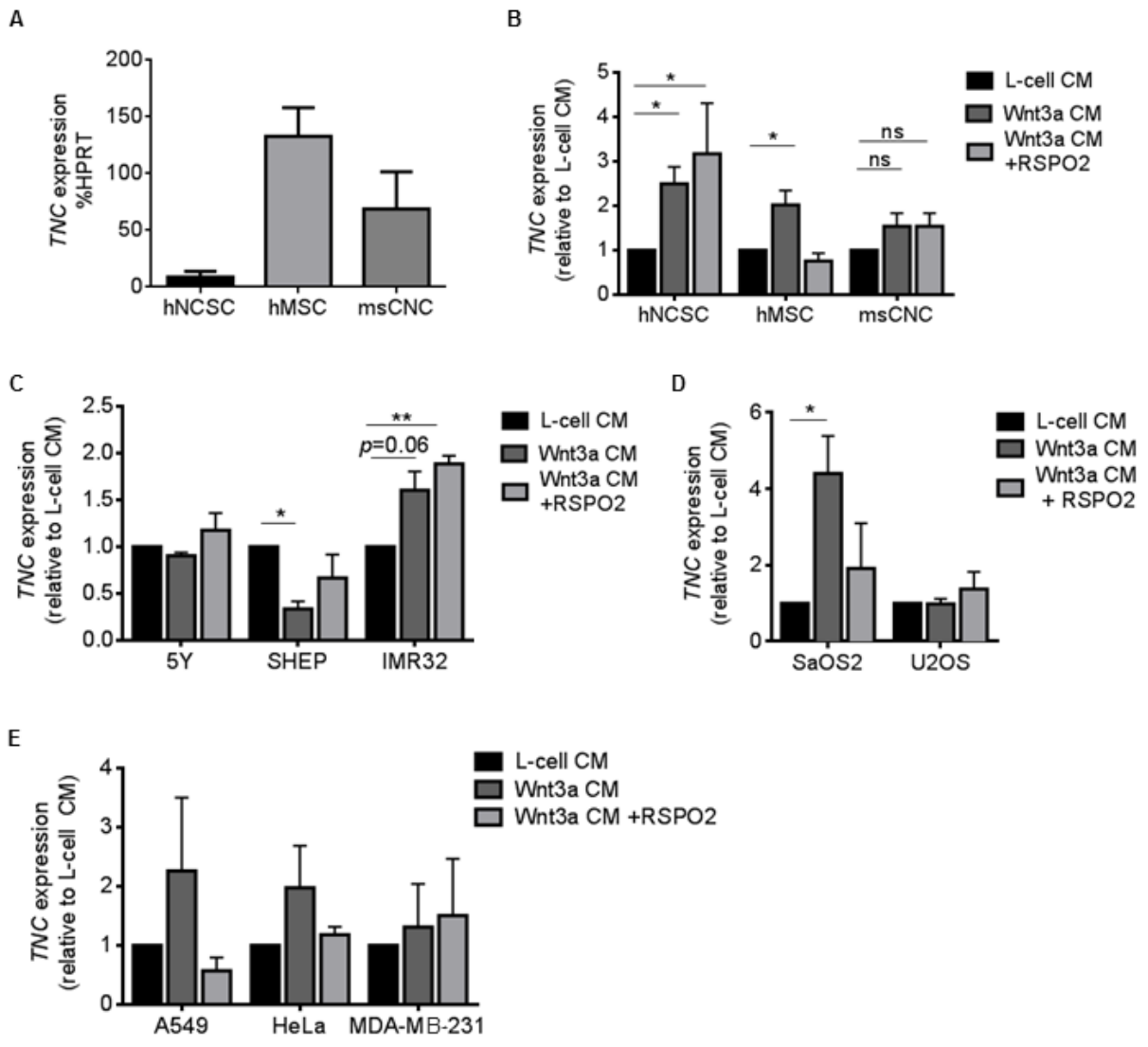


**Figure 3.3 TNC is expressed and variably induced by Wnt3a CM in stem cells and non-Ewing sarcoma tumors.**

(A) Basal *TNC* expression was measured in putative cells-of-origin by qRT-PCR. Stem cells (B), pediatric cancer cell lines derived from neuroblastoma (C), and osteosarcoma (D), and adult epithelial cancer cell lines (E) were stimulated with Wnt3a CM +/-RSPO2 and expression of *TNC* was measured by qRT-PCR. The regulation of *TNC* by Wnt3a was variable from tumor to tumor type, as well among cell lines of the same tumor type. All *p*-values were determined using the Student's t-test. *$p<0.05$.

### *TNC promotes Ewing sarcoma cell migration and tumorigenicity* in vivo

Having established that *TNC* is consistently regulated by Wnt/beta-catenin in Ewing sarcoma, we next sought to determine its role in pathogenesis through loss-of-function studies. TNC abrogation was achieved using shRNA delivered to cells by lentiviral transduction, and knockdown was verified using qRT-PCR to assess transcript levels (Fig. 3.4A), and immunocytochemistry to assess protein expression (Fig. 3.4B). In tumors, TNC can promote proliferation and migratory phenotypes in vitro. First, proliferation was assessed using an MTS assay. Knockdown of TNC had no effect on cell proliferation *(*Fig. 3.4C). Transwell assays were performed to assess migration, and revealed that loss of TNC strongly inhibited cell migration (Fig. 3.4D). The effects of TNC on tumorigenicity have not been described, so cells containing control or TNC knockdown were plated as single cells in soft agar and allowed to form colonies. After three weeks, shNS control cells readily formed colonies, but cells with TNC knockdown were severely inhibited in their ability to form anchorage-independent colonies (Fig 3.4E). Thus, loss of TNC results in dramatic reductions in migration and tumorigenicity that are independent of proliferation.

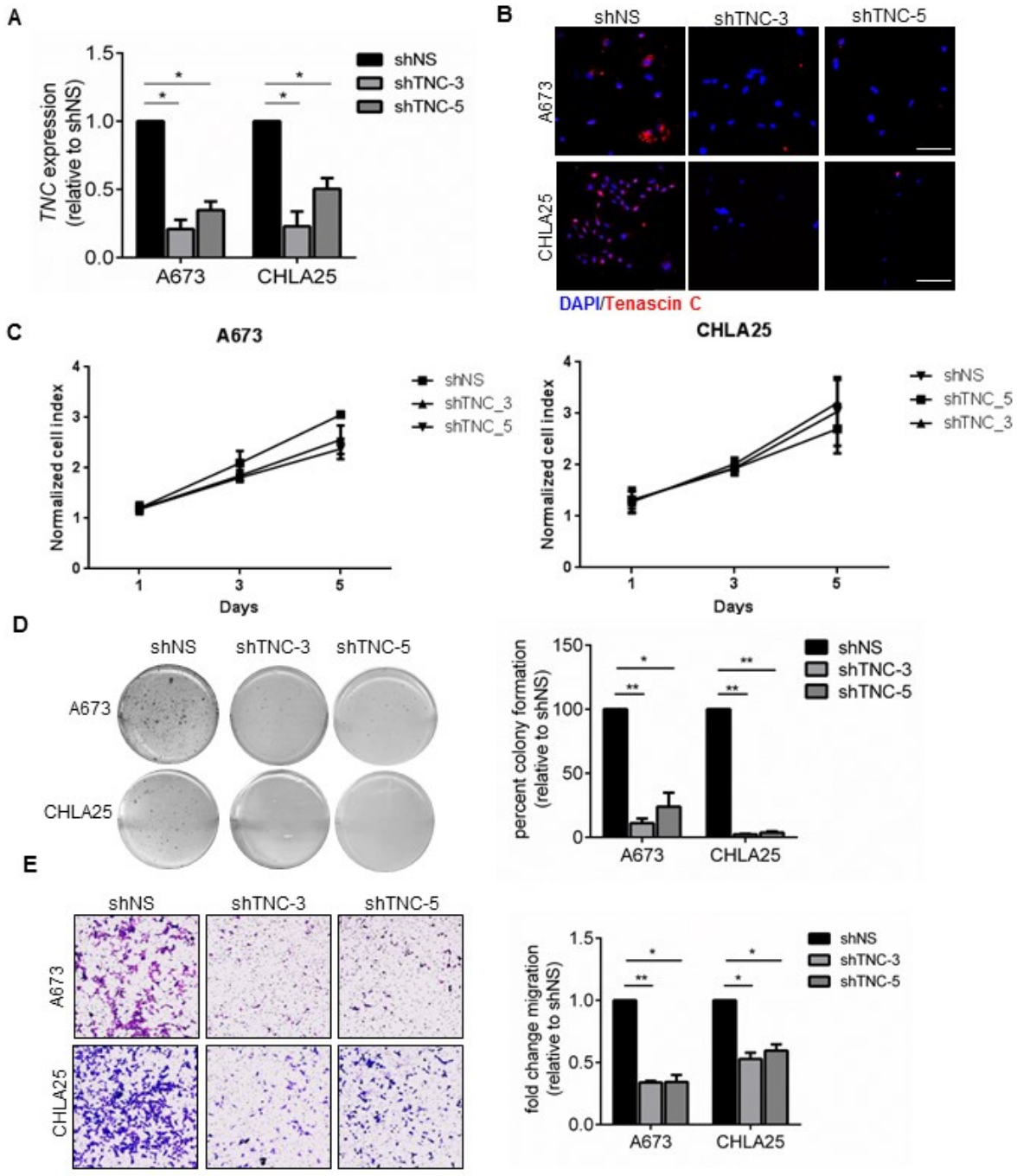


**Figure 3.4 Tenascin C promotes colony formation and migration *in vitro.***

Validation of tenascin C knockdown by qRT-PCR (A) and immunocytochemistry (B) in two Ewing sarcoma cell lines using two independent shRNAs targeting TNC.*P*-values were determined using the Student's t-test. *$p<0.05$. (C) shTNC cells have no significant changes in proliferation compared to shNS cells, as assessed by MTS assay. Differences between groups were not statistically significant as assessed by Student's t-test. (D) Loss of TNC strongly inhibits the ability of cells to form colonies in soft agar.

Data is shown as average colonies per well for n=3 independent experiments. *P*-values were determined using the Student's t-test. *$p<0.05$, **$p<0.01$. (E) Loss of TNC significantly inhibits transwell migration of Ewing sarcoma cells. Data is shown as average colorimetric absorbance of migrated cells for n=3 independent experiments. *P*-values were determined using the Student's t-test. *$p<0.05$, **$p<0.01$.

We next sought to determine if TNC mediates the migratory phenotype induced by Wnt3a. In transwell assays, control or TNC knockdown cells were induced to migrate by Wnt3a +/-RSPO2. In cells with TNC knockdown, a significant reduction of Wnt-induced migration was observed in both A673 (Fig. 3.5A) and CHLA25 (Fig. 3.5B) cells, indicating that the Wnt-induced migratory phenotype is mediated in part by TNC.

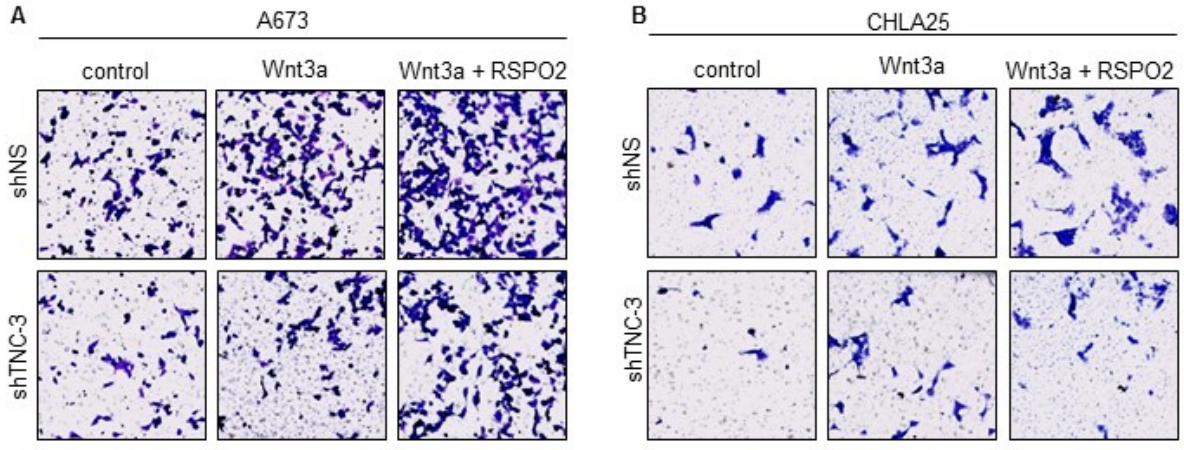


**Figure 3.5 Tenascin C mediates Wnt-induced migration.**

(A) A673 (B) CHLA25 cells transduced with lentivirus containing non-silencing (shNS) or shRNA against TNC (shTNC-3) were stimulated with control, Wnt3a, or Wnt3a +RSPO2 and allowed to migrate for 24 hr. TNC abrogation in part inhibits migration induced by Wnt.

### *TNC promotes in vivo* metastasis of Ewing sarcoma cells

To assess the impact of TNC knockdown *in vivo,* luciferase-tagged cells were similarly transduced with control non-silencing (shNS) or TNC knockdown vector (shTNC-3) (Fig. 3.6A). Cells were injected subcutaneously in Matrigel and tumor

formation was measured by calipers. After three weeks, A673 shNS readily formed tumors, while shTNC-3 cells failed to grow (Fig. 3.6B). TC32 cells are highly tumorigenic and express high levels of TNC, even with shRNA-mediated knockdown (Fig. 3.6A). Tumors formed from both control and TNC knockdown cells, although tumors with TNC were smaller on average (Fig. 3.6C). When TC32 cells were injected *via* tail vein into NOD-SCID mice, all but one of the control mice (7 of 8) formed metastatic tumors by seven weeks post-injection, whereas none of the TNC knockdown recipient mice showed evidence of tumor formation (0 of 7) (Fig. 3.6D,E), implicating TNC as important mediator of metastatic engraftment. Thus, like breast cancer cells [117], successful creation of metastatic tumors from circulating Ewing sarcoma cells is critically dependent on TNC, which we have identified to be induced in response to Wnt/beta-catenin activation. Based on these data, it appears likely that TNC is more important for metastatic engraftment compared to subcutaneous engraftment and tumor formation, especially in TC32 cells, which have high levels of TNC even upon shRNA-mediated knockdown (Fig, 3.6A). In A673, however, which has lower levels of TNC (Fig. 3.6A), it is likely that TNC is required for any tumor engraftment (Fig. 3.6B). These data together provide compelling evidence to support a model of Ewing sarcoma tumor plasticity linking Wnt/beta-catenin signaling to metastatic progression and poor clinical outcomes via induction of TNC.

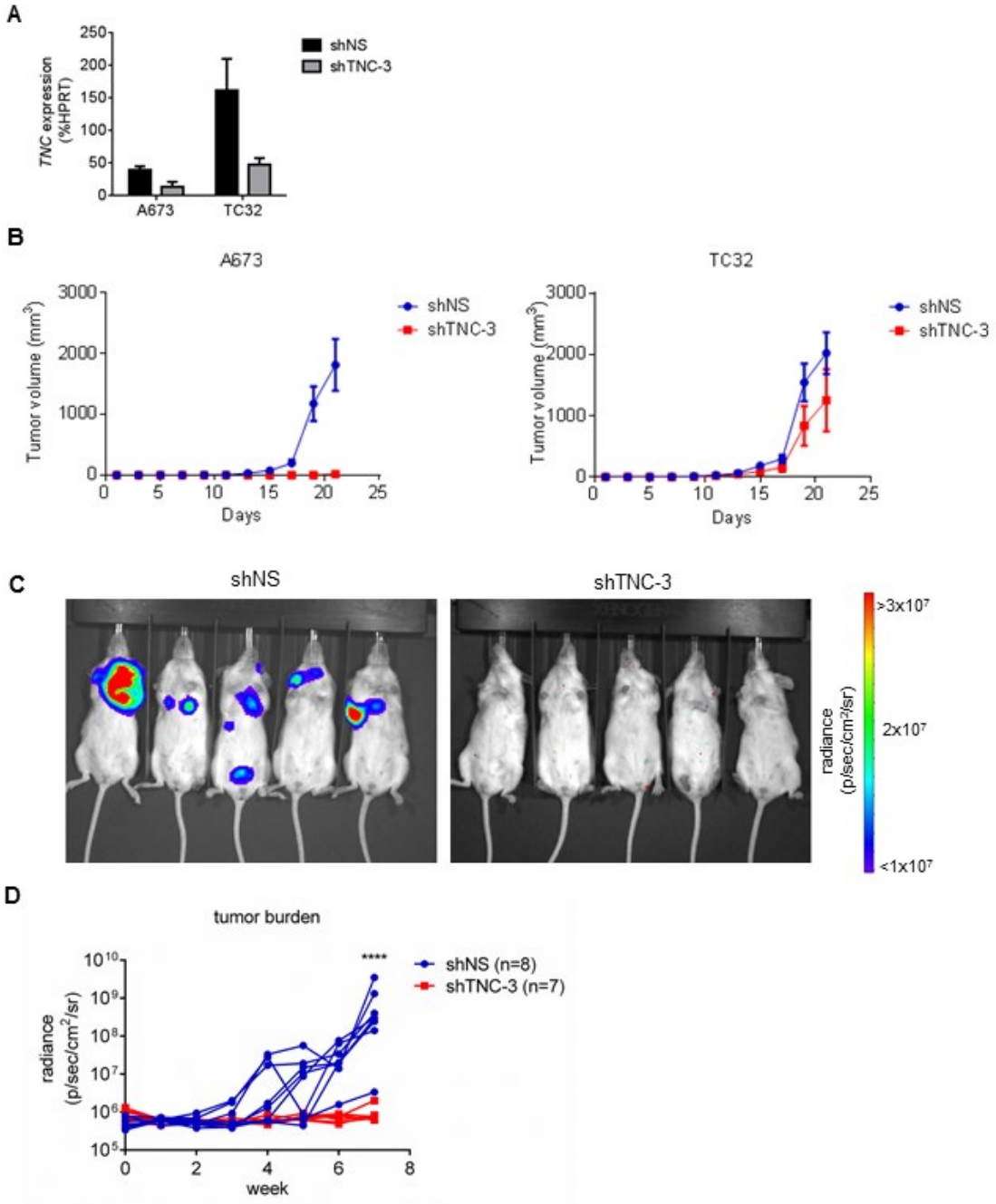


**Figure 3.6 Tenascin C promotes tumor engraftment and metastatic establishment *in* vivo.**

(A) A673 and TC32 GFP/luc-cells were transduced with lentivirus containing shNS or shTNC3 vectors, and knockdown of TNC was achieved in shTNC3 cells as assessed by qRT-PCR. Data is expressed as percent of the housekeeping gene *HPRT1.* (B) Cells in (A) were injected subcutaneously in Matrigel and tumor growth was monitored for three weeks by calipers. Abrogation of TNC dramatically inhibited tumor formation in A673 cells, while TNC knockdown in TC32 cells resulted in decreased proliferation. (C) TC32 cells containing TNC knockdown were injected intravenously via the tail vein and

followed by bioluminescence imaging for seven weeks (D). Loss of TNC in TC32 cells dramatically inhibited metastatic tumor formation. *P*-value was determined using the Student's t-test. ****$p<0.0001$.

## Discussion

In these studies, we have identified Tenascin C *(TNC)* as a critical and highly responsive target of Wnt/beta-catenin signaling in Ewing sarcoma. In all Ewing sarcoma cell lines tested, *TNC* was induced by Wnt3a, and this induction was even more pronounced in highly-Wnt responsive cells upon addition of RSPO2. Induction and potentiation of *TNC* by Wnt3a/RSPO2 was variably regulated in stem cells and other cancer cell lines. Functionally, we found that inhibition of TNC expression in part abrogates Wnt/RSPO2 induced migration in Ewing sarcoma cells, and also inhibits intrinsic Wnt-independent migration. Further, inhibition of TNC dramatically decreased the ability for Ewing sarcoma cells to form colonies in soft agar, thus reflecting a decrease in tumorigenicity. *In vivo* tumor formation was reduced, and lung engraftment of cells with *TNC* knockdown was virtually eliminated compared to control cells, identifying a key role for TNC tumor engraftment, especially in the setting of lung metastasis. Similar to how epithelial cells undergo phenotypic cell transitions to become more metastatic, these data suggest that Wnt/beta-catenin upregulate TNC to promote cell state transitions. Interestingly, TNC can induce EMT in epithelial cells [144-146] and is also found in vimentin positive cells [147], suggesting that it is also involved in the metastatic EMT of epithelial tumors. Since Ewing sarcoma cells are already in a mesenchymal state, perhaps acquisition of TNC via Wnt-mediated phenotypic transitions are analogous to EMT and ultimately result in induction of the same critical metastasis protein.

Although *TNC* has been described as a transcriptional target of Wnt/beta-catenin in other studies [143, 148], regulation of *TNC* expression by the Wnt pathway has not been well-validated in other cancers. Our studies reveal that induction of *TNC* in Ewing

sarcoma cells is robust compared to other cancers tested, and underscores the context-dependent nature of Wnt target genes. Interestingly, the regulation of *TNC* by Wnt3a/RSPO2 in NCSCs was most similar to its regulation in LGR5-high Ewing sarcoma cell lines. Alternatively, MSCs have a pattern of regulation characterized by induction by Wnt3a but down-regulation by Wnt3a+RSPO2, this same pattern was observed in the osteosarcoma cell line SaOS2. This may suggest that cells with more osteo-mesenchymal characteristics may be subject to feedback down-regulation of *TNC,* or other regulatory mechanisms. This difference in regulation among different cell types may be a reflection of the original cell-of-origin. Perhaps some Ewing sarcoma tumors arise from cells with strong NCSC characteristics, such as high LGR5 expression[3] and neuro-mesenchymal differentiation potential, whereas less Wnt-responsive Ewing sarcoma tumors, as well as other tumors like osteosarcoma, may arise from MSC-like cells. Differences in TNC induction are also likely affected by expression of LGRs and other Wnt pathway receptors, but gain-and-loss of function studies of these receptors are required to definitively understand their contributions to TNC regulation. In addition, chromatin accessibility strongly differs among different cell types and states of differentiation. Given the heterogeneous presentation of Ewing sarcoma tumors, perhaps reflecting different cells of origin, it is likely that chromatin accessibility may influence the ability for the individual Ewing sarcoma tumors and other cell types to induce TNC expression in response to Wnt/beta-catenin.

Heterogeneity of *TNC* expression is evident among patient transcript in published microarray data, and our studies reveal marked expression of TNC protein among individual cells in each cell line. It remains unknown if this heterogeneity is evident in primary tumors, and histological staining of a tumor microarray would greatly benefit our

understanding. For instance, it is unclear whether *TNC* expression is primarily in the tumor cells, the surrounding stroma, both, or variable between tumors. If there is variability among patients between predominantly stromal and tumor cell expression, it would be interesting to separate patients based on expression patterns and compare outcomes. Given that breast cancer cells up-regulate tenascin C during the metastatic cascade, and then the stroma re-establishes expression in secondary sites[117], one could hypothesize that patients whose tumor cells display the ability to express TNC might be more metastatically competent than tumors that only have stromal TNC expression.

In our studies, we observed that expression of TNC confers metastatic ability, and metastatic potential is dramatically reduced when its expression is abrogated. The mechanisms that mediate the migratory and metastatic potential remain unclear. The plethora of functions attributed to TNC provides many avenues for further exploration. One possibility is that TNC may modulate metastatic efficiency through cellular adhesion. In many contexts, tenascin C promotes de-adhesion from fibronectin to promote an intermediate state of adhesion conducive to migration, as strongly adherent cells do not move [134]. Despite this de-adhesive function, TNC also binds to numerous integrins [141]. Binding to certain integrin receptors combinations promotes cellular attachment, and thus may promote cellular attachment in distant metastatic sites. Further engagement of integrin receptors may also induce downstream signaling in stromal cells, which can induce expression of enzymes involved in matrix remodeling [149] and promote metastatic niche formation. TNC could also protect metastatic cells from anoikis, which is the process of apoptosis induced by cellular detachment. It has been shown that TNC promotes cell survival by activation of Akt [150]. Activation of Akt

in turn can protect cells from anoikis [151]. Thus, TNC expression may induce autocrine signaling required for survival during circulation and throughout the metastatic cascade. The heterogeneous expression of TNC among individual tumor cells in a cell line (Fig. 3.1C), may also be indicative of a paracrine signaling process, suggesting that TNC could have differential effects on cells within a cell line. Taken together, our data strongly warrants further explorations into the mechanisms of TNC-mediated tumor progression, and provides a novel therapeutic target for consideration of metastasis prevention in Ewing sarcoma.

## Experimental Procedures

*Cell lines and lentiviral transductions*

Ewing sarcoma cell lines were maintained in RPMI 1640 media (Gibco) supplemented with 10% FBS (Atlas Biologicals) and 2mM L-glutamine (Life Technologies). CHLA25, CHLA32, and STA-ET-8.2 were grown on plates coated with 0.2% gelatin. SaOS2 and U2OS, and HeLa were similarly maintained. MB-MDA-231 was maintained in DMEM containing 10% FBS. A549 was maintained in F12K media containing 10% FBS. shA673-1C cells were kindly provided by Dr. Olivier Delattre and maintained as previously described (21). SH-SY-5Y (abbreviated 5Y) and SHEP were maintained in MEM (Gibco). IMR32 were maintained in MEM supplemented with 7.5% sodium bicarbonate. L-cells (ATCC CRL-2648) and Wnt3a L-cells (ATCC CRL-2647) were cultured in DMEM (Gibco) with 10% FBS. All cells were verified to be mycoplasma negative and identities confirmed by STR profiling. Lentiviral production and transduction was performed as previously described (20), and the following plasmids were used: Addgene #24305 (7TGP), Addgene #24313 (EβP), Sigma TRCN0000230788 (shTNC-3), Sigma TRCN000015400 (shTNC-5), UM-vector core pLentilox-luciferase/GFP (luc-tagged). Cells were selected in puromycin (2 μg/mL).

*Generation of stem cells*

The stable cranial neural crest cell line were a gift from the Robert Maxson laboratory and were cultured adherently in a basal medium conditioned by STO feeder cells and supplemented with 25 ng/ml bFGF (R&D Systems) and 1,000 U/ml mouse LIF (Millipore) [152]. hMSC were a gift from the Paul Krebsbach lab and cultured in MEM

containing 10% Stem-cell grade FBS (Thermo Fisher). hNCSCs were derived from human embryonic stem cells as previously described[50].

*Analysis of gene expression*

Wnt targets were validated by quantitative RT-PCR, using standard methods as earlier described. The sequences of primers used are listed in Table 3.1.

| Gene | Forward primer sequence | Reverse primer sequence |
|---|---|---|
| *HPRT1* | TGACACTGGCAAAACAATGCA | GGTCCTTTTCACCAGCAAGCT |
| *TNC* | GCAGCTCCACACTCCAGGTA | TTCAGCAGAATTGGGGATT |
| *Hprt1* | AGTCCCAGCGTCGTGATTAG | TTTCCAAATCCTCGGCATAATGA |
| *Tnc* | ACGGCTACCACAGAAGCTG | ATGGCTGTTGTTGCTATGGCA |

**Table 3.1 Primer sequences used for qRT-PCR**

Immunofluorescence microscopy

Cells were grown on gelatin-coated coverslips and protein expression evaluated by standard techniques and immunofluorescence microscopy as previously described (20). Tenascin C was detected using anti-Tenascin C (Sigma, 1:100) primary followed secondary antibody (Alexafluor 594, 1:500). Slides were counterstained using DAPI (1:10,000) (Invitrogen), mounted using Prolong Gold (Molecular Probes, Life Technologies) and imaged using an Olympus CKX41 microscope with Nikon Elements software version 3.

*Proliferation assay*

$5x10^3$ cells were plated in triplicate on 96 well plates, and cells were allowed to proliferate for five days. Cell proliferation was monitored at days 0, 1, 3, and 5 using the CellTiter 96 AQueous One Solution Cell Proliferation Assay (Promega, Madison, WI)

according to the manufacturer's instructions. Colorimetric absorbance (490 nm) was quantified on a BioTek plate reader. Background readings for each day were subtracted from blank wells. Data is expressed as the normalized cell index, which is the background-corrected absorbance normalized to the day 0 reading.

*Migration assays*

$1x10^5$ cells in serum-free RPMI were added to transwells containing 0.8 μm pores with serum-containing media in the bottom chamber. After 24hr cells were fixed using a solution of 25% crystal violet and 25% methanol and membranes were imaged and then cells eluted using crystal violet in 10% acetic acid. Colorimetric absorbance (540 nm) was quantified on a BioTek plate reader.

*Colony formation assay*

Colony formation was assessed by plating a single cell suspension of $1 \times 10^4$ cells per well of six well plates in 0.35% noble agar on a layer of 0.5% noble agar. Colonies were stained with a solution of 0.005% crystal violet and counted three weeks later.

*In vivo assays*

To assess tumor growth, $2.5x10^5$ A673 or TC32 cells containing shNS or shTNC3 vectors were re-suspended in Matrigel and implanted subcutaneously into 10-12 week-old NOD SCID mice (strain 394, Charles River Laboratories, Wilmington, MA). Each mouse was implanted with a shNS tumor on the left flank and a shTNC-3 tumor on the right flank. Tumors were measured every other day by calipers, and tumor volume was determined using the formula $V=1/2ab^2$, where a is the longer dimension and b is the

shorter. To assess metastatic capacity, $1x10^6$ luciferase-labeled TC32 cells containing shNS or shTNC3 vectors were injected via tail vein into 10-12 week-old NOD SCID mice. Satisfactory injection of viable cells was confirmed by detection of light emission in the lungs of recipient mice 30 minutes after cell injection on a Xenogen IVIS bioluminescence system (Perkin Elmer, Waltham, MA). Imaging was repeated weekly and tumor burden quantified using Living Image software (Perkin Elmer, Waltham, MA). Mice were monitored for 7 weeks, at which point mice were euthanized due to signs of tumor-related ill health in control mice.

Statistics

Unless otherwise indicated, data are expressed as mean ± standard error of the mean (SEM) from a minimum of three independent experiments. The data were analyzed using GraphPad Prism software by Student's t-test and p-values $< 0.05$ considered significant.

## Chapter 4

## Prognostic and Therapeutic Significance of Wnt/beta-catenin signaling in the context of the ewing sarcoma Microenvironment


### Abstract

We have previously shown that Wnt/beta-catenin is heterogeneously active in Ewing sarcoma patient tumors, and that Wnt ligands similarly induce heterogeneous activation *in vitro*. Mechanistically, we found that Wnt/beta-catenin signaling antagonizes EWS/ETS transcriptional activity to promote metastatic phenotypes, in part through up-regulation of the metastasis gene tenascin C. In this chapter, we further investigated the clinical and therapeutic relevance of these findings, and expanded the scope of the effects of Wnt signaling to include potential interactions with the tumor microenvironment. In particular, we evaluated the prognostic significance of high nuclear beta-catenin in primary tumors, in addition to the downstream Wnt/beta-catenin target LEF-1. High expression of these molecules was significantly associated with poor clinical outcomes. LEF1 expression was correlated with 28/33 genes in a previously published signature of poor prognosis, as well as with genes involved in tumor microenvironment-mediated processes. To test the functional relevance of Wnt/beta-catenin activation in a physiologic microenvironment, cells with beta-catenin activation were grown the in the chick chorioallantoic membrane (CAM) assay, and a pronounced migratory and mild angiogenic phenotype were observed. Despite the angiogenic

phenotype in the CAM assay, as well as induction of angiogenesis-associated pathways in response to beta-catenin activation, no significant effects were seen on angiogenic endothelial differentiation. This was further supported by the fact that expression of CD31, an immunohistological marker of angiogenesis, had no prognostic significance in patient tumors. Finally, we therapeutically targeted the Wnt/beta-catenin pathway by neutralizing endogenous RSPO2 *in vivo* using the monoclonal antibody MT130-230, and show that this inhibition results in decreased metastatic incidence.

## Introduction

In order to generate therapeutic strategies to improve outcomes for patients, it is important to consider tumor biology in the context which tumors exist in patients—that is, in a physiologic microenvironment. The tumor stroma exists as a dynamic, multifaceted and interdependent ecosystem of cells, proteins, and ions. Key components of the microenvironment include the extracellular matrix, endothelial cells, immune cells, and fibroblasts, all of which can contribute to pathological processes. The bone microenvironment is particularly conducive to tumor growth and metastasis, as it is rich in cytokines and signaling molecules, and further possesses a well-defined cellular architecture, or “niche” that is conducive to stem cell maintenance and homeostasis [153, 154]. Tumor cells can co-opt this niche for their own survival [155]. Further, Ewing sarcoma is a highly osteolytic tumor, and its clinical presentation is characterized by extensive bone destruction. This osteolysis occurs though tumor-mediated activation of osteoclasts, and results in release of growth factors including TGF-beta, IGF-1, and PDGF, which can in turn signal back to tumor cells, promoting growth and further tumor progression [153].

Although the specialized bone microenvironment is particularly conducive to Ewing sarcoma tumor growth and development, the fact that Ewing sarcoma cells in extra-skeletal tissue demonstrates that some tumors do not require the relatively specialized environment of the bone, and further may directly modify their surroundings to better suit their needs. It is likely that tumor interactions with the stroma have clinical and biological significance. In a study to define gene signatures associated with poor prognosis, whole genome expression profiling revealed that Ewing sarcoma patients with poor clinical outcomes demonstrated enrichment for genes involved in integrin,

chemokine, and angiogenic pathways [113], thus suggesting microenvironment-mediated processes.

Given the lack of activating Wnt pathway mutations in tumors, and further absence of autocrine Wnt/beta-catenin activation in Ewing sarcoma cells lines, it is likely that tumors with evidence of nuclear beta-catenin are responding to Wnt ligands provided by the tumor microenvironment. Indeed cancer associated fibroblasts (CAFs) in the stroma [156], as well as normal osterix positive cells are a source of Wnt ligands [77] in the microenvironment, suggesting that microenvironment involvement promotes Wnt/beta-catenin activation. It further remains unknown, however, if Wnt/beta-catenin activation in Ewing sarcoma also influences the microenvironment. In the following studies, we investigate the prognostic and functional significance of Wnt/beta-catenin activation both in and on the tumor microenvironments, and explore putative downstream pathways including IGF1 and TGF-beta, which provide opportunities for crosstalk. Finally, we attempt to therapeutically target the Wnt/beta-catenin pathway by neutralizing endogenous RSPO2 *in vivo*, and show that this inhibition results in decreased metastatic incidence.

## Results

### *Beta-catenin/LEF1 expression results in poor clinical outcomes*

In Chapter 2, we analyzed a small tumor microarray (TMA) of patient biopsies for evidence of Wnt/beta-catenin activation. In some of these biopsies, we found that beta-catenin was detectable in both the cytoplasmic and nuclear compartments, and revealed marked inter- and intra-tumoral heterogeneity. Of the six tumors that robustly expressed nuclear beta-catenin, all (100%) relapsed. Nuclear beta-catenin was low or undetectable in 31 patients, and 18 (58%) relapsed. With similar methodology as previously described, we used tissue from a new and larger, clinically annotated tissue microarray (TMA), denoted as TMA9, to perform more detailed immunohistological analyses on a larger patient sample size. The new TMA included data for 108 patients, with multiples records for each patient. Of these patients, 51 Ewing sarcoma patient samples were able to be utilized for further analysis. The TMA was stained for beta-catenin, and staining was quantified using AQuA technology. Correlation with nuclear beta-catenin expression and overall/event free survival was determined. Patients with evidence of elevated nuclear beta-catenin (Fig. 4.1A) experienced significantly worse overall survival and progression free survival, further supporting our earlier findings that elevated nuclear beta-catenin is associated with worse clinical outcomes.

As detailed in Chapter 2, the Wnt pathway gene *LEF1* is strongly induced by Wnt/beta-catenin activation, and patients with evidence of high *LEF1* transcript expression experienced worse outcomes. In addition to transcript data, we next sought to determine if LEF1 protein expression was similarly regulated and associated with a poor prognosis. In keeping with our transcript data, we found that cells stimulated with

Wnt3a +/- RSPO2 strongly upregulated protein expression of LEF1 (Figure 4.1B). To determine if patients with high levels of LEF1 protein expression experience poor clinical outcomes, we stained TMA9 for LEF1. Of note, we found LEF1 expression to be highly heterogeneous and only expressed in a minority of tumor cells (Fig. 4.1C). As shown by Kaplan-Meier survival analysis, patients with high LEF1 protein expression experienced very poor overall and event free survival (Fig. 4.1D). All five patients with high LEF1 expression did not experience long-term survival, and died of their disease with an average timespan of one year. Thus, our findings with LEF1 protein expression are strongly concordant with our aforementioned findings using *LEF1* transcript expression.

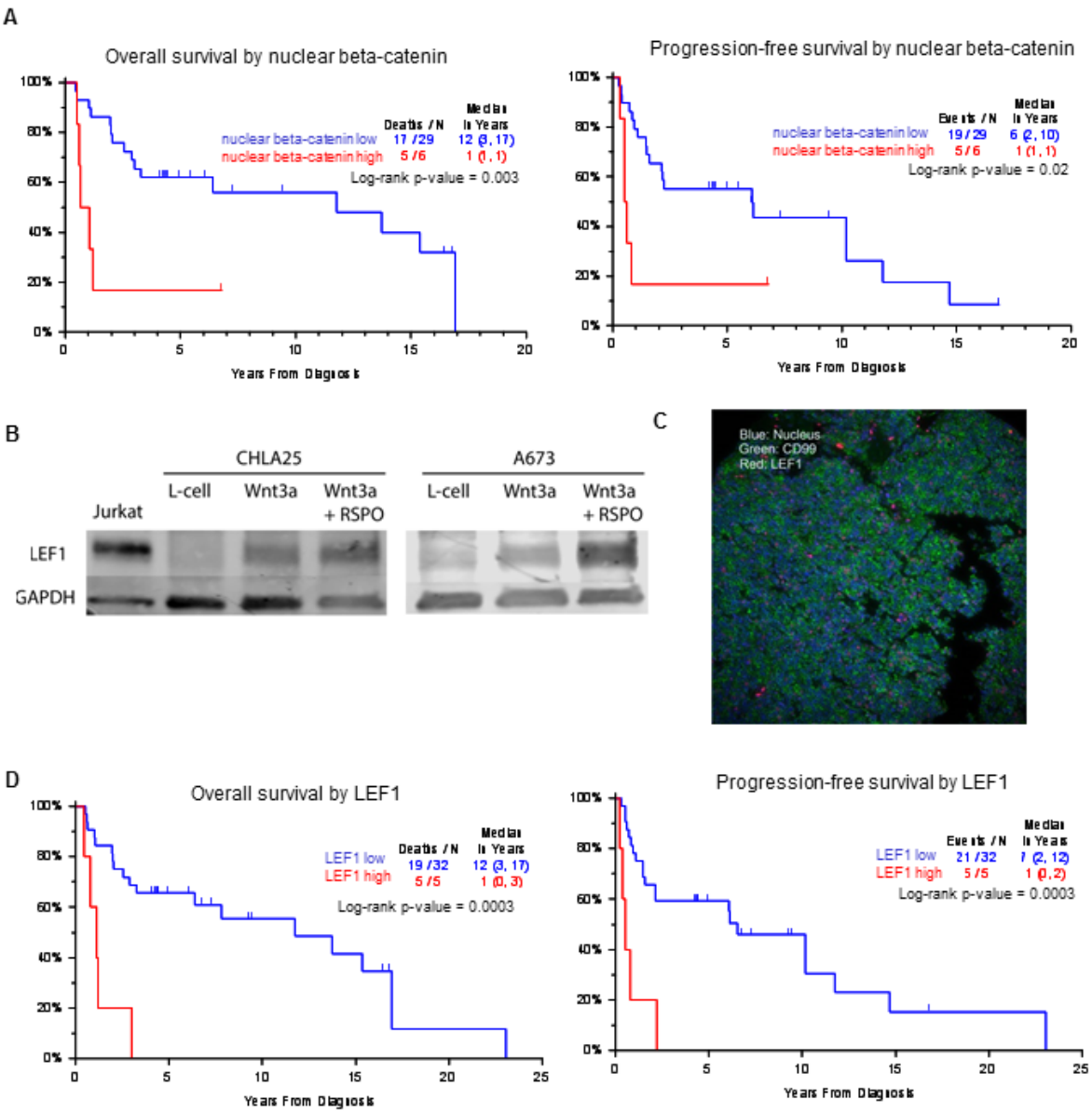


**Figure 4.1. High LEF1 expression is associated with poor prognostic and stroma-associated genes.**

(A) Patients with high nuclear beta-catenin experienced worse overall (left) and event-free survival (right). (B) LEF1 expression is strongly induced in cells with Wnt/beta-catenin stimulation. (C) LEF1 expression is detectable and heterogeneous in a metastatic Ewing sarcoma tumor biopsy (red). Tumor cells are marked by CD99 (green) and nuclei are stained with DAPI (blue). (D) High levels of LEF1 protein expression are associated with worse overall (left) and event-free survival (right).

### *LEF1 expression is correlated with a stroma-enriched poor prognostic signature in Ewing sarcoma patients*

A recently published study of 46 Ewing sarcoma patients who were uniformly treated on Children's Oncology Group (COG) therapeutic studies (GSE 63157) found that expression of 33 genes was associated with a poor prognosis [113]. Notably, this signature was enriched in tumors with significant stromal involvement; however, how the stroma contributes to aggressive disease is unclear. Given that Wnt and RSPO ligands are abundant in the microenvironment, we hypothesized that stroma-induced Wnt-beta catenin signaling may contribute to pathogenesis. Again using *LEF1* as a transcriptional readout of Wnt/beta-catenin signaling, we interrogated if *LEF1* expression was correlated with expression of poor prognosis genes. Remarkably, *LEF1* expression was strongly correlated with 28 out of 33 genes prognostic genes (Fig. 4.2A), even though *LEF1* itself was not a gene found to be a marker of poor prognosis in this analysis. Many of these highly correlated genes are known mediators of angiogenesis and other tumor-stroma interactions. This relationship between LEF-1 targets and candidate poor prognosis genes was reproduced in an independent set of 117 tumors (Fig. 4.2B). In the COG dataset, the extent of stromal contamination in each patient was recorded, and we observed that patients with stromal-rich tumors had significantly higher *LEF1* expression than patients with stromal-poor tumors (Fig. 4.2C). These data support our hypothesis that Wnt ligands provided by the stromal microenvironment activate Wnt/LEF1 and result in poor outcomes and aggressive disease.

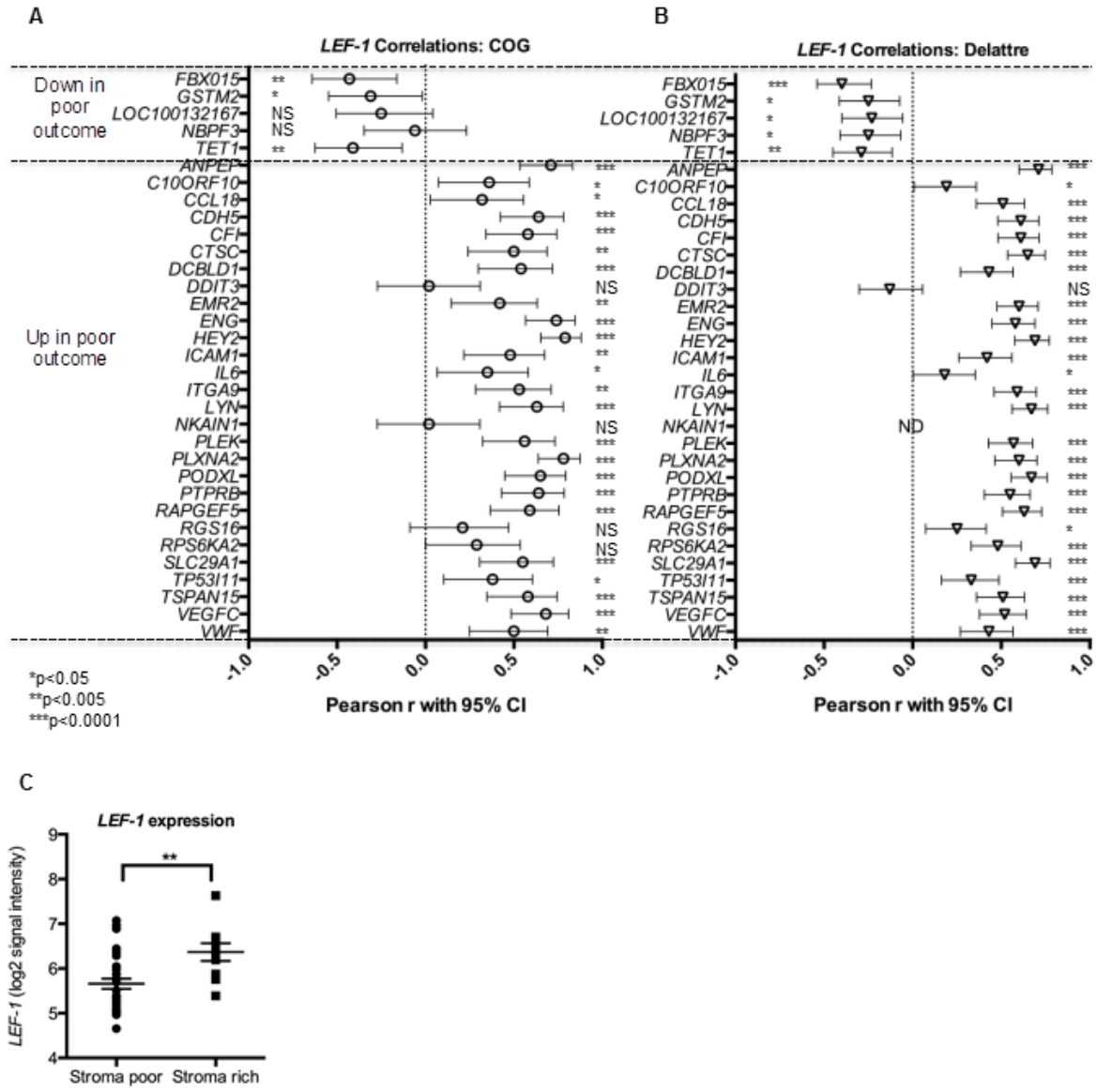


**Figure 4.2. *LEF1* expression is associated with a poor prognostic signature and high stromal content.**

(A) *LEF1* expression is correlated with expression of the 33 genes associated with a poor prognostic signature in COG patients as well as in the Delattre dataset (B) ND indicates no data available for indicate gene. *P*-values are indicated as shown in figure; NS indicates not significant. (C) Patients with stroma-rich tumors express higher levels of LEF1 than those with stroma-poor tumors. **P<0.01.

Having established that patients with evidence of Wnt/beta-catenin and LEF1 expression experience poor prognoses, we next sought to determine if the reverse question was true: do patients who experience poor prognoses have any common evidence of Wnt/beta-catenin activity? We interrogated a previously performed microarray analysis [3], in which gene expression of tumors from four patients who died of their disease within one year were compared to 10 tumors, in which patients experienced long term survival. In this dataset, 311 genes were upregulated twofold or more in the patients with aggressive disease. Of the top ten most significantly overlapping datasets in the Molecular Signatures database (MSigDB), genes containing CTTTGT LEF1 binding sites in their promoters were significantly enriched (Table 4.1). Further consistent with our earlier hypothesis that antagonism of EWS/FLI1 activity promotes aggressive disease, of the 261 genes upregulated twofold or more in patients who experiencing long-term survival, the most significantly enriched dataset was for genes up-regulated by EWS-FLI1 (Table 4.2). This suggests that patients with a good prognosis have predominant and likely un-antagonized transcriptional activation by EWS/ETS proteins.

**Table 1.** MSigDB gene set enrichment analysis for 311 genes with >2-fold higher expression in patients with aggressive disease.

| | Gene Set Name | # Genes in Gene Set (K) | # Genes in Overlap (k) | k/K | p-value | FDR q-value |
|---|---|---|---|---|---|---|
| 1 | BLALOCK_ALZHEIMERS_DISEASE_DN | 1237 | 54 | 0.0437 | 1.06E-28 | 5.88E-25 |
| 2 | CAGGTG_V$E12_Q6 | 2485 | 72 | 0.029 | 2.55E-27 | 7.04E-24 |
| 3 | SMID_BREAST_CANCER_LUMINAL_B_DN | 564 | 36 | 0.0638 | 9.42E-25 | 1.74E-21 |
| 4 | ONDER_CDH1_TARGETS_2_DN | 464 | 33 | 0.0711 | 3.11E-24 | 4.30E-21 |
| 5 | MEISSNER_BRAIN_HCP_WITH_H3K4ME3_AND_H3K27ME3 | 1069 | 45 | 0.0421 | 2.60E-23 | 2.87E-20 |
| 6 | SMID_BREAST_CANCER_BASAL_UP | 648 | 36 | 0.0556 | 1.01E-22 | 9.32E-20 |
| 7 | AACTTT_UNKNOWN | 1890 | 57 | 0.0302 | 2.45E-22 | 1.93E-19 |
| 8 | MCLACHLAN_DENTAL_CARIES_UP | 253 | 25 | 0.0988 | 4.33E-22 | 2.99E-19 |
| 9 | CHEN_METABOLIC_SYNDROM_NETWORK | 1210 | 46 | 0.038 | 5.04E-22 | 3.10E-19 |
| **10** | **CTTTGT_V$LEF1_Q2** | **1972** | **56** | **0.0284** | **9.94E-21** | **5.49E-18** |

**Table 4.1. MSigDB gene set enrichment analysis for** 311 genes with at >2-fold higher expression in patients with aggressive disease

The top 10 overlapping gene sets for the 311 genes with at least 2 fold higher expression in patients who experienced aggressive disease. Genes with LEF1 binding sites in the promoter were significantly enriched within this dataset.

**Table 2.** MSigDB gene set enrichment analysis for 261 genes with >2-fold higher expression in patients experiencing long-term survival.

| | Gene Set Name | # Genes in Gene Set (K) | # Genes in Overlap (k) | k/K | p-value | FDR q-value |
|---|---|---|---|---|---|---|
| 1 | **RIGGI_EWING_SARCOMA_PROGENITOR_UP** | **430** | **26** | **0.0605** | **3.74E-21** | **2.06E-17** |
| 2 | ZWANG_TRANSIENTLY_UP_BY_1ST_EGF_PULSE_ONLY | 1839 | 39 | 0.0212 | 2.52E-15 | 6.97E-12 |
| 3 | REACTOME_GENERIC_TRANSCRIPTION_PATHWAY | 352 | 16 | 0.0455 | 1.42E-11 | 2.61E-08 |
| 4 | MIKKELSEN_NPC_ICP_WITH_H3K4ME3 | 445 | 17 | 0.0382 | 4.88E-11 | 6.74E-08 |
| 5 | TGGAAA_V$NFAT_Q4_01 | 1896 | 33 | 0.0174 | 8.56E-11 | 9.46E-08 |
| 6 | NIKOLSKY_BREAST_CANCER_19Q13.1_AMPLICON | 22 | 6 | 0.2727 | 6.85E-10 | 6.31E-07 |
| 7 | RODRIGUES_THYROID_CARCINOMA_ANAPLASTIC_DN | 537 | 16 | 0.0298 | 6.45E-09 | 5.09E-06 |
| 8 | MIKKELSEN_ES_ICP_WITH_H3K4ME3 | 718 | 18 | 0.0251 | 1.03E-08 | 6.56E-06 |
| 9 | MIKKELSEN_MEF_LCP_WITH_H3K4ME3 | 128 | 9 | 0.0703 | 1.07E-08 | 6.56E-06 |
| 10 | BOQUEST_STEM_CELL_CULTURED_VS_FRESH_UP | 425 | 14 | 0.0329 | 1.69E-08 | 9.32E-06 |

**Table 4.2. MSigDB gene set enrichment analysis for 261 with >2-fold higher expression in patients experiencing long-term survival.**

The top 10 overlapping gene sets for the 261 genes with at least 2 fold higher expression patients who experienced long-term survival. The most enriched pathway was for EWS/FLI-1 induced genes, suggesting that high EWS/ETS activity is associated with a better prognosis.

To gain further insight into the pathways that are associated with high *LEF1* expression, we ranked genes in the COG dataset by correlation with *LEF1,* and performed gene set enrichment analysis (GSEA), on the genes with a correlation r>05. The top most significantly correlated datasets are shown in Table 4.3. Significantly, among genes highly correlated with *LEF1* expression are genes that are down-regulated by EWS/ETS, consistent with our hypothesis that activation of Wnt/beta-

catenin signaling is associated with antagonism of EWS/ETS. Other top hits are pathways associated with TGF-beta/Smad signaling, blood vessel development, ECM, and focal adhesion. Taken together, these data lead us to hypothesize that in addition to EWS/ETS antagonism, activation of Wnt/beta-catenin signaling alters tumor-microenvironment interactions.

**Table 3.** MSigDB gene set enrichment analysis for genes with significantly correlated with *LEF1* (r>0.5).

| | Gene Set Name | # Genes in Gene Set (K) | # Genes in Overlap (k) | k/K | p-value | FDR q-value |
|---|---|---|---|---|---|---|
| 1 | KOINUMA_TARGETS_OF_SMAD2_OR_SMAD3 | 824 | 66 | 0.0801 | 1.38E-25 | 6.50E-24 |
| 2 | ZHU_CMV_ALL_DN | 128 | 30 | 0.2344 | 1.08E-25 | 5.13E-24 |
| 3 | KEGG_ECM_RECEPTOR_INTERACTION | 84 | 26 | 0.3095 | 6.64E-26 | 3.20E-24 |
| 4 | LANDIS_ERBB2_BREAST_TUMORS_324_DN | 149 | 32 | 0.2148 | 4.92E-26 | 2.39E-24 |
| 5 | LIAN_LIPA_TARGETS_6M | 74 | 25 | 0.3378 | 4.72E-26 | 2.32E-24 |
| 6 | ROY_WOUND_BLOOD_VESSEL_UP | 50 | 22 | 0.44 | 3.84E-26 | 1.91E-24 |
| 7 | SANSOM_APC_TARGETS_DN | 366 | 46 | 0.1257 | 3.18E-26 | 1.60E-24 |
| 8 | FARMER_BREAST_CANCER_CLUSTER_5 | 19 | 16 | 0.8421 | 3.19E-26 | 1.60E-24 |
| 9 | KEGG_CELL_ADHESION_MOLECULES_CAMS | 134 | 31 | 0.2313 | 2.55E-26 | 1.31E-24 |
| 10 | QI_PLASMACYTOMA_UP | 259 | 40 | 0.1544 | 2.09E-26 | 1.08E-24 |
| 11 | SWEET_LUNG_CANCER_KRAS_UP | 491 | 53 | 0.1079 | 8.58E-27 | 4.50E-25 |
| 12 | NADLER_OBESITY_UP | 61 | 24 | 0.3934 | 5.93E-27 | 3.15E-25 |
| 13 | REACTOME_HEMOSTASIS | 466 | 52 | 0.1116 | 5.39E-27 | 2.89E-25 |
| 14 | *RIGGI_EWING_SARCOMA_PROGENITOR_DN* | 191 | 36 | 0.1885 | 5.17E-27 | 2.80E-25 |
| 15 | GOBERT_OLIGODENDROCYTE_DIFFERENTIATION_DN | 1080 | 78 | 0.0722 | 3.59E-27 | 1.97E-25 |
| 16 | KEGG_FOCAL_ADHESION | 201 | 37 | 0.1841 | 2.43E-27 | 1.35E-25 |
| 17 | REACTOME_COLLAGEN_FORMATION | 58 | 24 | 0.4138 | 1.34E-27 | 7.55E-26 |
| 18 | BRUINS_UVC_RESPONSE_LATE | 1137 | 81 | 0.0712 | 8.49E-28 | 4.83E-26 |
| 19 | PASINI_SUZ12_TARGETS_DN | 315 | 45 | 0.1429 | 4.54E-28 | 2.61E-26 |
| 20 | LENAOUR_DENDRITIC_CELL_MATURATION_DN | 128 | 32 | 0.25 | 2.78E-28 | 1.62E-26 |
| 21 | MARKEY_RB1_ACUTE_LOF_UP | 215 | 39 | 0.1814 | 1.69E-28 | 1.00E-26 |
| 22 | WANG_MLL_TARGETS | 289 | 44 | 0.1522 | 1.17E-28 | 7.01E-27 |
| 23 | DUTERTRE_ESTRADIOL_RESPONSE_24HR_DN | 505 | 56 | 0.1109 | 7.52E-29 | 4.55E-27 |
| 24 | WIELAND_UP_BY_HBV_INFECTION | 101 | 30 | 0.297 | 4.46E-29 | 2.74E-27 |
| 25 | *KINSEY_TARGETS_OF_EWSR1_FLI1_FUSION_DN* | 329 | 47 | 0.1429 | 2.89E-29 | 1.80E-27 |

**Table 4.3. MSigDB gene set analysis for genes significantly correlated with *LEF1* (r>0.5).**

The top 25 pathways of gene sets most significantly correlated with *LEF1* (r>0.5) in primary tumors are shown and reveal pathways involved in Smad signaling and blood vessel formation, as well as correlation with EWS/FLI-1-repressed genes.

### *Activation of beta-catenin signaling induces cell spreading and an angiogenic phenotype* in ovo

In order to substantiate the correlative patient data, we sought to study the effects of Wnt/beta-catenin activation in Ewing sarcoma cells in a physiologic microenvironment. Thus, we took advantage of the chick chorioallantoic membrane (CAM) assay. The CAM assay is ideal for understanding tumor microenvironment interactions because it contains stromal and endothelial cells, and a fully intact basement membrane. We reasoned that this assay would not only assess tumor growth and migration, but would also help us investigate the potential angiogenic signatures detected in analyses shown in Figure 4.2 and Table 4.3. A673 cells containing either an empty vector on constitutively active beta-catenin construct (EβP) were seeded in equal numbers on the surface of the CAM of E11.5 eggs. Cells were allowed to grow for 72 hr, after which CAMs containing tumor cells were dissected out, fixed, and imaged on a stereomicroscope. After 72 hr of growth, we observed that empty vector control cells grew as cohesive tumor masses (Fig. 4.3A left panels) that did not spread across the CAM (Fig 4.3B, top panels) and had well-demarcated edges (Fig. 4.3C, top panels). In comparison, cells transduced with the constitutively active beta-catenin construct exhibited more diffuse growth (Fig. 4.3A**,** right panels), often spread across the CAM (Fig. 4.3B, bottom panels), and had infiltrative margins (Fig. 4.3C, bottom panels). The spreading and blood vessel density of the tumors was assessed by quantifying the area of GFP-positive cells and vessels covered by the CAM. This revealed that EβP cells covered a significantly larger surface area than cells containing an empty vector (Fig. 4.3D). Further, we noticed that the EβP tumors contained a larger surface area of blood

vessels (Fig. 4.3E). Of note, the overall density of vessels in EβP tumors was not significantly different (Fig. 4.3F), yet revealed a trend toward increased angiogenesis.

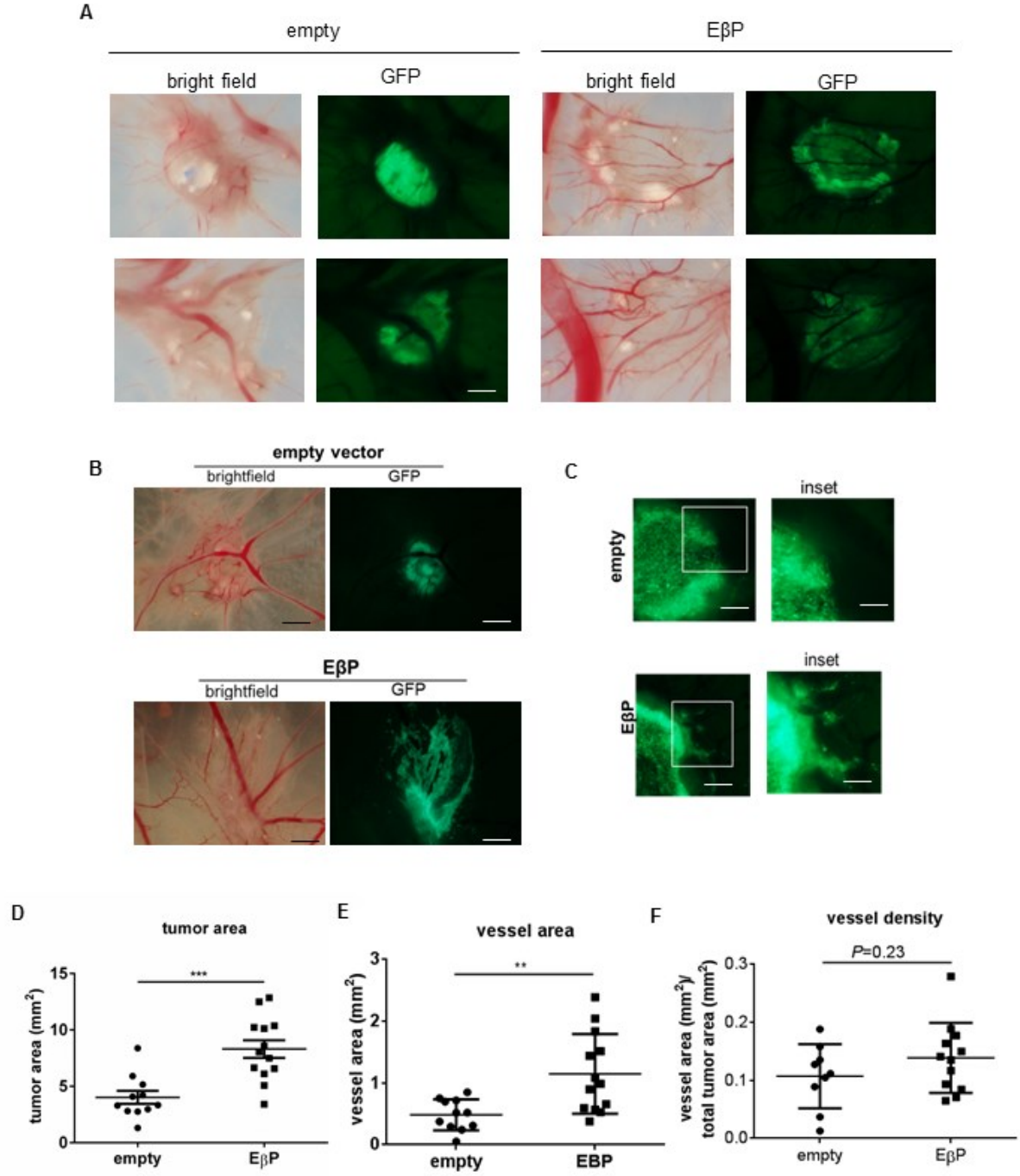


**Figure 4.3. Beta-catenin activation promotes cell spreading and angiogenesis in the chick chorioallantoic membrane (CAM) assay.**

(A) GFP-labeled A673 cells transduced with control (empty vector) or constitutively active beta-catenin (EβP) were grown on chorioallantoic membranes (CAMs) and spreading of the tumor was observed by bright field and fluorescence microscopy. Scale bar = 500 μm. (B) Compared to empty tumors, some EβP tumors demonstrate extensive spreading, shown in the bottom panels. Scale bar = 2 mm. (C) Representative high-magnification images of tumor borders reveals more infiltrative edges in EβP cells compared to controls Scale bar = 250 μm, inset =100 μm. (D) Spreading of tumors was quantified by measuring the area of GFP-positivity. Quantification of *n*=11(empty) and *n*=13 (EβP) independent experiments (mean ± SEM). Significance was determined using a Student's t-test. ***$p<0.001$. (E) Vessel area was determined by measuring the area of red pixels within the area of GFP-positivity of samples as in (D). Significance was determined using a Student's t-test. **$p<0.01$. (F) Vessel density was determined by dividing the tumor vessel area (E) for an individual tumor by its corresponding overall tumor area (D).

### *Wnt/beta-catenin signaling induces expression of angiogenesis-related genes but does not induce secretion of pro-angiogenic factors*

Using our RNA-seq expression data in Chapter 2, as well as the prognostic gene signature in Fig. 4.3, we identified a small set of genes as putative candidates of angiogenic signature that included IGF-1, IL-6, and CYR61. By qRT-PCR, we observed a trend toward up-regulation of these genes by Wnt3a CM and/or RSPO2 (Fig. 4.4A), and modest but significant up-regulation of all three genes in EβP cells (Fig. 4.4B). Induction of IGF-1 was particularly interesting, because the IGF-1 receptor (IGF-1R) is an established EWS/FLI-1-regulated oncogene for which targeted monoclonal antibodies have been designed, and are currently in clinical trials for Ewing sarcoma patients. To further understand the effects of Wnt/beta-catenin signaling on the IGF-1/IGF-1R pathway, we performed an immunoblot analysis for IGF-IR, as well as for IGF-R that has undergone phosphorylation at the tyrosine 1135, as this is one of the key initiating events of IGF-I signaling. Although no significant changes were observed in A673 cells treated with CM, a dramatic increase was observed in IGF-1R as well as p-Y1135-IGF-1R expression in cells EβP cell (Fig. 4.4C). This suggested that potent

constitutive activation of beta-catenin induces either autocrine or paracrine IGF-1/IGF-1R signaling and may contribute to angiogenesis or other beta-catenin mediated processes.

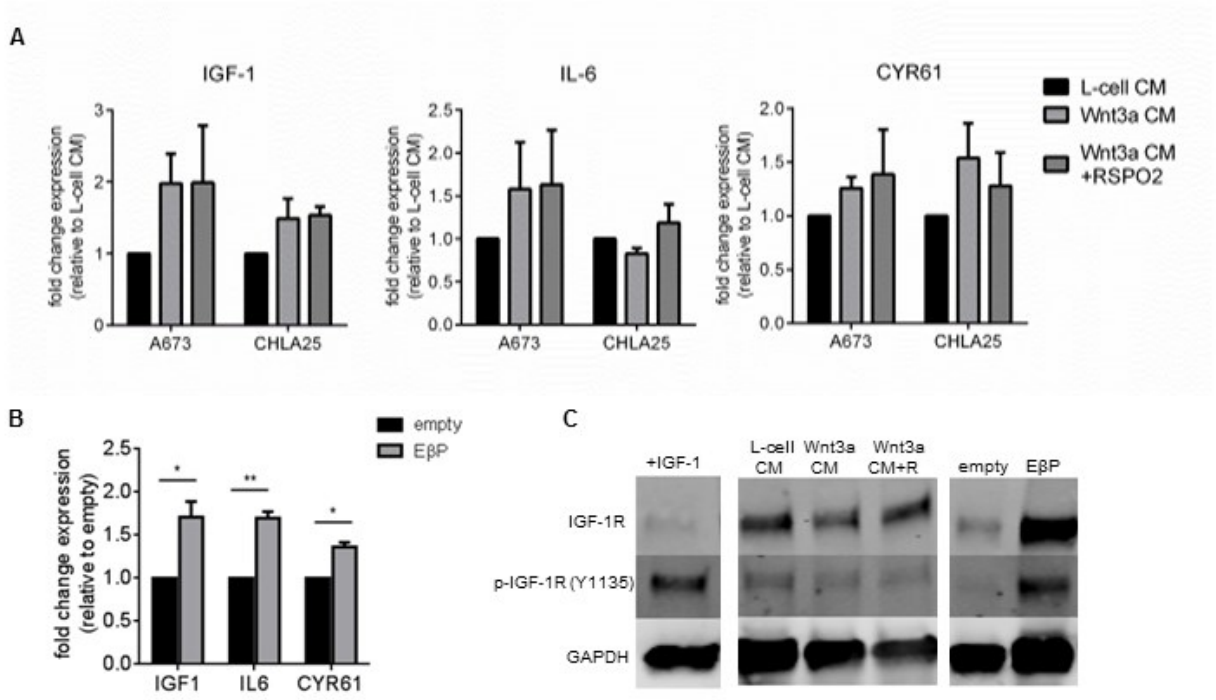


**Figure 4.4. Genes involved in angiogenesis are up-regulated by Wnt/beta-catenin signaling.**

A) A673 and CHLA25 cells were stimulated with Wnt3a CM+/- RSPO2, and expression of IGF1, IL6, and CYR61 was assessed by qRT-PCR. A trend toward up-regulation was apparent in both cell lines, although differences between treatment groups were not statistically significant. (B) Expression of the same genes was assessed by qRT-PCR in A673 cells transduced with either an empty vector or constructively beta-catenin construct (EβP). All genes were significantly upregulated in beta-catenin activated cells. **p*<0.05, ***p*<0.01. (C) Little differences were observed in IGF-R expression or activation as assessed by Western blotting for IGF-1R and auto-phosphorylation IGF-1R at Y1135 in Wnt-stimulated A673 cells, but a dramatic induction of IGF-1R activation was observed in EβP cells compared to control.

To determine if up-regulation of these angiogenesis-associated genes results in functional secretion of pro-angiogenic factors, we took advantage of an *in vitro* angiogenesis assay in which human umbilical endothelial cells (HUVECs)

spontaneously undergo differentiation and form capillary-like tubes. In the absence of angiogenic growth factors, HUVECs undergo apoptosis when plated on Matrigel within 16 hr, but addition of growth factors promotes angiogenic tube formation (Fig. 4.5A). These conditions were used as negative and positive controls, respectively. To test the effects of Wnt/beta-catenin signaling on this process, Ewing sarcoma cells were stimulated with L-cell CM or Wnt3a CM +/-RSPO2, and the total media was collected after 48 hr (total tumor-CM). HUVECs were plated in media lacking angiogenic growth factors, and then either L-cell/Wnt CM or total tumor-CM was added. Tube formation was assessed after 16 hr. Although L-cell and Wnt3a CM alone supported tube formation, no appreciable differences were observed when HUVECs were cultured in total tumor-CM from Wnt/beta-catenin-stimulated A673 or CHLA25 (Fig. 4.5B). Further, when CM from A673 cells containing empty vector control or EβP cells was added, similar results were observed (Fig. 4.5C). Taken together, these results suggest that Wnt/beta-catenin-activated Ewing sarcoma cells do not secrete pro-angiogenic factors.

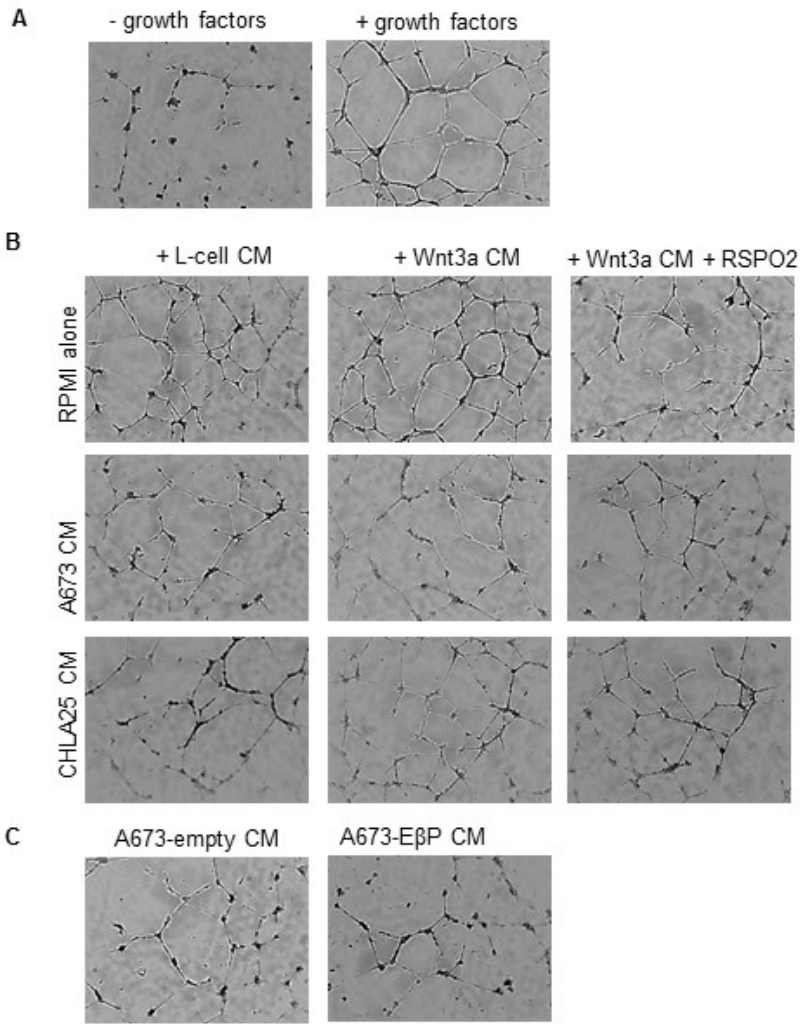


**Figure 4.5. CM from Wnt-activated cells does not promote angiogenesis..**

(A) HUVECs plated on Matrigel underwent apoptosis after 16 hr in the absence of growth factors (left) but spontaneously differentiated to form angiogenic tubules in the presence of angiogenic growth factors (right). These conditions were used as negative and positive controls, respectively. (B) A673 and CHLA25 cells were stimulated with L-cell CM or Wnt3a CM +/- RSPO2 for 48 hr, then all media was collected and added to HUVECs. L-cell CM or Wnt3a CM +/- RSPO2 mixed with RPMI was used as a control (top panels). All CM was able to promote some angiogenic tubule formation, although no significant differences existed between groups. (C) CM from A673 cells transduced with either an empty vector or constructively beta-catenin construct (EβP) was collected after 48 hr in culture and added to HUVECs on Matrigel. No differences in tubule formation were apparent.

### *Wnt/beta-catenin signaling induces TGF-beta genes*

Our RNA-seq dataset revealed that TGFB2 and TGFBR2 were two genes that were significantly regulated in sorted, highly Wnt-responsive cells (Fig 2.7B). In table 4.3, we observed a strong association with genes associated with LEF1 expression and the Smad/TGF-beta signaling pathway. To validate these findings, we performed qRT-PCR on Wnt/beta-catenin activated cells and found a trend toward up-regulation with Wnt3a CM (Fig. 4.6A), and consistent induction of TGFB2 and TGFBR2 in cells containing constitutively active beta-catenin (Fig. 4.6B). To determine if up-regulation of TGFB2 results in autocrine TGF-beta signaling, we performed an immunoblot assay for phospho-Smad2 and total Smad2/3. Phosphorylation of Smad2 results from engagement of TGF-beta receptors and leads to activation of Smad4 and transcription of downstream TGF-beta target genes. In A673 cells stimulated with Wnt3a CM +/- RSPO2 (Fig. 4.6C) or in EβP cell (Fig. 4.6D), we saw little evidence of Smad-2 phosphorylation suggesting that Wnt/beta-catenin-signaling-induced TGFB2 expression does not induce TGF-beta/Smad signaling. We also observed up-regulation of TGFBR2, so we question if induction of this receptor “primed” cells to be more responsive to TGF-beta ligands. After stimulation for 1 hr with TGF-beta-1, we observed robust induction of phospho-Smad2/3 in all conditions (Fig. 4.6C), with little notable differences among samples, suggesting that TGFBR2 up-regulation does not significantly contribute to TGF-beta ligand responsiveness.

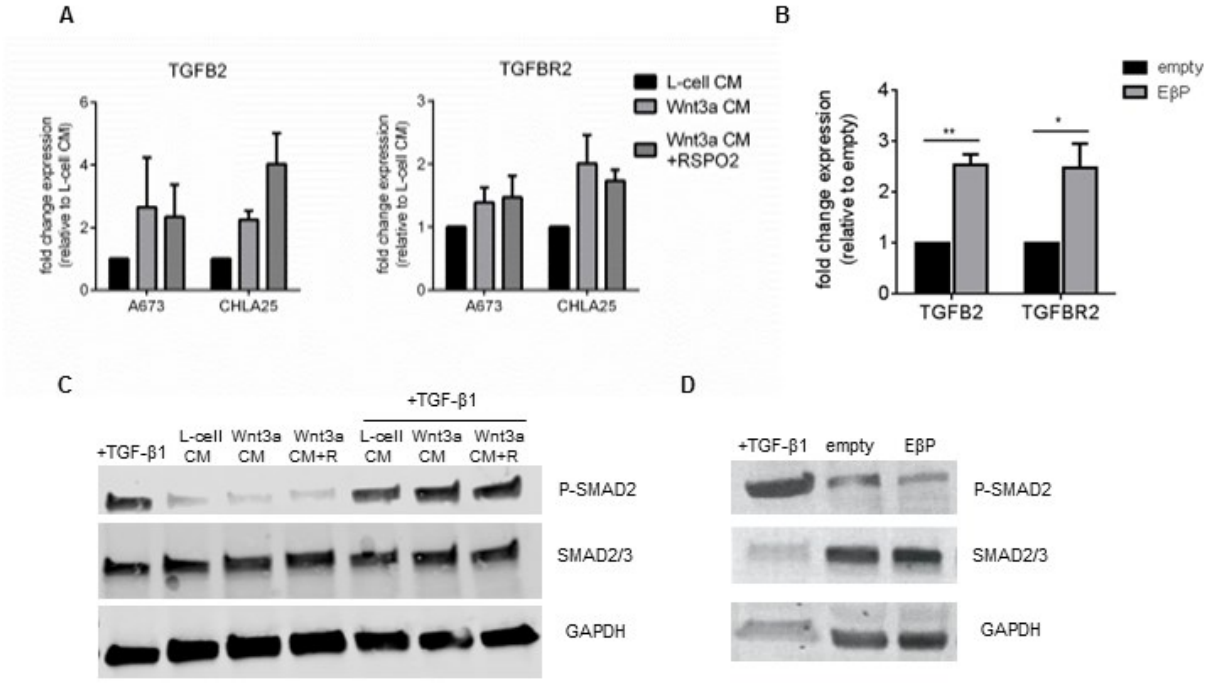


**Figure 4.6. TGFB2 and TGBR2 are induced by Wnt/beta-catenin signali**ng.

(A) A673 and CHLA25 cells were stimulated with Wnt3a CM+/- RSPO2, and expression of TGFB2 and TGFBR2 was assessed by qRT-PCR. A trend toward up-regulation was apparent in both cell lines, although differences between treatment groups were not statistically significant. (B) Expression of TGFB2 and TGFBR2 was assessed by qRT-PCR in A673 cells transduced with either an empty vector or constructively beta-catenin construct (EβP). Both genes were significantly upregulated in beta-catenin activated cells. *$p$<0.05, **$p$<0.01. (C) Little differences were observed in TGF-beta activation as assessed by Western blotting for phosphorylation of Smad2 in Wnt-stimulated A673 cells with or without TGF-beta exposure for 1 hr. (D) No apparent difference was observed in phospho-Smad2 in A673 cells in EβP cells compared to control.

### *Pharmacologic inhibition of RSPO2 does not affect tumor burden but inhibits the incidence of distant metastases*

We have providing compelling data that the Wnt/beta-catenin pathway is a mediator of metastatic disease in Ewing sarcoma. In collaboration with OncoMed Pharmaceuticals, we sought to determine if this pathway can be effectively targeted in Ewing sarcoma by the anti-RSPO2 monoclonal antibody MT130-230. First, to determine if the antibody

blocks RSPO2 *in vitro,* we stimulated with A673-7TGP reporter cells with Wnt3a CM +RSPO2 in the presence of saline or 100 mg/mL MT130-230. As shown in Fig. 4.7A, MT-130-230 partially blocks the RSPO2-mediated potentiation of Wnt/beta-catenin-TCF activity. We next assessed the effects of the antibody on subcutaneous tumor growth. In order to assess the efficacy of the antibody as a therapeutic option in established tumors, cells were first allowed to engraft and form small tumors. Once tumors were 200-500 $mm^3$ in volume, weekly intraperitoneal (IP) administration of MT130-230 was started. Not unexpectedly, inhibition of RSPO2 had no significant effect on subcutaneous growth of A673 or TC32 tumors (Fig. 4.7B).

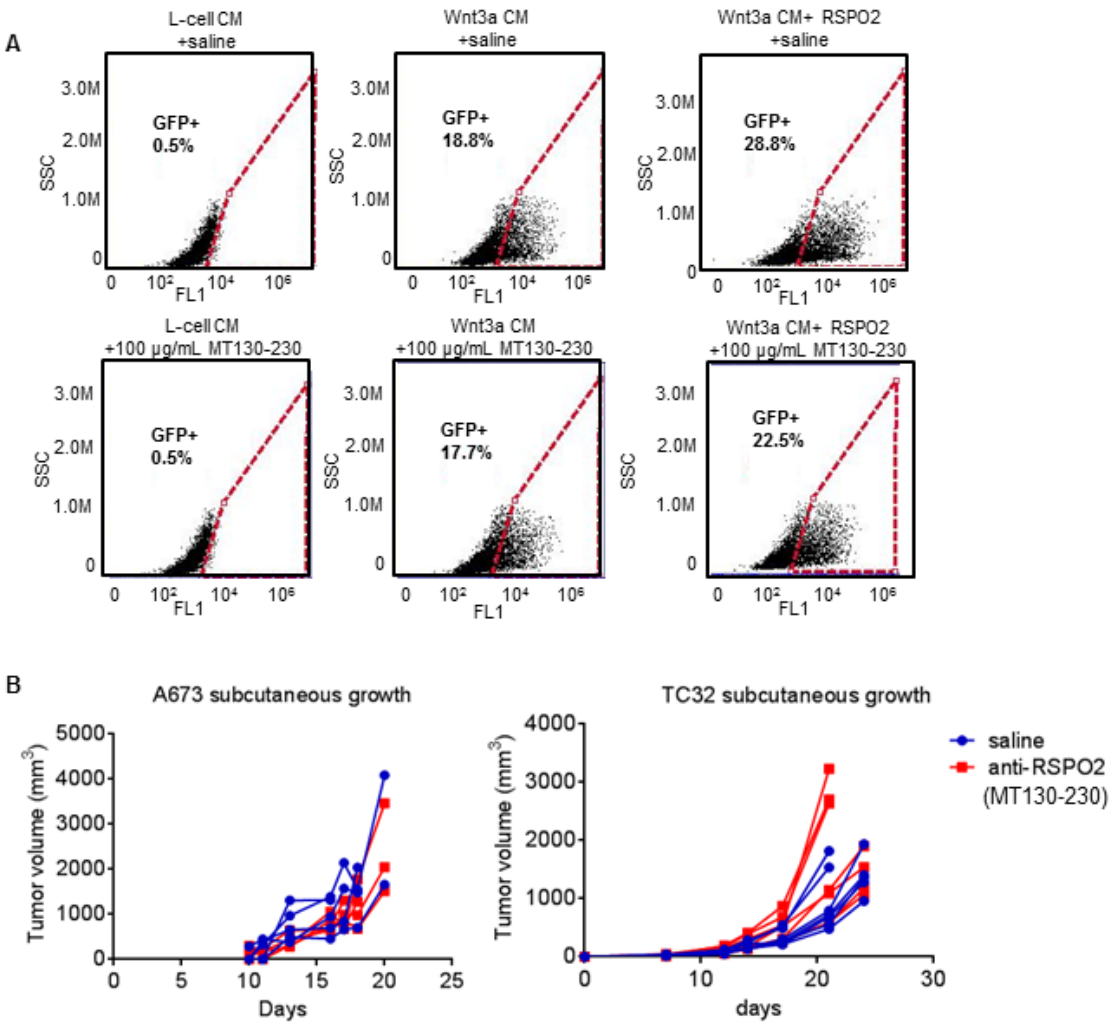


**Figure 4.7. The monoclonal antibody against RSPO2 MT130-230 blocks RSPO2-mediated potentiation of Wnt signaling but has no effect on subcutaneous tumor growth**.

(A) The ability of MT130-230 was determined by stimulating A673-7TGP reporter cells with Wnt3a CM +/- RSPO2 in the presence of saline (top panels) or 100 µg/ml MT130-230, and assessing Wnt activity by flow cytometry. MT130-230 moderately blocked the RSPO2-mediated potentiation of reporter activity. (B) A673 (left) and TC32 (right) cells were implanted subcutaneously, and weekly IP administration of MT130-230 was started once tumors reached 200-500 $mm^3$ in volume. No significant differences were observed between groups.

To determine if RSPO2 inhibition had any effects on suppression of metastasis, we sought to use a model that recapitulates the entire metastatic cascade. Since Ewing

sarcoma cell lines do not effectively metastasize from subcutaneous tumors, and tail vein metastasis assays only model the steps of survival in the circulation, extravasation, and distant tumor formation, we utilized the sub-renal capsule model as a method to assess the full metastatic cascade. In this study, TC32 cells were directly injected under the capsule of the kidney via ultrasound-guided needle and catheter. A primary tumor was established in the kidney, which is a highly vascularized organ thus providing ample opportunity for tumor cells to access the bloodstream. Weekly IP injection of MT130-230 was started at the time of tumor implantation. Primary tumor growth and appearance of large metastases was followed via bioluminescence imaging (Fig 4.8A). After six weeks, each mouse was individually euthanized and its kidney containing the primary tumor was removed (Fig. 4.8B). Immediately following dissection, the remaining organs were imaged by bioluminescence *ex vivo,* and the number of overt metastases, as well as the bioluminescent tumor burden of distant metastases was measured (Fig 4.8C). Representative images of metastases detected *ex vivo* are shown in Fig. 4.8D. Upon comparison of mice treated with saline and mice treated with MT130-230, we observed that both groups efficiently formed large primary tumors, and there was no notable difference in primary tumor burden (Fig. 4.8E). Upon primary tumor removal, all mice had evidence of distant metastases, and the bioluminescent signal intensity was largely similar (Fig. 4.8F). This suggests that once metastases grew, there was no apparent different difference in tumor burden generated. However, the overall number of distant metastases was strikingly reduced in mice treated with MT130-230 (Fig. 4.9D, G). Mice treated with saline had numerous metastatic nodules throughout the body and especially in the GI system, whereas mice treated with MT130-230 had fewer nodules, although they were similar in size to those in saline-treated mice one established. Taken

together, these data suggest that inhibition of RSPO2 via MT130-230 has little effect on the growth of Ewing sarcoma cells, but significantly reduces the ability of primary Ewing sarcoma tumors to seed distant organs with metastases.

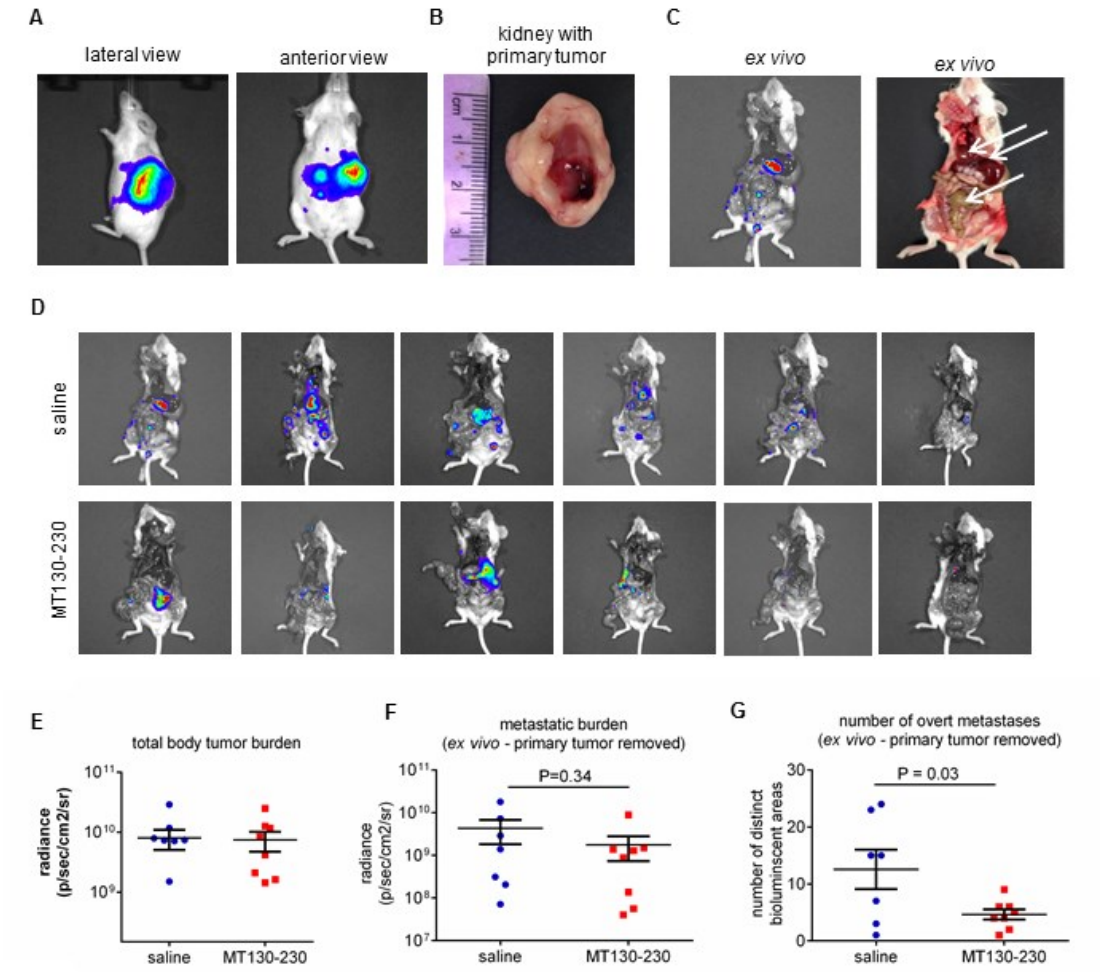


**Figure 4.8. Inhibition of RSPO2 does not affect tumor burden but inhibits the number of metastatic nodules in a sub-renal capsule model of metastasis.**

(A) After ultrasound-guided injection into the sub-renal space, luciferase-tagged TC32 cells formed primary tumors and tumor growth was monitored by bioluminescence for six weeks. (B) Representative image showing that primary tumors grew in and around the kidney. (C) After kidney and primary tumor were dissected out as in (B), mice were immediately re-imaged *ex vivo*, and metastases were detected by bioluminescent imaging (left panels) and confirmed as tumor nodules (arrows) upon inspection (right panel). (D) Representative *ex vivo* images of tumor burden from mice treated with saline control (top panels) or the anti-RSPO2 antibody MT130-230. No difference was observed in primary (E) tumor or metastatic (F) tumor burden between groups. Data is expressed as radiance in each mouse. (G) Distinct areas of bioluminescent signal were

counted, and revealed that mice treated with MT130-230 had significantly less metastatic nodule formation than mice treated with saline.

## Discussion

In these studies, we provide evidence that patients with high nuclear beta-catenin and LEF1 protein expression experience poor clinical outcomes. Further, tumors with high levels of *LEF1* transcript expression are stroma-rich, and *LEF1* expression is correlated with expression of genes in a validated poor prognostic signature. Notably, these genes are enriched for stromal- and angiogenesis-related genes, signifying that tumor-microenvironment interactions are important for tumor progression. These data suggest that the LEF1 transcription factor may directly induce expression of these genes in tumor cells and/or indirectly induce changes in the local microenvironment that lead to recruitment of stromal cells that express these genes and promote tumor progression. Although stroma- and angiogenesis-associated genes including TGFB2, CYR61, IL6, and IGF1 are induced by Wnt/beta-catenin signaling, activation of Wnt/beta-catenin signaling did not induce differentiation of HUVECs in a tube formation assay, indicating it is unlikely that any significant pro-angiogenic secreted factors are produced in response to Wnt/beta-catenin activation. Instead, the induction of angiogenesis observed in the CAM assay may be secondary to the increased cell spreading and coverage of a larger surface area and thus increased cell-cell contact of cancer cells and endothelial cells. Direct cell-cell interactions can induce angiogenesis, notably through membranous beta-catenin [157] or TNC [133, 158], raising the possibility that cell-cell contact mediated angiogenesis may occur in Ewing sarcoma and this may be mediated by both Wnt-dependent and Wnt-independent mechanisms.

Interestingly, cells with a constitutively active beta-catenin more reproducibly upregulated the angiogenesis and TGF-beta associated genes than cells stimulated by Wnt CM. This is likely in part due to the heterogeneity of the Wnt response, and the fact

that not all cells may induce gene expression in response to Wnt3a CM. If cells were sorted on the basis of Wnt activity, as in Chapter 2, we might observe more dramatic regulation of the genes and pathways. Further EβP cells are generated by lentiviral transduction followed by selected in puromycin, ensuring all cells in the population have expression of the constitutively active beta-catenin construct. This uniformity likely results in more consistent induction of expression of downstream target genes. Our findings that TGFBR2 is induced in highly Wnt responsive cells also raises the intriguing possibility that Wnt/beta-catenin signaling may "prime" highly Wnt-responsive cells to be more responsive to other ligands in the microenvironment, such as members of the TGF-beta family. The role of TGF-beta/Smad signaling in Ewing sarcoma is relatively unexplored but is considered tumor suppressive due to the fact that it weakly inhibits proliferation[24]. Like Wnt signaling, TGF-beta signaling is highly context dependent [159], so although TGF-beta signaling is currently considered tumor suppressive in Ewing sarcoma, other context-dependent roles in tumorigenesis cannot be ruled out. It is possible that TGF-beta activation that may promote a migratory or an invasive phenotype, as it does in other tumors under certain conditions [159, 160]. Wnt/beta-catenin and TGF-beta pathway crosstalk has been well-studied and implicated in tumorigenesis, and in some contexts can result in synergistic regulation of target genes [161, 162]. Future investigations into the nature of TGF-beta signaling in Ewing sarcoma, and potential cross-talk with the Wnt/beta-catenin pathway, such as the effects of TGF-beta on Wnt/beta-catenin target gene regulation, would undoubtedly provide important insights.

Another particularly interesting finding is that constitutively active beta-catenin strongly induces IGF-1R and its phosphorylation. Although this effect was not apparent

in A673 stimulated with Wnt ligands, an effect might be present but masked or diluted by the presence of cells that are not Wnt-responsive. Sorting on the basis of Wnt activity, or investigation of more cell lines may result in more apparent induction. Induction of IGF-1R signaling is extremely important for Ewing sarcoma biology, because monoclonal antibodies against IGF-1R are currently in clinical trials for advanced Ewing sarcoma disease [163, 164]. Most Ewing sarcoma cell lines and clinical samples exhibit activation of autocrine IGF-1R phosphorylation by IGF-1, and inhibition of IGF-1R results in cell death and tumor regression in animal models[164, 165]. The overall effect of early clinical trials revealed that some patients experienced dramatic inhibition of tumor growth by anti IGF-1R therapy, whereas other patients were unresponsive or developed resistance [166]. The mechanisms that mediate resistance to IGF-1R inhibition are unknown. The striking induction of IGF-1R and its auto-phosphorylation observed in cells with constitutively active beta-raise the fascinating possibility that Wnt/beta-catenin signaling may be a mediator of anti-IGF-1R therapy resistance.

Finally, our early findings that anti-RSPO2 therapy may decrease the incidence of metastases provide evidence that the Wnt/beta-catenin pathway may be amenable to therapeutic targeting in Ewing sarcoma. Despite the modest reduction of TCF reporter activity upon administration of the anti-RSPO2 monoclonal antibody MT130-230, we observed a striking difference in the number of metastatic nodules formed after *in vivo* using the sub-renal capsule metastasis model. Subcutaneously, we observed no differences in tumor growth upon MT130-230 administration, and this is reflected by the fact that when metastatic tumors did grow in the sub-renal capsule model, there was little difference in the overall tumor burden. Given that Wnt/beta-catenin has little effect

on proliferation of Ewing sarcoma cells [3], (Fig. 2.11B), it is not unexpected that pharmacologic inhibition has little effect on tumor outgrowth. The overall incidence of metastatic foci, however, was decreased, and emphasizes the idea that tumor size is not the only therapeutic outcome that should be assessed. Reduction of metastatic seeding by this single agent is impressive, especially considering the fact that RSPO2 inhibition only inhibited RSPO2-mediated potentiation of Wnt activity, but did not significantly reduce Wnt activity alone. (Fig.4.7A). Thus, combination therapy of MT130-230 and an inhibitor of the Wnt ligand/receptor interaction, such as with the monoclonal antibody OMP-18R5 (currently in clinical trials) [88, 167, 168], may result in even greater benefits. Together the studies provide compelling evidence for further preclinical investigation toward the use of anti-RSPO/Wnt therapeutics for metastasis inhibition in Ewing sarcoma.

## Experimental Procedures

*Cell culture and lentiviral transductions*

Ewing sarcoma cell lines A673, CHLA25, and TC32 were kindly provided by Dr. Timothy Triche (CHLA, Los Angeles, CA, USA), Dr. Heinrich Kovar (CCRI, St. Anna Kinderkrebsforschung, Vienna, Austria), and the COG cell bank (cogcell.org). Identities of the cells were verified by short tandem repeat (STR) profiling. Cells were routinely tested for mycoplasma contamination, and were verified to be negative for all studies. Cells were cultured in RPMI 1640 media (Gibco) supplemented with 10% fetal bovine serum (FBS)(Atlas Biologicals) and 2mM L-glutamine (Life Technologies). CHLA25 was grown on plates coated with 0.2% gelatin. L-cells (ATCC CRL-2648) and Wnt3a L-cells (ATCC CRL-2647) were cultured in DMEM (Gibco) supplemented with 10% FBS. Human umbilical vascular endothelial cells (HUVEC) were obtained from Lonza and cultured in EGM-2 (Lonza). Lentiviral production and transduction was performed as previously described [3]. For generation of 7TGP reporter cells, plasmids #24305 (Addgene) was used [110]. For generation of EβP cells, plasmid #24313 (Addgene) was used. The constitutively active beta-catenin element was removed using BamHI to generate EβP-empty vector.

*TMA assembly, immunohistochemistry, and automated quantitative analysis (AQuA)*

A tumor microarray was assembled as described in Chapter 2 and denoted as TMA9. Samples were obtained from the files of the Department of Pathology, University of Michigan Medical Center, Ann Arbor, MI. The University of Michigan Institutional Review Board provided a waiver of informed consent to obtain these samples. The TMA contains108 cases of Ewing sarcoma tumors with multiple clinical records 51 patients

were used for analysis. The TMA was stained with antibodies against beta-catenin, LEF1, and CD31. Protein expression in individual tumors was quantified using AQUA technology as previously described in Chapter 2.

*Clinical correlations analysis*

Optimal method was applied to select the best cut-point for total beta-catenin, cytoplasmic beta-catenin, nuclear beta-catenin, LEF1, and CD31 primary tumor AQUA data. The method of Kaplan-Meier was used to estimate overall survival and event-free survival. Log-rank tests were used to compare survival distributions. LEF1 transcript data was obtained from a recently published, clinically annotated dataset from the Children's Oncology Group (COG) (GSE 63157 [113] and GSE 34620 [125]). Log-rank tests were used to compare survival distributions. Correlations with *LEF1* were measured by Pearson correlation and 95% confidence intervals determined.

*Gene set enrichment analysis (GSEA)*

Generation of a list of significantly overlapping datasets was computed using the Molecular Signatures Database v4.05 (MSigDB)[109]. An *in vivo* signature of Wnt/beta-catenin signaling was generated by ranking genes based on correlation with *LEF1* expression in the clinically annotated dataset from the Children's Oncology Group (COG) (GSE 63157 [113]), and gene set enrichment analysis (GSEA) was performed by using the GseaPreranked function of GSEA v2.1.0 software (Broad Institute).

*Chick chorioallantoic membrane (CAM) assay*

Fertilized eggs were obtained from the Michigan State University Department of Animal

Science Poultry Farm. Immediately upon arrival, eggs were placed in a humidified, rocking incubator (G.Q.F. Manufacturing, Savannah, GA) at 37°C for 11 days (E11). On E11, eggs were assessed for viability of the embryo using a handheld light source (G.Q.F. Manufacturing, Savannah, GA). Eggs containing non-viable embryos were discarded. The chorioallantoic membrane (CAM) was "dropped" as previously described [169, 170], and $1x10^6$ GFP-labeled A673 cells were placed on the CAM in 10 µL of 2.5% growth-factor reduced Matrigel (BD Biosciences) in PBS. Cells were incubated for three days without rocking. On E14, the CAM was dissected out and fixed for 1 hr in 4% paraformaldehyde. Tumors on the CAM were identified and imaged by GFP fluorescence and bright field microscopy on an Olympus SZX16 Stereo-Dissecting macroscope and analyzed using NIS-Elements Imaging software. Cell spreading was assessed by measuring the surface area of GFP on the CAM, and vessel density was determined by quantifying the area of red pixels within the area of the tumor (as determined by GFP).

*Analysis of gene expression*

Wnt targets were validated by quantitative RT-PCR, using standard methods as previously described in earlier chapters. The sequences of primers used are listed in Table 4.4.

| Gene | Forward primer sequence | Reverse primer sequence |
|---|---|---|
| *HPRT1* | TGACACTGGCAAAACAATGCA | GGTCCTTTTCACCAGCAAGCT |
| *CYR61* | ACCGCTCTGAAGGGGATCT | ACTGATGTTTACAGTTGGGCTG |
| *IGF1* | GCTCTTCAGTTCGTGTGTGGA | GCCTCCTTAGATCACAGCTCC |
| *IL6* | CCTGAACCTTCCAAAGATGGC | TTCACCAGGCAAGTCTCCTCA |
| *TGFB2* | CAGCACACTCGATATGGACCA | CCTCGGGCTCAGGATAGTCT |
| *TGFBR2* | AATGTGAAGGTGTGGAGAC | GGTAGGCAGTGGAAAGAG |

**Table 4.4. Primer sequences used for qRT-PCR.**

*Western blots*

Lysis buffer, prepared by adding 1 tablet each of cOmplete protease inhibitor and PhosStop phosphatase inhibitor (Roche, Switzerland) to RIPA buffer, was added directly to culture plates after aspiration of culture media and washing 1x with PBS buffer. Cells were mechanically separated from the surface of the culture plate and then the lysate transferred to 1.5 mL micro-centrifuge tube and sonicated on ice for 5 cycles of 20 seconds, with 1 minute pauses. Total protein concentration was estimated using the Bio-Rad protein assay (Bio-Rad, Richmond, CA) and 50mg of total protein was loaded on 4-15% Mini-PROTEAN polyacrylamide gel. The protein samples were electrophoresed and transferred to nitrocellulose membranes (Invitrogen). The membranes were blocked for 1 hr at RT with a 1:1 mixture of Odyssey blocking buffer (LI-COR). The membranes were then incubated with primary antibody overnight at 4 °C. Primary antibodies were diluted in 5% (w/v) BSA in TBS buffer containing 0.1% Tween-20 (TBS-T) at the following concentrations: rabbit anti-LEF1 (1:150, Sigma-Aldrich), mouse anti-glyceraldehyde-3-phosphate dehydrogenase (GAPDH) monoclonal antibody (1:200, AbCam), rabbit anti-IGF-I Receptor β (1:1,000, Cell Signaling) and rabbit anti-Phospho-IGF-I Receptor β (Tyr1135) (1:1,000, Cell Signaling.) The membranes were washed three times with TBS-T for 5 minutes with shaking and then incubated with secondary antibodies, which were diluted in 1% BSA in TBS-T as follows: IRDye 800CW goat anti-rabbit (1:10,000, LI-COR) and IRDye 680RD goat anti-mouse (1:10,000, LI-COR.) The membranes were washed twice more with TBS-T and once with TBS buffer. Finally, membranes were visualized with an Odyssey infrared imaging system (LI-COR.)

*HUVEC tube formation assay*

Tube formation assays were performed in the method of Arnaoutova *et al* [171]. Briefly, 96 well plates were coated with 50 µl of growth-factor reduced Matrigel (BioRad) and incubated at 37°C for 30 min. HUVECs were plated at a density of $1.5x10^4$ cells per well in either growth factor-reduced (EBM) media, or media supplemented with the growth factors (EGM) provided by the EGM Bullet Kit (Lonza). Generation of tumor CM was achieved by collecting the conditioned media from cells cultured in 6-well plates for 24 or 48 hr, and then was added in a 1:1 ratio with EBM to experimental samples. Morphology was assessed after 16 hr on an Olympus CKX41 microscope with Nikon Elements software version 3.

*Assessment of MT130-230 activity*

Stably transduced A673-7TGP cells were stimulated with 1:1 RPMI1640 supplemented with 5% FBS and 1% L-glutamine and CM +/- RSPO2 for 48 hr, with either saline control or 100 µg/mL MT130-230. Cells were dissociated using Accutase (Millipore) and fluorescence was measured using an Accuri C6 cytometer.

*Subcutaneous tumor growth*

$1x10^6$ A673 or TC32 cells were re-suspended in Matrigel and implanted subcutaneously into 10-12 week-old NOD SCID mice (strain 394, Charles River Laboratories, Wilmington, MA). Tumors were measured every other day by calipers, and tumor volume was determined using the formula $V=1/2ab^2$, where 'a' is the longer dimension and 'b' is the shorter dimension. Once tumors reached 200-500$mm^3$, weekly

administration of the anti-RSPO2 monoclonal antibody MT130-230 was administered intraperitoneally at a dose of 20 mg/kg or an equal volume of saline as a control. Mice were euthanized once tumors reached 18mm in any dimension.

In vivo s*ub-renal capsule model*

$2x10^5$ luciferase-tagged TC32 cells were directly injected under the capsule of the kidney via ultrasound-guided needle and catheter. Weekly IP injections of 20 mg/kg MT130-230 or an equal volume of saline was started at the time of tumor implantation. Primary tumor growth and appearance of large metastases was followed weekly via bioluminescence imaging as previously described. After six weeks, each mouse was first injected with luciferin and the primary tumor was imaged. Mice were then euthanized 5 minutes after luciferase injection, and its kidney containing the primary tumor was removed via dissection. Immediately following kidney dissection, the remaining organs were imaged by bioluminescence *ex vivo,* and the number of overt metastases, as well as the bioluminescent tumor burden of distant metastases was measured via bioluminescence and macroscopic visualization with the aid of ULAM-PCAR.

# Chapter 5

# Discussion

## Introduction

The Wnt/beta-catenin signaling pathway has a significant role in the pathogenesis of multiple cancers; however, its role in Ewing sarcoma is largely unknown. Previous work by our lab implicated the Wnt-modulatory receptor LGR5 as a mediator of aggressive disease, yet the mechanism of its contribution remained elusive. Emerging evidence supported a role for potentiation of Wnt/beta-catenin signaling by RSPOs through LGR5, and we thus hypothesized that LGR5 contributes to aggressive disease via activation of Wnt/beta-catenin. To date, however, there has been little evidence that Wnt/beta-catenin has a role in the development or progression of this tumor. The work in this dissertation set out to determine the extent to which the Wnt/beta-catenin signaling pathway is involved in Ewing sarcoma pathogenesis, and to further determine the downstream effects of activated signaling.

Through investigation of primary tumor samples, we have discovered that focal nuclear beta-catenin is detectable in a subset of Ewing sarcoma patients. Importantly, patients whose tumors have nuclear beta-catenin experience worse clinical outcomes and overall survival compared to patients whose tumors lack beta-catenin. These findings are supported by the fact that in separate study, patients who had high levels of

LEF1, a readout of Wnt/beta-catenin signaling, similarly experienced worse outcomes and rates of survival compared to patients whose tumors had low levels of LEF1. Taken together, these findings demonstrate that patients with evidence of Wnt/beta-catenin activation harbor aggressive disease.

Given the evidence that Wnt/beta-catenin signaling contributes to poor outcomes in patients, we used *in vitro* and *in vivo* models to probe the mechanism of how Wnt/beta-catenin signaling mediates this effect. We first recognized that in cell lines, the response to Wnt ligands was heterogeneous at the level of individual cells within a cell line, and also among different cell lines. These findings reflected our observation that Wnt/beta-catenin was focal and heterogeneous within individual tumor biopsies, but was also highly variable between different patients as well. We then investigated the downstream effects of Wnt/beta-catenin activation in Ewing sarcoma cell lines, with particular focus on the most highly Wnt-responsive cells. Through RNA-sequencing and functional studies, we discovered that activation of Wnt/beta-catenin paradoxically inhibits EWS-ETS transcriptional activity, and promotes a phenotypic transition from a proliferative to a migratory and metastatic state. In addition, the metastasis-associated molecule Tenascin C (TNC) was identified as a gene that was consistently induced by Wnt/beta-catenin signaling. We validated its role as a mediator of both Wnt-mediated and Wnt-independent migration, and also established its significant role in promotion of metastasis. Regulation of TNC by Wnt/beta-catenin was not consistent in other cell types, thus underscoring the context-dependent nature of genes regulated by Wnt/beta-catenin signaling.

We further investigated how Wnt/beta-catenin activation might contribute to pathogenesis in the scope of the tumor microenvironment. In particular, we found that

patient tumors with high LEF1 expression had higher stromal content in biopsies than tumors with low expression, and LEF1 expression correlated strongly with expression of stroma-and angiogenesis-related genes. Experimentally, we found that high LEF1 expression induced by beta-catenin promoted a migratory phenotype on a physiologic basement membrane. We also observed that an angiogenic phenotype was induced, and this was likely through direct tumor-microenvironment interactions rather than through induction of secreted pro-angiogenic factors. Taken together, these findings suggest a model in which Wnt/RSPO activation inhibits EWS/FLI1 and results in a phenotypic transition from a proliferative to a more aggressive state characterized by an increase in migration, metastasis, and possible microenvironment involvement (Fig. 5.1).

In Chapter 4 we also investigated if the RSPO/Wnt/beta-catenin pathway could be therapeutically targeted *in vivo*. Although the anti-RSPO2 antibody MT130-230 showed a decrease in the number of metastatic foci, our findings suggest that targeted inhibition is moderately effective at metastatic prevention, and warrant preclinical investigation for the use of additional inhibitors of the Wnt signaling pathway, as broader Wnt pathway inhibition may be more desirable for therapeutic intervention, which will be further discussed in this chapter.

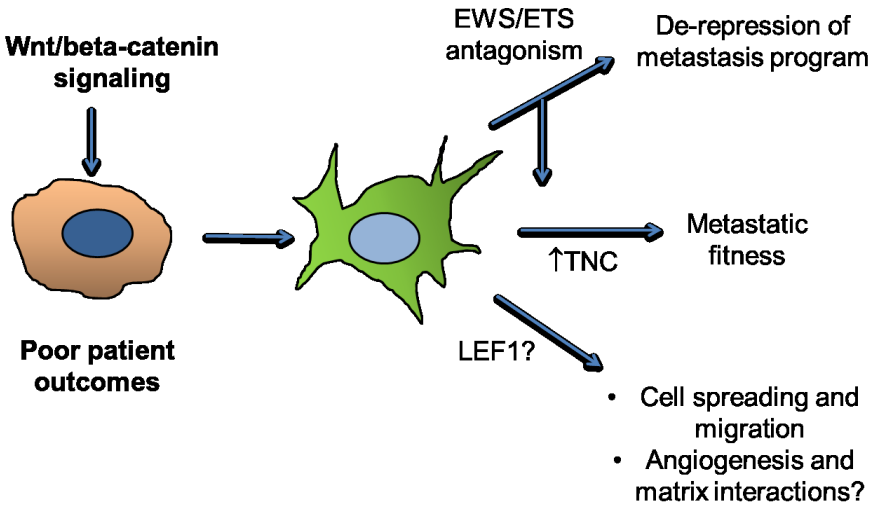


**Figure 5.1 Model of the downstream effects of activated Wnt/beta-catenin signaling on Ewing sarcoma cells.**

Wnt/beta-catenin activation in Ewing sarcoma cells promotes poor outcomes in patients through induction of migratory and metastatic phenotypes via EWS/ETS antagonism and TNC induction. Microenvironment interactions, through Wnt/LEF1-mediated modification of angiogenesis and signaling pathway and matrix crosstalk, may also contribute to aggressive disease, but further investigation is required to elucidate the specific contributions of these factors.

## Implications for Wnt/beta-catenin biology

The Wnt/beta-catenin signaling is an evolutionarily conserved pathway that has generated an enormous body of work given its crucial role in development and cancer pathogenesis. The events in its signaling cascade are well-characterized and are reproducible in most cells. In Ewing sarcoma, we have found that the Wnt/beta-catenin signaling cascade is functionally intact in that 'canonical' Wnt3a ligands result in expected stabilization and nuclear accumulation of beta-catenin, leading to an increase in 7xTCF reporter activity and transcription of established and well-described target genes *AXIN2* and *LEF1*. These downstream effects are recapitulated by GSK3-beta inhibition and by ectopic expression of constitutively active beta-catenin and cannot be

induced by the non-canonical ligand Wnt5a. Thus in Ewing sarcoma, the Wnt/beta-catenin signaling cascade proceeds largely in manner consistent with published literature. Further, the context-dependent nature of transcriptional regulation of Wnt target genes is consistent with published literature. While known targets of Wnt/beta-catenin signaling such as *CCND1* and *CMYC* are not regulated in Ewing sarcoma, the less-conventional target gene *TNC* is reproducibly induced. In addition to context-dependent regulation of downstream target genes, this work further supports the idea that the phenotypic and functional response of cells to Wnt stimulation are context dependent, namely that the proliferative phenotype induced by Wnt/beta-catenin in many epithelial cancers is not recapitulated in Ewing sarcoma, but rather a migratory phenotype is induced, perhaps reminiscent of its putative neural crest and/or mesenchymal origins.

A relatively novel finding of this work is that not all cells in a given cell line activate the Wnt/beta-catenin signaling cascade, and the responsive proportions vary among cells lines. This heterogeneity was observed at a cellular level by heterogeneous nuclear beta-catenin localization as well as transcriptionally by heterogeneous activation of the 7TGP-reporter. Evidence for examples of heterogeneous Wnt activation in other cancers is deliberated in the discussion of Chapter 2, yet the mechanism of this heterogeneity in Ewing sarcoma remains unclear. Our leading hypothesis is that LGR5 and other cell surface receptors, such as Fzs and LRPs, are variably expressed on individual cells. Intracellular regulators of Wnt/beta-catenin signaling are less likely to be heterogeneously expressed, as most Ewing sarcoma cell lines have uniform absence of Wnt/beta-catenin activation, indicating that the destruction complex is functional intact in all cells. Further, pharmacologic GSK3-beta inhibition revealed that all cells possess the

ability to respond intracellularly, as almost 100% of cells activated reporter activity following exposure. Thus, the source of heterogeneity is likely to occur at the cell surface, especially given the highly heterogeneous expression of LGR5 by cell lines and primary tumors. The factors that contribute to LGR5 heterogeneity are also unknown, but LGR5 expression is likely to be regulated epigenetically, rather than through genetic mechanisms. Yet another source of heterogeneity *in vivo* that should be considered is the microenvironment. Differential responsiveness of cells to signaling molecules has been described *in vivo*¸ as it was recently published that squamous cell carcinomas cells exhibit heterogeneous activation of the TGF-beta pathway [120]. In this study, TGF-beta ligand distribution was found to be expressed by the vasculature and immune cells in the tumor microenvironment, generating regional TGF-beta signaling within subpopulations of the tumor. Similarly, since Wnt ligands are short-range signaling molecules, the physical proximity of Wnt-secreting cells, such as osterix-positive bone cells [77], to Ewing sarcoma cells could further contribute to the complexity of the heterogeneous Wnt activation we observed in primary tumors.

## Implications for Ewing sarcoma pathogenesis

Ever since the first implication of a role for Wnt/beta-catenin signaling in Ewing sarcoma in 2004, there have been suggestions in the literature but few dedicated investigations into the role of the this pathways in this tumor. In this work, we provide the first evidence that Wnt/beta catenin acts as a contributor to metastasis. It is important to note that Wnt/beta catenin activation only occurs in a minority of biopsies, indicating that either some but not all tumors may use this mechanism to promote metastasis, or that other tumors may have activation but may not be detectable upon

biopsy due to heterogeneous staining within a tumor. The contribution and potential cross-talk of other established metastatic pathways, such as ERBB4/Rac signaling and SDF-1/CXCR4, to Wnt-mediated metastasis remains unknown but could providing interesting insight toward mechanisms of disease progression.

In this study, we established that the set of genes regulated by Wnt/beta-catenin is distinct in Ewing sarcoma, and has little overlap with Wnt/beta-catenin activation in other cell types. Published gene sets involving the Wnt pathway were not frequently observed in our GSEA analyses. The unique specificity of transcriptional targets in Ewing sarcoma, but not other cells may be influenced by it developmental origins as discussed in Chapter 3, but also be affected by the profound dysregulation of epigenetic modifiers in Ewing sarcoma. For instance, Polycomb group (PcG) proteins BMI1 [172-174] and EZH2 [21] are overexpressed in Ewing sarcoma. PcG proteins regulated histone modifications that serve to promote activation or repression of numerous genes. In Ewing sarcoma, PcG dysregulation results in aberrant repression of many genes and inappropriate activation of others [175]. In addition to epigenetic dysregulation by PcG, EWS/FLI-1 itself has recently been described to act as a pioneer factor, meaning that the fusion protein opens chromatin and creates novel epigenetic enhancer regions [15], thus resulting in alterations in gene expression. Taking this together, the chromatin status of classic Wnt/beta-catenin target genes is likely to be considerably different in Ewing sarcoma compared to other cells, and thus may drastically affect what genes are accessible to TCF/LEF transcription factor binding.

Ewing sarcoma cells express a complement of Wnt ligands and receptors, but for the most part, no autocrine signaling is observed in any of the cell lines tested. It is intriguing that expression of these ligands does not activate signaling. In contrast, other

sarcomas [89] and breast cancer similarly express numerous Wnts, but this results in and autocrine activation that can be blocked by SFRPs [176, 177]. Even though there is transcript expression of numerous Wnt genes, it remains unknown if there is sufficient protein expression of Wnts for autocrine activation, because detailed studies of protein expression of Wnt signaling components have not been performed, and are difficult due to lack of suitable antibodies for many components of the signaling cascade. The receptor complexes and components of the signaling cascade are likely to contribute, but cannot be fully responsible for suppressing basal Wnt activation, as all cell lines exhibit some degree of Wnt responsiveness when assessed by TCF reporter assays. The possible explanation is that most cells inherently exhibit tight regulation of Wnt activity. This is achieved via the regulation by the destruction complex, as well as through fine-tuned regulation of the sub-cellular localization of ligands and receptors. In addition, we have shown that Wnt activation does not promote proliferation and antagonizes proliferative transcriptional programs, thus creating no selective growth advantage for cells to exhibit autocrine Wnt signaling.

An important implication of this work is that Wnt/beta-catenin signaling provides a biological mechanism by which EWS/FLI-1 activity may be reduced and lead to metastasis. Recent studies have provided a novel mechanism of Ewing sarcoma metastasis by which inhibition of EWS/FLI-1 results in de-repression of critical cytoskeleton genes including ZYX. In these studies, EWS/FLI-1 inhibition was generated via RNAi technology, yet little discussion was provided of how EWS/FLI-1 levels might be reduced endogenously in patients. This raised the question of whether or not EWS/FLI-1 levels could actually change *in vivo* or in patient tumors, and if the observed metastatic phenotype was just an artifact of *in vitro* manipulation. In this work,

we show that it is possible that Wnt/beta-catenin signaling may reduce EWS/FLI-1 transcript levels in some cell lines, which could contribute to reduced EWS/FLI-1 expression. Importantly, however, regardless of the extent of repression of EWS/FLI1 transcript expression, functional inhibition of EWS/FLI-1 activity was observed in all cell lines tested. Thus, Wnt/beta-catenin activation might act as a biological mechanism by which EWS/FLI-1 activity is functionally reduced, thus phenocopying the effects of RNAi-mediated inhibition.

Further evidence that inhibition of EWS/FLI-1 promotes metastasis is emerging. Unpublished work presented by Olivier Delattre at the 2015 Advances in Pediatric Cancer Research independently validated the previous findings [60] that RNAi-mediated inhibition of EWS-FLI1 promotes lung engraftment *in vivo* [178]. In addition, heterogeneous expression of EWS/FLI-1-regulated cell surface proteins was observed, suggesting that EWS/FLI-1 levels are heterogeneous at the level of single cells [178]. This raises the possibility that heterogeneous EWS/FLI-1 levels may be yet another contributor to the heterogeneous Wnt/beta-catenin signaling observed in Ewing sarcoma cells, as we have shown that EWS/FLI-1 knockdown strongly enhances the response of A673 cell to Wnt ligands. These findings are of considerable importance, as specific EWS/FLI-1 inhibitors are an ongoing topic of intense investigation. Compounds such as mithramycin specifically inhibit EWS/FLI-1 activity and reduce tumor growth and formation [34], but the effects of EWS/FLI-1 inhibitors on metastatic phenotypes is unknown. Hopefully, these drugs will actually eradicate tumor cells rather than merely reduce EWS/FLI-1 levels and inhibit tumor proliferation, as there is a possibility that reduced, nonzero levels of EWS/FLI-1 may result in devastating metastatic phenotypes.

As these therapeutics are optimized and transition into clinical trials, particular care and attention should be paid to determine the effects on metastatic phenotypes.

## Considerations for therapy

The observations we have made using data from primary patient tumors in conjunction with our experimental findings demonstrate the importance of the Wnt/beta-catenin signaling pathway in the pathogenesis of Ewing sarcoma. Both early and modern studies of colorectal carcinoma have demonstrated the irrefutable importance of this pathway in oncogenesis, which has been further supported by numerous studies in other cancer types. Thus, there has been significant interest in generating Wnt pathway inhibitors that may be useful in several cancer types. Our findings in Ewing sarcoma further broaden the utility of such therapeutics. Unlike other tumors, in which oncogenic dysregulation of Wnt/beta-catenin promotes tumor initiation, proliferation, and primary tumor growth, we have found that Wnt/beta-catenin promotes metastatic phenotypes. As it follows, targeted inhibition of the Wnt signaling pathway may be beneficial to patients in order to prevent the formation of distant metastases or relapse. Thus, different endpoints may be required for determining the efficacy of inhibitors of Wnt/beta-catenin signaling inhibitors. As demonstrated by our findings with an anti-RSPO2 antibody, inhibition of the RSPO2/LGR5 interaction resulted in no changes in primary tumor growth either subcutaneously or in the renal capsule, however, inhibition decreased the formation of distant metastases. It is becoming more appreciated that when testing new therapeutics, in both pre-clinical and clinical studies, tumor shrinkage should not be the only end point determined, and this idea should hold true for Ewing

sarcoma as well. Although it may be clinically unfeasible, especially in Ewing sarcoma patients, factors such as time to progression and prevalence of distant metastases, as well as overall and event free survival should be included when assessing the efficacy of new therapeutics.

Numerous levels of the Wnt/beta-catenin signaling cascade have potential for therapeutic intervention, including (1) Wnt ligand secretion (2) Wnt ligand/receptor interactions (3) intracellular pathway regulators, (4) nuclear partner transcription factors, and (5) epigenetic status of target genes. Numerous small molecule and biologic inhibitors of these are currently in phase I clinical trials. The porcupine inhibitor LGK974 is an example of a drug that acts at the level of Wnt ligand secretion [179], and is currently under pre-clinical and clinical investigation Wnt-driven solid tumors [88]. Since it is likely that Wnt ligands are provided by Ewing sarcoma microenvironment, porcupine inhibitors might be useful as an adjuvant therapy. Similarly, inhibition at the level of Wnt ligand/receptor interactions is also likely to be useful and the aforementioned drug, OMP-18R5, is an example of a monoclonal antibody that should be considered [168]. Other drugs in this category in clinical trials include OMP-54F28, which is a FZD8 mimetic that binds to Wnt ligands [180]. The evidence we provided in here and in the aforementioned chapters suggest that these therapeutics, acting at any level of the Wnt/beta-catenin signaling cascade, should be considered in Ewing sarcoma patients with evidence of Wnt/beta-catenin activation.

## Concluding remarks

Throughout this dissertation, we provide the first evidence for activation of Wnt/beta-catenin signaling in a subset of Ewing sarcoma patients. Through *in vitro* and

*in vivo* studies, we have discovered that the downstream effects of activated Wnt/beta-catenin signaling result in metastatic phenotypes via novel mechanisms, namely through inhibition of EWS/ETS and up-regulation of metastasis genes, including TNC. We further raise the possibility that Wnt/beta-catenin signaling may influence the tumor microenvironment and contribute to signaling of other pathways important in Ewing sarcoma pathogenesis. In light of the recent advances toward development of Wnt pathway and EWS/FLI1 inhibitors, the data presented in this dissertation provide strong rationale to begin pre-clinical investigation for the use of Wnt inhibitors in Ewing sarcoma models of metastasis. It is my hope that these studies will eventually lay a foundation for discoveries that will lead to the eradication of metastasis in this terrible disease.

## References


1. Balamuth, N.J. and R.B. Womer, *Ewing's sarcoma.* Lancet Oncol, 2010. **11**(2): p. 184-92.
2. Lawlor, E.R. and P.H. Sorensen, *Twenty Years on: What Do We Really Know about Ewing Sarcoma and What Is the Path Forward?* Crit Rev Oncog, 2015. **20**(3-4): p. 155-71.
3. Scannell, C.A., et al., *LGR5 is Expressed by Ewing Sarcoma and Potentiates Wnt/beta-Catenin Signaling.* Front Oncol, 2013. **3**: p. 81.
4. Clevers, H. and R. Nusse, *Wnt/beta-catenin signaling and disease.* Cell, 2012. **149**(6): p. 1192-205.
5. Womer, R.B., et al., *Randomized controlled trial of interval-compressed chemotherapy for the treatment of localized Ewing sarcoma: a report from the Children's Oncology Group.* J Clin Oncol, 2012. **30**(33): p. 4148-54.
6. Le Deley, M.C., et al., *Cyclophosphamide compared with ifosfamide in consolidation treatment of standard-risk Ewing sarcoma: results of the randomized noninferiority Euro-EWING99-R1 trial.* J Clin Oncol, 2014. **32**(23): p. 2440-8.
7. Armstrong, G.T., et al., *Aging and risk of severe, disabling, life-threatening, and fatal events in the childhood cancer survivor study.* J Clin Oncol, 2014. **32**(12): p. 1218-27.
8. Bernstein, M., et al., *Ewing's sarcoma family of tumors: current management.* Oncologist, 2006. **11**(5): p. 503-19.
9. Grier, H.E., *The Ewing family of tumors. Ewing's sarcoma and primitive neuroectodermal tumors.* Pediatr Clin North Am, 1997. **44**(4): p. 991-1004.
10. Scotlandi, K., et al., *CD99 engagement: an effective therapeutic strategy for Ewing tumors.* Cancer Res, 2000. **60**(18): p. 5134-42.
11. Arvand, A. and C.T. Denny, *Biology of EWS/ETS fusions in Ewing's family tumors.* Oncogene, 2001. **20**(40): p. 5747-54.
12. Sankar, S. and S.L. Lessnick, *Promiscuous partnerships in Ewing's sarcoma.* Cancer Genet, 2011. **204**(7): p. 351-65.
13. Kovar, H., *Blocking the road, stopping the engine or killing the driver? Advances in targeting EWS/FLI-1 fusion in Ewing sarcoma as novel therapy.* Expert Opin Ther Targets, 2014. **18**(11): p. 1315-28.
14. Guillon, N., et al., *The oncogenic EWS-FLI1 protein binds in vivo GGAA microsatellite sequences with potential transcriptional activation function.* PLoS One, 2009. **4**(3): p. e4932.
15. Riggi, N., et al., *EWS-FLI1 utilizes divergent chromatin remodeling mechanisms to directly activate or repress enhancer elements in Ewing sarcoma.* Cancer Cell, 2014. **26**(5): p. 668-81.
16. Tomazou, E.M., et al., *Epigenome mapping reveals distinct modes of gene regulation and widespread enhancer reprogramming by the oncogenic fusion protein EWS-FLI1.* Cell Rep, 2015. **10**(7): p. 1082-95.

17. Owen, L.A., A.A. Kowalewski, and S.L. Lessnick, *EWS/FLI mediates transcriptional repression via NKX2.2 during oncogenic transformation in Ewing's sarcoma.* PLoS One, 2008. **3**(4): p. e1965.
18. Smith, R., et al., *Expression profiling of EWS/FLI identifies NKX2.2 as a critical target gene in Ewing's sarcoma.* Cancer Cell, 2006. **9**(5): p. 405-16.
19. Kinsey, M., et al., *EWS/FLI and its downstream target NR0B1 interact directly to modulate transcription and oncogenesis in Ewing's sarcoma.* Cancer Res, 2009. **69**(23): p. 9047-55.
20. Kinsey, M., R. Smith, and S.L. Lessnick, *NR0B1 is required for the oncogenic phenotype mediated by EWS/FLI in Ewing's sarcoma.* Mol Cancer Res, 2006. **4**(11): p. 851-9.
21. Richter, G.H., et al., *EZH2 is a mediator of EWS/FLI1 driven tumor growth and metastasis blocking endothelial and neuro-ectodermal differentiation.* Proc Natl Acad Sci U S A, 2009. **106**(13): p. 5324-9.
22. Sankar, S., et al., *Mechanism and relevance of EWS/FLI-mediated transcriptional repression in Ewing sarcoma.* Oncogene, 2013. **32**(42): p. 5089-100.
23. Sankar, S., et al., *Reversible LSD1 inhibition interferes with global EWS/ETS transcriptional activity and impedes Ewing sarcoma tumor growth.* Clin Cancer Res, 2014. **20**(17): p. 4584-97.
24. Hahm, K.B., et al., *Repression of the gene encoding the TGF-beta type II receptor is a major target of the EWS-FLI1 oncoprotein.* Nat Genet, 1999. **23**(2): p. 222-7.
25. Im, Y.H., et al., *EWS-FLI1, EWS-ERG, and EWS-ETV1 oncoproteins of Ewing tumor family all suppress transcription of transforming growth factor beta type II receptor gene.* Cancer Res, 2000. **60**(6): p. 1536-40.
26. Agra, N., et al., *Lysyl oxidase is downregulated by the EWS/FLI1 oncoprotein and its propeptide domain displays tumor supressor activities in Ewing sarcoma cells.* PLoS One, 2013. **8**(6): p. e66281.
27. Brohl, A.S., et al., *The genomic landscape of the Ewing Sarcoma family of tumors reveals recurrent STAG2 mutation.* PLoS Genet, 2014. **10**(7): p. e1004475.
28. Crompton, B.D., et al., *The genomic landscape of pediatric Ewing sarcoma.* Cancer Discov, 2014. **4**(11): p. 1326-41.
29. Tirode, F., et al., *Genomic landscape of Ewing sarcoma defines an aggressive subtype with co-association of STAG2 and TP53 mutations.* Cancer Discov, 2014. **4**(11): p. 1342-53.
30. Uren, A. and J.A. Toretsky, *Ewing's sarcoma oncoprotein EWS-FLI1: the perfect target without a therapeutic agent.* Future Oncol, 2005. **1**(4): p. 521-8.
31. Houghton, P.J., et al., *Evaluation of cytarabine against Ewing sarcoma xenografts by the pediatric preclinical testing program.* Pediatr Blood Cancer, 2010. **55**(6): p. 1224-6.
32. Grohar, P.J., et al., *Dual targeting of EWS-FLI1 activity and the associated DNA damage response with trabectedin and SN38 synergistically inhibits Ewing sarcoma cell growth.* Clin Cancer Res, 2014. **20**(5): p. 1190-203.
33. Grohar, P.J., et al., *Identification of an inhibitor of the EWS-FLI1 oncogenic transcription factor by high-throughput screening.* J Natl Cancer Inst, 2011. **103**(12): p. 962-78.

34. Osgood, C.L., et al., *Identification of mithramycin analogs with improved targeting of the EWS-FLI1 transcription factor.* Clin Cancer Res, 2016.
35. Barber-Rotenberg, J.S., et al., *Single enantiomer of YK-4-279 demonstrates specificity in targeting the oncogene EWS-FLI1.* Oncotarget, 2012. **3**(2): p. 172-82.
36. Lamhamedi-Cherradi, S.E., et al., *An Oral Formulation of YK-4-279: Preclinical Efficacy and Acquired Resistance Patterns in Ewing Sarcoma.* Mol Cancer Ther, 2015. **14**(7): p. 1591-604.
37. Celli, R. and G. Cai, *Ewing Sarcoma/Primitive Neuroectodermal Tumor of the Kidney: A Rare and Lethal Entity.* Arch Pathol Lab Med, 2016. **140**(3): p. 281-5.
38. Shek, T.W., et al., *Ewing sarcoma of the small intestine.* J Pediatr Hematol Oncol, 2001. **23**(8): p. 530-2.
39. Vallonthaiel, A.G., et al., *Ewing Sarcoma of Urinary Bladder Showing EWSR1 Rearrangement on FISH Analysis and Unique Response to Chemotherapy.* Clin Genitourin Cancer, 2016. **14**(2): p. e183-6.
40. Osborn, H.A., et al., *Ewing's sarcoma of the masseter muscle.* J Laryngol Otol, 2011. **125**(9): p. 978-81.
41. Majid, N., et al., *Bilateral ewing sarcoma/primitive neuroectodermal tumor of the breast: a very rare entity and review of the literature.* Case Rep Oncol Med, 2013. **2013**: p. 964568.
42. Tasli, F., et al., *An unusual tumor of the breast - extraskeletal ewing sarcoma.* Curr Health Sci J, 2014. **40**(1): p. 75-7.
43. Zhang, D.W., et al., *[Primitive neuroectodermal tumor/Ewing's sarcoma of the penis in children: a case report and review of the literature].* Zhonghua Nan Ke Xue, 2012. **18**(12): p. 1115-8.
44. Kallala, R., et al., *Primary extraskeletal Ewing sarcoma involving the carotid artery: a case report and review of the current literature.* Ann R Coll Surg Engl, 2012. **94**(4): p. e141-3.
45. Ewing, J., *Diffuse Endothelioma of the Bone.* Proceedings of the New York Pathological Society, 1921. **192**(21): p. 17-24.
46. van der Schaft, D.W., et al., *Tumor cell plasticity in Ewing sarcoma, an alternative circulatory system stimulated by hypoxia.* Cancer Res, 2005. **65**(24): p. 11520-8.
47. Tirode, F., et al., *Mesenchymal stem cell features of Ewing tumors.* Cancer Cell, 2007. **11**(5): p. 421-9.
48. Staege, M.S., et al., *DNA microarrays reveal relationship of Ewing family tumors to both endothelial and fetal neural crest-derived cells and define novel targets.* Cancer Res, 2004. **64**(22): p. 8213-21.
49. Riggi, N., et al., *EWS-FLI-1 modulates miRNA145 and SOX2 expression to initiate mesenchymal stem cell reprogramming toward Ewing sarcoma cancer stem cells.* Genes Dev, 2010. **24**(9): p. 916-32.
50. von Levetzow, C., et al., *Modeling initiation of Ewing sarcoma in human neural crest cells.* PLoS One, 2011. **6**(4): p. e19305.
51. Deneen, B. and C.T. Denny, *Loss of p16 pathways stabilizes EWS/FLI1 expression and complements EWS/FLI1 mediated transformation.* Oncogene, 2001. **20**(46): p. 6731-41.

52. Lessnick, S.L., C.S. Dacwag, and T.R. Golub, *The Ewing's sarcoma oncoprotein EWS/FLI induces a p53-dependent growth arrest in primary human fibroblasts.* Cancer Cell, 2002. **1**(4): p. 393-401.
53. Sainz-Jaspeado, M., et al., *Caveolin-1 modulates the ability of Ewing's sarcoma to metastasize.* Mol Cancer Res, 2010. **8**(11): p. 1489-500.
54. Tirado, O.M., et al., *Caveolin-1 (CAV1) is a target of EWS/FLI-1 and a key determinant of the oncogenic phenotype and tumorigenicity of Ewing's sarcoma cells.* Cancer Res, 2006. **66**(20): p. 9937-47.
55. Wiles, E.T., et al., *ZEB2 Represses the Epithelial Phenotype and Facilitates Metastasis in Ewing Sarcoma.* Genes Cancer, 2013. **4**(11-12): p. 486-500.
56. Krook, M.A., et al., *Stress-induced CXCR4 promotes migration and invasion of ewing sarcoma.* Mol Cancer Res, 2014. **12**(6): p. 953-64.
57. Sand, L.G., et al., *CXCL14, CXCR7 expression and CXCR4 splice variant ratio associate with survival and metastases in Ewing sarcoma patients.* Eur J Cancer, 2015. **51**(17): p. 2624-33.
58. Mendoza-Naranjo, A., et al., *ERBB4 confers metastatic capacity in Ewing sarcoma.* EMBO Mol Med, 2013. **5**(7): p. 1019-34.
59. Chaturvedi, A., et al., *Molecular dissection of the mechanism by which EWS/FLI expression compromises actin cytoskeletal integrity and cell adhesion in Ewing sarcoma.* Mol Biol Cell, 2014. **25**(18): p. 2695-709.
60. Chaturvedi, A., et al., *The EWS/FLI Oncogene Drives Changes in Cellular Morphology, Adhesion, and Migration in Ewing Sarcoma.* Genes Cancer, 2012. **3**(2): p. 102-16.
61. Li, L., et al., *Second cysteine-rich domain of Dickkopf-2 activates canonical Wnt signaling pathway via LRP-6 independently of dishevelled.* J Biol Chem, 2002. **277**(8): p. 5977-81.
62. Mao, B., et al., *LDL-receptor-related protein 6 is a receptor for Dickkopf proteins.* Nature, 2001. **411**(6835): p. 321-5.
63. Clevers, H., *Wnt/beta-catenin signaling in development and disease.* Cell, 2006. **127**(3): p. 469-80.
64. Matushansky, I., R.G. Maki, and C. Cordon-Cardo, *A context dependent role for Wnt signaling in tumorigenesis and stem cells.* Cell Cycle, 2008. **7**(6): p. 720-4.
65. Herr, P., G. Hausmann, and K. Basler, *WNT secretion and signalling in human disease.* Trends Mol Med, 2012. **18**(8): p. 483-93.
66. Cruciat, C.M. and C. Niehrs, *Secreted and transmembrane wnt inhibitors and activators.* Cold Spring Harb Perspect Biol, 2013. **5**(3): p. a015081.
67. Brott, B.K. and S.Y. Sokol, *Regulation of Wnt/LRP signaling by distinct domains of Dickkopf proteins.* Mol Cell Biol, 2002. **22**(17): p. 6100-10.
68. Mao, C.D. and S.W. Byers, *Cell-context dependent TCF/LEF expression and function: alternative tales of repression, de-repression and activation potentials.* Crit Rev Eukaryot Gene Expr, 2011. **21**(3): p. 207-36.
69. Kawano, Y. and R. Kypta, *Secreted antagonists of the Wnt signalling pathway.* J Cell Sci, 2003. **116**(Pt 13): p. 2627-34.
70. Carmon, K.S., et al., *R-spondins function as ligands of the orphan receptors LGR4 and LGR5 to regulate Wnt/beta-catenin signaling.* Proc Natl Acad Sci U S A, 2011. **108**(28): p. 11452-7.

71. de Lau, W., et al., *The R-spondin/Lgr5/Rnf43 module: regulator of Wnt signal strength.* Genes Dev, 2014. **28**(4): p. 305-16.
72. Schuijers, J. and H. Clevers, *Adult mammalian stem cells: the role of Wnt, Lgr5 and R-spondins.* EMBO J, 2012. **31**(12): p. 2685-96.
73. Ruffner, H., et al., *R-Spondin potentiates Wnt/beta-catenin signaling through orphan receptors LGR4 and LGR5.* PLoS One, 2012. **7**(7): p. e40976.
74. van Amerongen, R. and R. Nusse, *Towards an integrated view of Wnt signaling in development.* Development, 2009. **136**(19): p. 3205-14.
75. Luis, T.C., et al., *Canonical wnt signaling regulates hematopoiesis in a dosage-dependent fashion.* Cell Stem Cell, 2011. **9**(4): p. 345-56.
76. Alonso, L. and E. Fuchs, *Stem cells in the skin: waste not, Wnt not.* Genes Dev, 2003. **17**(10): p. 1189-200.
77. Tan, S.H., et al., *Wnts produced by Osterix-expressing osteolineage cells regulate their proliferation and differentiation.* Proc Natl Acad Sci U S A, 2014. **111**(49): p. E5262-71.
78. Zhong, Z., N.J. Ethen, and B.O. Williams, *WNT signaling in bone development and homeostasis.* Wiley Interdiscip Rev Dev Biol, 2014. **3**(6): p. 489-500.
79. Fearon, E.R., *Molecular genetics of colorectal cancer.* Annu Rev Pathol, 2011. **6**: p. 479-507.
80. Seshagiri, S., et al., *Recurrent R-spondin fusions in colon cancer.* Nature, 2012. **488**(7413): p. 660-4.
81. Majid, S., S. Saini, and R. Dahiya, *Wnt signaling pathways in urological cancers: past decades and still growing.* Mol Cancer, 2012. **11**: p. 7.
82. Polakis, P., *Wnt signaling in cancer.* Cold Spring Harb Perspect Biol, 2012. **4**(5).
83. Malanchi, I., et al., *Cutaneous cancer stem cell maintenance is dependent on beta-catenin signalling.* Nature, 2008. **452**(7187): p. 650-3.
84. Mazieres, J., et al., *Wnt signaling in lung cancer.* Cancer Lett, 2005. **222**(1): p. 1-10.
85. Schepers, A.G., et al., *Lineage tracing reveals Lgr5+ stem cell activity in mouse intestinal adenomas.* Science, 2012. **337**(6095): p. 730-5.
86. Shtutman, M., et al., *The cyclin D1 gene is a target of the beta-catenin/LEF-1 pathway.* Proc Natl Acad Sci U S A, 1999. **96**(10): p. 5522-7.
87. He, T.C., et al., *Identification of c-MYC as a target of the APC pathway.* Science, 1998. **281**(5382): p. 1509-12.
88. Kahn, M., *Can we safely target the WNT pathway?* Nat Rev Drug Discov, 2014. **13**(7): p. 513-32.
89. Vijayakumar, S., et al., *High-frequency canonical Wnt activation in multiple sarcoma subtypes drives proliferation through a TCF/beta-catenin target gene, CDC25A.* Cancer Cell, 2011. **19**(5): p. 601-12.
90. Uren, A., et al., *Wnt/Frizzled signaling in Ewing sarcoma.* Pediatr Blood Cancer, 2004. **43**(3): p. 243-9.
91. Endo, Y., et al., *Wnt-3a and Dickkopf-1 stimulate neurite outgrowth in Ewing tumor cells via a Frizzled3- and c-Jun N-terminal kinase-dependent mechanism.* Mol Cell Biol, 2008. **28**(7): p. 2368-79.
92. Endo, Y., et al., *Wnt-3a-dependent cell motility involves RhoA activation and is specifically regulated by dishevelled-2.* J Biol Chem, 2005. **280**(1): p. 777-86.

93. Greer, Y.E. and J.S. Rubin, *Casein kinase 1 delta functions at the centrosome to mediate Wnt-3a-dependent neurite outgrowth.* J Cell Biol, 2011. **192**(6): p. 993-1004.
94. Grumolato, L., et al., *Canonical and noncanonical Wnts use a common mechanism to activate completely unrelated coreceptors.* Genes Dev, 2010. **24**(22): p. 2517-30.
95. Tanaka, M., et al., *Ewing's sarcoma precursors are highly enriched in embryonic osteochondrogenic progenitors.* J Clin Invest, 2014. **124**(7): p. 3061-74.
96. Navarro, D., et al., *The EWS/FLI1 oncogenic protein inhibits expression of the Wnt inhibitor DICKKOPF-1 gene and antagonizes beta-catenin/TCF-mediated transcription.* Carcinogenesis, 2010. **31**(3): p. 394-401.
97. Miyagawa, Y., et al., *EWS/ETS regulates the expression of the Dickkopf family in Ewing family tumor cells.* PLoS One, 2009. **4**(2): p. e4634.
98. Hauer, K., et al., *DKK2 mediates osteolysis, invasiveness, and metastatic spread in Ewing sarcoma.* Cancer Res, 2013. **73**(2): p. 967-77.
99. Hu-Lieskovan, S., et al., *Sequence-specific knockdown of EWS-FLI1 by targeted, nonviral delivery of small interfering RNA inhibits tumor growth in a murine model of metastatic Ewing's sarcoma.* Cancer Res, 2005. **65**(19): p. 8984-92.
100. Katoh, M., *Integrative genomic analyses of WNT11: transcriptional mechanisms based on canonical WNT signals and GATA transcription factors signaling.* Int J Mol Med, 2009. **24**(2): p. 247-51.
101. Jin, Z., et al., *Wnt5a promotes ewing sarcoma cell migration through upregulating CXCR4 expression.* BMC Cancer, 2012. **12**: p. 480.
102. Endo, M., et al., *Insight into the role of Wnt5a-induced signaling in normal and cancer cells.* Int Rev Cell Mol Biol, 2015. **314**: p. 117-48.
103. Potratz, J., et al., *Receptor tyrosine kinase gene expression profiles of Ewing sarcomas reveal ROR1 as a potential therapeutic target in metastatic disease.* Mol Oncol, 2015.
104. Kemper, K., et al., *Monoclonal antibodies against Lgr5 identify human colorectal cancer stem cells.* Stem Cells, 2012. **30**(11): p. 2378-86.
105. Hirsch, D., et al., *LGR5 positivity defines stem-like cells in colorectal cancer.* Carcinogenesis, 2014. **35**(4): p. 849-58.
106. Barker, N., et al., *Identification of stem cells in small intestine and colon by marker gene Lgr5.* Nature, 2007. **449**(7165): p. 1003-7.
107. Nam, J.S., T.J. Turcotte, and J.K. Yoon, *Dynamic expression of R-spondin family genes in mouse development.* Gene Expr Patterns, 2007. **7**(3): p. 306-12.
108. Friedman, M.S., S.M. Oyserman, and K.D. Hankenson, *Wnt11 promotes osteoblast maturation and mineralization through R-spondin 2.* J Biol Chem, 2009. **284**(21): p. 14117-25.
109. Subramanian, A., et al., *Gene set enrichment analysis: a knowledge-based approach for interpreting genome-wide expression profiles.* Proc Natl Acad Sci U S A, 2005. **102**(43): p. 15545-50.
110. Fuerer, C. and R. Nusse, *Lentiviral vectors to probe and manipulate the Wnt signaling pathway.* PLoS One, 2010. **5**(2): p. e9370.
111. Webb, B.A., R. Eves, and A.S. Mak, *Cortactin regulates podosome formation: roles of the protein interaction domains.* Exp Cell Res, 2006. **312**(6): p. 760-9.

112. Murphy, D.A. and S.A. Courtneidge, *The 'ins' and 'outs' of podosomes and invadopodia: characteristics, formation and function.* Nat Rev Mol Cell Biol, 2011. **12**(7): p. 413-26.
113. Volchenboum, S.L., et al., *Gene Expression Profiling of Ewing Sarcoma Tumors Reveals the Prognostic Importance of Tumor-Stromal Interactions: A Report from the Children's Oncology Group.* J Pathol Clin Res, 2015. **1**(2): p. 83-94.
114. Anastas, J.N. and R.T. Moon, *WNT signalling pathways as therapeutic targets in cancer.* Nat Rev Cancer, 2013. **13**(1): p. 11-26.
115. Reya, T. and H. Clevers, *Wnt signalling in stem cells and cancer.* Nature, 2005. **434**(7035): p. 843-50.
116. Nguyen, D.X., et al., *WNT/TCF signaling through LEF1 and HOXB9 mediates lung adenocarcinoma metastasis.* Cell, 2009. **138**(1): p. 51-62.
117. Oskarsson, T., et al., *Breast cancer cells produce tenascin C as a metastatic niche component to colonize the lungs.* Nat Med, 2011. **17**(7): p. 867-74.
118. Pisco, A.O. and S. Huang, *Non-genetic cancer cell plasticity and therapy-induced stemness in tumour relapse: 'What does not kill me strengthens me'.* Br J Cancer, 2015. **112**(11): p. 1725-32.
119. Meacham, C.E. and S.J. Morrison, *Tumour heterogeneity and cancer cell plasticity.* Nature, 2013. **501**(7467): p. 328-37.
120. Oshimori, N., D. Oristian, and E. Fuchs, *TGF-beta promotes heterogeneity and drug resistance in squamous cell carcinoma.* Cell, 2015. **160**(5): p. 963-76.
121. Yang, J. and R.A. Weinberg, *Epithelial-mesenchymal transition: at the crossroads of development and tumor metastasis.* Dev Cell, 2008. **14**(6): p. 818-29.
122. Tsai, J.H. and J. Yang, *Epithelial-mesenchymal plasticity in carcinoma metastasis.* Genes Dev, 2013. **27**(20): p. 2192-206.
123. Davidson, G., et al., *Cell cycle control of wnt receptor activation.* Dev Cell, 2009. **17**(6): p. 788-99.
124. Vermeulen, L., et al., *Wnt activity defines colon cancer stem cells and is regulated by the microenvironment.* Nat Cell Biol, 2010. **12**(5): p. 468-76.
125. Postel-Vinay, S., et al., *Common variants near TARDBP and EGR2 are associated with susceptibility to Ewing sarcoma.* Nat Genet, 2012. **44**(3): p. 323-7.
126. Watanabe, T., et al., *Distal colorectal cancers with microsatellite instability (MSI) display distinct gene expression profiles that are different from proximal MSI cancers.* Cancer Res, 2006. **66**(20): p. 9804-8.
127. Nocito, A., et al., *Tissue microarrays (TMAs) for high-throughput molecular pathology research.* Int J Cancer, 2001. **94**(1): p. 1-5.
128. Applebaum, M.A., et al., *Comparative evaluation of strategies for quantifying signaling pathway proteins in Ewing sarcoma.* Appl Immunohistochem Mol Morphol, 2014. **22**(8): p. 593-9.
129. Wang, F., et al., *RNAscope: a novel in situ RNA analysis platform for formalin-fixed, paraffin-embedded tissues.* J Mol Diagn, 2012. **14**(1): p. 22-9.
130. Patro, R., S.M. Mount, and C. Kingsford, *Sailfish enables alignment-free isoform quantification from RNA-seq reads using lightweight algorithms.* Nat Biotechnol, 2014. **32**(5): p. 462-4.

131. Robinson, M.D., D.J. McCarthy, and G.K. Smyth, *edgeR: a Bioconductor package for differential expression analysis of digital gene expression data.* Bioinformatics, 2010. **26**(1): p. 139-40.
132. Lowy, C.M. and T. Oskarsson, *Tenascin C in metastasis: A view from the invasive front.* Cell Adh Migr, 2015. **9**(1-2): p. 112-24.
133. Orend, G. and R. Chiquet-Ehrismann, *Tenascin-C induced signaling in cancer.* Cancer Lett, 2006. **244**(2): p. 143-63.
134. Midwood, K.S. and G. Orend, *The role of tenascin-C in tissue injury and tumorigenesis.* J Cell Commun Signal, 2009. **3**(3-4): p. 287-310.
135. Behrem, S., et al., *Distribution pattern of tenascin-C in glioblastoma: correlation with angiogenesis and tumor cell proliferation.* Pathol Oncol Res, 2005. **11**(4): p. 229-35.
136. Shao, H., J.M. Kirkwood, and A. Wells, *Tenascin-C Signaling in melanoma.* Cell Adh Migr, 2015. **9**(1-2): p. 125-30.
137. Schnyder, B., et al., *Distribution pattern of tenascin-C in normal and neoplastic mesenchymal tissues.* Int J Cancer, 1997. **72**(2): p. 217-24.
138. Akbareian, S.E., et al., *Enteric neural crest-derived cells promote their migration by modifying their microenvironment through tenascin-C production.* Dev Biol, 2013. **382**(2): p. 446-56.
139. Bronner-Fraser, M., *Distribution and function of tenascin during cranial neural crest development in the chick.* J Neurosci Res, 1988. **21**(2-4): p. 135-47.
140. Tucker, R.P. and S.E. McKay, *The expression of tenascin by neural crest cells and glia.* Development, 1991. **112**(4): p. 1031-9.
141. Yoshida, T., T. Akatsuka, and K. Imanaka-Yoshida, *Tenascin-C and integrins in cancer.* Cell Adh Migr, 2015. **9**(1-2): p. 96-104.
142. Watanabe, G., et al., *Induction of tenascin-C by tumor-specific EWS-ETS fusion genes.* Genes Chromosomes Cancer, 2003. **36**(3): p. 224-32.
143. Beiter, K., et al., *beta-Catenin regulates the expression of tenascin-C in human colorectal tumors.* Oncogene, 2005. **24**(55): p. 8200-4.
144. Katoh, D., et al., *Binding of alphavbeta1 and alphavbeta6 integrins to tenascin-C induces epithelial-mesenchymal transition-like change of breast cancer cells.* Oncogenesis, 2013. **2**: p. e65.
145. Nagaharu, K., et al., *Tenascin C induces epithelial-mesenchymal transition-like change accompanied by SRC activation and focal adhesion kinase phosphorylation in human breast cancer cells.* Am J Pathol, 2011. **178**(2): p. 754-63.
146. Takahashi, Y., et al., *Tumor-derived tenascin-C promotes the epithelial-mesenchymal transition in colorectal cancer cells.* Anticancer Res, 2013. **33**(5): p. 1927-34.
147. Dandachi, N., et al., *Co-expression of tenascin-C and vimentin in human breast cancer cells indicates phenotypic transdifferentiation during tumour progression: correlation with histopathological parameters, hormone receptors, and oncoproteins.* J Pathol, 2001. **193**(2): p. 181-9.
148. Cohen, E.D., et al., *Wnt signaling regulates smooth muscle precursor development in the mouse lung via a tenascin C/PDGFR pathway.* J Clin Invest, 2009. **119**(9): p. 2538-49.

149. Tremble, P., R. Chiquet-Ehrismann, and Z. Werb, *The extracellular matrix ligands fibronectin and tenascin collaborate in regulating collagenase gene expression in fibroblasts.* Mol Biol Cell, 1994. **5**(4): p. 439-53.
150. Jang, J.H. and C.P. Chung, *Tenascin-C promotes cell survival by activation of Akt in human chondrosarcoma cell.* Cancer Lett, 2005. **229**(1): p. 101-5.
151. Diaz-Montero, C.M., J.N. Wygant, and B.W. McIntyre, *PI3-K/Akt-mediated anoikis resistance of human osteosarcoma cells requires Src activation.* Eur J Cancer, 2006. **42**(10): p. 1491-500.
152. Ishii, M., et al., *A stable cranial neural crest cell line from mouse.* Stem Cells Dev, 2012. **21**(17): p. 3069-80.
153. Redini, F. and D. Heymann, *Bone Tumor Environment as a Potential Therapeutic Target in Ewing Sarcoma.* Front Oncol, 2015. **5**: p. 279.
154. Shiozawa, Y., K.J. Pienta, and R.S. Taichman, *Hematopoietic stem cell niche is a potential therapeutic target for bone metastatic tumors.* Clin Cancer Res, 2011. **17**(17): p. 5553-8.
155. Shiozawa, Y., et al., *Human prostate cancer metastases target the hematopoietic stem cell niche to establish footholds in mouse bone marrow.* J Clin Invest, 2011. **121**(4): p. 1298-312.
156. Placencio, V.R., et al., *Stromal transforming growth factor-beta signaling mediates prostatic response to androgen ablation by paracrine Wnt activity.* Cancer Res, 2008. **68**(12): p. 4709-18.
157. Menge, T., et al., *Human mesenchymal stem cells inhibit endothelial proliferation and angiogenesis via cell-cell contact through modulation of the VE-Cadherin/beta-catenin signaling pathway.* Stem Cells Dev, 2013. **22**(1): p. 148-57.
158. Tanaka, K., et al., *Tenascin-C regulates angiogenesis in tumor through the regulation of vascular endothelial growth factor expression.* Int J Cancer, 2004. **108**(1): p. 31-40.
159. Massague, J., *TGFbeta signalling in context.* Nat Rev Mol Cell Biol, 2012. **13**(10): p. 616-30.
160. Padua, D. and J. Massague, *Roles of TGFbeta in metastasis.* Cell Res, 2009. **19**(1): p. 89-102.
161. Guo, X. and X.F. Wang, *Signaling cross-talk between TGF-beta/BMP and other pathways.* Cell Res, 2009. **19**(1): p. 71-88.
162. Attisano, L. and E. Labbe, *TGFbeta and Wnt pathway cross-talk.* Cancer Metastasis Rev, 2004. **23**(1-2): p. 53-61.
163. Pappo, A.S., et al., *A phase 2 trial of R1507, a monoclonal antibody to the insulin-like growth factor-1 receptor (IGF-1R), in patients with recurrent or refractory rhabdomyosarcoma, osteosarcoma, synovial sarcoma, and other soft tissue sarcomas: results of a Sarcoma Alliance for Research Through Collaboration study.* Cancer, 2014. **120**(16): p. 2448-56.
164. Schoffski, P., et al., *An open-label, phase 2 study evaluating the efficacy and safety of the anti-IGF-1R antibody cixutumumab in patients with previously treated advanced or metastatic soft-tissue sarcoma or Ewing family of tumours.* Eur J Cancer, 2013. **49**(15): p. 3219-28.

165. Scotlandi, K., et al., *Insulin-like growth factor I receptor-mediated circuit in Ewing's sarcoma/peripheral neuroectodermal tumor: a possible therapeutic target.* Cancer Res, 1996. **56**(20): p. 4570-4.
166. Jiang, Y., J. Ludwig, and F. Janku, *Targeted therapies for advanced Ewing sarcoma family of tumors.* Cancer Treat Rev, 2015. **41**(5): p. 391-400.
167. Smith, D., et al., *First-in-human evaluation of the human monoclonal antibody vantictumab (OMP-18R5; anti-Frizzled) targeting the WNT pathway in a Phase I study for patients with advanced solid tumors.* J. Clin. Onc. Abstr., 2013. **31**(2540).
168. Gurney, A., et al., *Wnt pathway inhibition via the targeting of Frizzled receptors results in decreased growth and tumorigenicity of human tumors.* Proc Natl Acad Sci U S A, 2012. **109**(29): p. 11717-22.
169. Kunzi-Rapp, K., et al., *Chorioallantoic membrane assay: vascularized 3-dimensional cell culture system for human prostate cancer cells as an animal substitute model.* J Urol, 2001. **166**(4): p. 1502-7.
170. Sys, G.M., et al., *The in ovo CAM-assay as a xenograft model for sarcoma.* J Vis Exp, 2013(77): p. e50522.
171. Arnaoutova, I. and H.K. Kleinman, *In vitro angiogenesis: endothelial cell tube formation on gelled basement membrane extract.* Nat Protoc, 2010. **5**(4): p. 628-35.
172. Cooper, A., et al., *Ewing tumors that do not overexpress BMI-1 are a distinct molecular subclass with variant biology: a report from the Children's Oncology Group.* Clin Cancer Res, 2011. **17**(1): p. 56-66.
173. Douglas, D., et al., *BMI-1 promotes ewing sarcoma tumorigenicity independent of CDKN2A repression.* Cancer Res, 2008. **68**(16): p. 6507-15.
174. Hsu, J.H. and E.R. Lawlor, *BMI-1 suppresses contact inhibition and stabilizes YAP in Ewing sarcoma.* Oncogene, 2011. **30**(17): p. 2077-85.
175. Svoboda, L.K., et al., *Overexpression of HOX genes is prevalent in Ewing sarcoma and is associated with altered epigenetic regulation of developmental transcription programs.* Epigenetics, 2014. **9**(12): p. 1613-25.
176. Schlange, T., et al., *Autocrine WNT signaling contributes to breast cancer cell proliferation via the canonical WNT pathway and EGFR transactivation.* Breast Cancer Res, 2007. **9**(5): p. R63.
177. Benhaj, K., K.C. Akcali, and M. Ozturk, *Redundant expression of canonical Wnt ligands in human breast cancer cell lines.* Oncol Rep, 2006. **15**(3): p. 701-7.
178. Delattre, O., *Genetic and phenotypic diversity in Ewing sarcoma*, in *AACR Special Conference: Advances in Pediatric Cancer Research: From Mechanisms and Models to Treatment and Survivorship*. 2015: Fort Lauderdale, Florida.
179. Liu, J., et al., *Targeting Wnt-driven cancer through the inhibition of Porcupine by LGK974.* Proc Natl Acad Sci U S A, 2013. **110**(50): p. 20224-9.
180. Le, P.N., J.D. McDermott, and A. Jimeno, *Targeting the Wnt pathway in human cancers: therapeutic targeting with a focus on OMP-54F28.* Pharmacol Ther, 2015. **146**: p. 1-11.